A taxonomic and phylogenetic study of *Nephroselmis* Stein (Prasinophyceae, Chlorophyta)

Trevor Graham Bell

School of Animal, Plant and Environmental Sciences
University of the Witwatersrand, Johannesburg

A dissertation submitted to the Faculty of Science, University of the Witwatersrand, in fulfilment of the requirements for the Degree of Master of Science

Johannesburg, May 2008

Frontispiece

Phase contrast light microscopy of the external morphology of *Nephroselmis spinosa*

Declaration

This dissertation is the result of my own work, except where the work of others is explicitly referenced. This work has not been submitted for another qualification to this or any other University.

____

Trevor Graham Bell

____

Date

Acknowledgements

Thanks are extended to my supervisors, Prof. Stuart Sym and Dr Glynis Goodman-Cron, and my research committee, Prof. Dave Mycock, Prof. Richard Pienaar and Prof. Graham Alexander. Thanks are also due to Mr Claudio Marangoni, the School of Animal, Plant and Environmental Sciences in the Faculty of Science at the University of the Witwatersrand, and the Head of School, Prof. Kevin Balkwill. The staff of the Electron Microscope Unit provided support and assistance – thanks to Prof. Mike Witcomb, Ms Caroline Lalkhan and Mr Abe Seema. Thanks also to the staff of the inter-library loan section of the Library at the University of the Witwatersrand.

Dr Jacob Larsen from the University of Copenhagen kindly provided scans of Stein's original 1878 drawings of *Nephroselmis olivacea*. Dr Ute Schwaibold of the University of the Witwatersrand kindly translated Schiller's 1926 original German description of *Nephroselmis marina* into English.

Support and understanding were provided in generous measure by Karl van Wyk, Ramon Nogueira and Pippa Wing. Very special and heartfelt thanks are extended to my parents, Lesley and Keith, without whose generosity, understanding and support this work would never have been possible.

Funding received from the Department of Environmental Affairs and Tourism (DEAT), the National Research Foundation (NRF) and the University of the Witwatersrand is also gratefully acknowledged.

– T.

Abstract

The Prasinophycean genus *Nephroselmis* Stein is a group of largely marine, photosynthetic, scaly biflagellates which has undergone several taxonomic changes since its erection in 1878. The taxonomy and phylogeny of the genus was investigated in the present study using separate and combined morphological and molecular maximum parsimony cladistic analyses. New data from light and electron microscopy were combined with data from the literature. Partial 18S gene molecular data from fresh material and from GenBank were included.

Seven species of *Nephroselmis* were confirmed as discrete entities: *N. anterostigmatica*, *N. astigmatica*, *N. olivacea*, *N. pyriformis*, *N. rotunda*, *N. spinosa* and *N. viridis*. The existing generic and specific descriptions are emended. Samples of *N. fissa*, *N. gaoae*, *N. marina* and *N. minuta* could not be sourced from culture collections or opportunistic sampling, and as no detailed and reliable electron microscopic work is available for these species, they were not included and could not be confirmed by this study.

The cladistic analyses undertaken in this study confirmed that the genus *Nephroselmis* is monophyletic. Reweighted morphological cladistic analysis yielded distinct clades within the genus, grouped predominantly by body scale number and scale complexity. Partial 18S molecular cladistic analysis agreed well with the morphological analysis, as did the combined analysis. *N. pyriformis*, which shows the greatest number of plesiomorphic features and possesses the simplest scale morphology, was placed in a basal position in all three analyses. The greatest scale complexity is found in *N. anterostigmatica* and *N. astigmatica*, which occured as sister species in all three analyses. Eyespot modifications are found in these two species only: *N. astigmatica* lacks an eyespot and the eyespot of *N. anterostigmatica* is atypically located on the anterior surface of the cell. *N. olivacea* and *N. viridis* show intermediate scale complexity and were placed as sister species in all three analyses.

The relationship between *N. rotunda* and *N. spinosa* varied between the three analyses. The reweighted morphological cladistic analysis placed *N. rotunda*, which has three body scale layers, in its own clade, between *N. pyriformis*, which has two body scale layers, and the clade consisting of all other *Nephroselmis* species, which possess four or five body scale layers. The partial 18S molecular cladistic analysis grouped *N. rotunda* and *N. spinosa* in a clade sister to the *N. olivacea* / *N. viridis* clade. The combined analysis grouped *N. rotunda* and *N. spinosa* in a clade sister to the remaining *Nephroselmis* species. The only freshwater species, *N. olivacea*, occured in a clade with *N. viridis* (in a more derived position), rather than in a basal position or alone in a clade. This is consistent with *N. olivacea* having adapted to a freshwater environment as a result of, for example, a marine overwash event. Of the nine other genera included in the molecular analysis, *Dolichomastix*, *Mamiella*, *Pseudoscourfieldia* and *Tetraselmis* appeared as the sister clade of *Nephroselmis*.

Contents

List of Tables

List of Figures

For Lesley and Keith

"But morphology is a much more complex subject than it at first appears"
— Charles Darwin (1872: 385)

Chapter 1

Introduction

1.1 Identification and Classification

Historically, nanoplankton[1] species have not enjoyed prominence when identifying marine organisms, often being dismissed on species lists as "unidentifiable flagellates" (Tomas, 1997). Identification typically requires detailed microscopy (dissecting, compound, scanning and transmission), access to live cultures and adequate preservation techniques (Tomas, 1997; Graham and Wilcox, 2000). Identification can also be difficult as no definitive, global key exists for all algal species (Graham and Wilcox, 2000), although web-based keys[2] are becoming more popular, as are online databases of algae, such as the one maintained by Guiry and Guiry (2008). The term "algae", in its historical sense, encompasses a wide range of unicellular organisms and is certainly not a phylogenetically valid term. Accurate identification can only be achieved by careful observation of features and structures at both the light and electron microscope level (Tomas, 1997). In most cases, a suite of features is required in order to arrive at an accurate species-level identification. It is becoming increasingly important to accurately identify species, particularly with regard to environmental changes and the understanding of species successions (Tomas, 1997). The challenges presented by conservation and biodiversity issues as well as harmful toxic algal blooms rely on accurate species identifications (Tomas, 1997). Furthermore, the compilation of distribution data requires accurate identification of species. It is estimated that all the algal species described to date (approximately 36,000) represent only 10% of the total number of species (John and Maggs, 1997).

1.2 The Class Prasinophyceae

The kingdom Viridiplantae *sensu* Cavalier-Smith (1981) is a monophyletic lineage of eukaryotes, consisting of the phylum Streptophyta (the true land plants[3] and several green algal lines which were previously considered part of the Charophyceae) and the phylum Chlorophyta (the "green algae") (Nayakama *et al.*, 1998; Marin and Melkonian, 1999). Synapomorphic characters of the Viridiplantae include a chloroplast with a double membrane, containing chlorophyll *a* and *b*, stacked thylakoids, interplastidial starch and "stellate structure"-type flagellar transition region (Melkonian, 1984; Nayakama *et al.*, 1998).

[1] Plankton in the size range 2 – 20μm (Sieburth, 1979).

[2] Examples (accessed 13 September 2007): *http://silicasecchidisk.conncoll.edu/Algal-ED_finished.html* and *http://www.phycology.net/Content/PNetContent.cfm?MID=133*

[3] Embryophytes, the non-vascular bryophytes, and the vascular pteridophytes and spermatophytes.

The Chlorophyta – photosynthetic aquatic flagellates, most of which are unicellular – comprise four classes: the Chlorophyceae, the Prasinophyceae, the Trebouxiophyceae and the Ulvophyceae.

The name Prasinophyceae [originally termed "Prasinophycinées" by Chadefaud (1960)] is derived from "prasinos", the Greek word for "green", rather than from the genus *Prasinocladus* (Moestrup and Throndsen, 1988) as Mattox and Stewart (1984) incorrectly suspected. The class Prasinophyceae very loosely can be defined as "green flagellates with scales". The group is considered to be the most primitive of the green algae and to have given rise to all other classes of green algae and the true land plants (Sym and Pienaar, 1993). That is, they are considered ancestral to the Streptophyta and the rest of the Chlorophyta (Nayakama *et al.*, 1998; Marin and Melkonian, 1999). Scaly green flagellates are located in a basal position within the Chlorophyta [Norris (1980); Steinkötter *et al.* (1994); see others in Steinkötter *et al.* (1994)]. However, the prasinophytes, represented by *Tetraselmis*, did not appear in a basal position in a ribosomal study of eukaryotes (Lipscomb *et al.*, 1998). However, as only one genus from the prasinophytes was included in the study, the results may not be very robust. Additionally, *Tetraselmis* is an atypical prasinophyte in that it produces a theca and appears only distantly related to the prasinophytes (Steinkötter *et al.*, 1994).

Cladistic analyses of nuclear-encoded small-subunit (SSU) 18S and 26S ribosomal RNA (rRNA) sequence data have shown that the class Prasinophyceae [termed Micromonadophyceae *sensu* Mattox and Stewart (1984) by Kantz *et al.* (1990)] is not monophyletic (Kantz *et al.*, 1990; Steinkötter *et al.*, 1994). This was confirmed by Nayakama *et al.* (1998) who report that the prasinophytes are paraphyletic or even polyphyletic. Phylogenetic analyses of 18S rRNA sequences from other scaly green flagellates are needed in order to determine whether the origin of this class is polyphyletic or paraphyletic (Steinkötter *et al.*, 1994). Despite this, Moestrup (1991) proposed that the class may deserve the status of a phylum (Prasinophyta).

The class is diverse, exhibiting a wide variety of forms. All members are unicellular, with the cell body and flagella covered by non-mineralized organic scales (Melkonian, 1990). No characters have yet been discovered which unite all prasinophytes and also exclude other green algae and other algal classes (Steinkötter *et al.*, 1994; Nayakama *et al.*, 1998). This is not surprising, as the group is not monophyletic. Lists of diagnostic characters for the class have been suggested, however; a summary of these is provided in Table 1.1. Moestrup and Throndsen (1988) define the class by the presence of hair scales on the flagella and very long basal bodies, although they note that *Mesostigma* lacks hair scales. *Mesostigma* has subsequently been designated the type genus for the class Mesostigmatophyceae Marin *et* Melkonian within the phylum Charophyta (Marin and Melkonian, 1999). The presence of scales has also been suggested as a feature supporting delineation at the class level (Manton and Parke, 1960), but naked flagellates such as *Micromonas* and *Scourfieldia* have subsequently been placed into the Prasinophyceae as a result of pigment studies or very long basal bodies being present (Moestrup, 1991). Other exceptions exist, such as the flagella of the genus *Prasinopapilla* Inouye gen. ined. arising from an anterior papilla rather than from a flagellar pit (Sym and Pienaar, 1993; Daugbjerg *et al.*, 1995). Further exceptions are *Tetraselmis* and *Scherffelia*, the only genera in the class to posses thecae (compact cells walls) which are formed by the fusing of body scales. Extensive details of exceptions are provided by Sym and Pienaar (1993). Many of the features previously considered as diagnostic of the class Prasinophyceae (such as scales, flagellar pits, long basal bodies and parallel basal bodies) are now considered to be symplesiomorphic characters, as they are found in other green algal groups (Steinkötter *et al.*, 1994).

Table 1.1. Summary of features of the class Prasinophyceae

From Manton and Parke (1960); Moestrup and Throndsen (1988); Melkonian (1990); Sym and Pienaar (1993); Steinkötter *et al.* (1994); Daugbjerg *et al.* (1995).

Feature	**Exceptions**
Scales (made in the Golgi apparatus) composed of at least one of the three 2-keto sugar acids (KDO, 5-OMeKDO and DHA).	*Micromonas*, *Scourfieldia* (naked) *Tetraselmis*, *Scherffelia* (theca/cell wall)
Hair-scales (tubular flagellar hairs) occur in two opposite rows along the flagella.	*Mesostigma* [Now a charophyte (Marin and Melkonian, 1999)]
Pigments include chlorophyll *a* and *b*, Mg2,4D, xanthophylls (prasinoxanthin, siphonein, lutein, violaxanthin and neoxanthin). Siphonaxanthin has recently been reported in *Nephroselmis* (Yoshii *et al.*, 2005; Yoshii, 2006).	
Flagellated stages which are capable of division.	*Tetraselmis*, *Scherffelia*
Flagella inserted in localized cell depression (flagellar pit).	*Prasinopapilla*
Blunt-ended flagella tips.	*Mantoniella*
Basal bodies (kinetosomes) usually parallel, greater than 500nm (600–900nm), held together by at least a distal and proximal connective, in a counterclockwise absolute configuration, with microtubular roots attached at least to basal body 1; basal apparatus is usually asymmetric.	*Tetraselmis*, *Scherffelia*
Parabasal Golgi bodies (located near the basal bodies).	
Chloroplast is single, cup-shaped, with the open end orientated towards the flagella pole.	*Tetraselmis*, *Pyramimonas cyrtoptera*
Pyrenoid present	*Scherffelia*, *Bathycoccus*
Pyrenoid located opposite the flagella and variably surrounded by starch.	*Mantoniella*
Nucleus located laterally and associated with a well-developed system II fibre (rhizoplast) which runs between the basal apparatus and the chloroplast plasmalemma.	*Tetraselmis*, *Scherffelia*
Mannitol possibly the principle soluble carbohydrate.	
Extrusomes present.	

Members of the Prasinophyceae are found in symbiotic relationships with a wide variety of other organisms. The marine flatworm *Convoluta roscoffensis* Graff provides the specific name for its symbiont, *Tetraselmis convolutae* (Parke & Manton) Norris *et al.* (Parke and Manton, 1967), as is the case with the dinoflagellate *Noctiluca scintillans* (Macartney) Koifoid *et* Swezy (= *Noctiluca miliaris* Suriray) and its symbiont *Pedinomonas noctilucae* (Subrahmanyan) Sweeney (Sweeney, 1976). The radiolarian *Thalassolampe margarodes* Haeckel and *Pedinomonas symbiotica* M. Cachon & Caram share a symbiotic relationship (Cachon and Caram, 1979). An unidentified strain of *Nephroselmis* has recently been shown to be a symbiont of the katablepharid *Hatena arenicola* Okamoto *et* Inouye (Okamoto and Inouye, 2005, 2006). *Hatena* appears to be highly selective, only forming a symbiotic relationship with a particular strain of *Nephroselmis* (Okamoto and Inouye, 2006). The prasinophyte *Ostreococcus tauri* C. Courties & M.-J. Chrétiennot-Dinet is the smallest known eukaryote, with cell dimensions of less than 1μm (Courties *et al.*, 1994; Chrétiennot-Dinet *et al.*, 1995).

Since its creation (Chadefaud, 1960; Christensen, 1962), the class Prasinophyceae has undergone several revisions, for example Chadefaud (1977). Two extensive reviews of the class have been published (Norris, 1980; Sym and Pienaar, 1993) and various classification systems for the class have been provided historically. Sym and Pienaar (1993) review the two main alternative classification systems: that of Moestrup and Throndsen (1988) as modified by Moestrup (1991) and Guillard *et al.* (1991), and that of Melkonian (1990), and nominate to follow the latter system in their paper. The present study will also follow the classification system of the class as proposed by Melkonian (1990). Within this system, the 16 genera belonging to the class Prasinophyceae are divided across the following four orders: Mamiellales (5 genera), Pseudoscourfieldiales (2 genera), Chlorodendrales (2 genera) and Pyraminonadales (7 genera, including *Prasinopapilla* gen. ined.). The order Pseudoscourfieldiales consists of two families, Pseudoscourfieldiaceae (which contains only *Pseudoscourfieldia*) and Nephroselmidaceae (which contains only *Nephroselmis*). A summary of the features of the four orders of the Prasinophyceae is provided in Table 1.2.

1.3 The Genus *Nephroselmis*

The genus *Nephroselmis*, erected by Stein (Figure 1.1) in 1878 (Stein, 1878), is placed in the phylum Chlorophyta, class Prasinophyceae[4], order Pseudoscourfieldiales and family Nephroselmidaceae[5] (Melkonian, 1990; Sym and Pienaar, 1993). The exact number of species within the genus is debatable, although nine are suggested by Suda (2003). The type species is *Nephroselmis olivacea* Stein (Figure 1.2), which is the only known freshwater species in the genus[6]. Interestingly, it is also the only species of the genus in which sexual reproduction has been observed (Suda and Watanabe, 1989; Suda *et al.*, 2004). The eight other species considered to comprise the genus are marine (Suda, 2003). The existence of another nine species is uncertain. In addition to this, four new species have yet to be described formally [S Suda, pers. comm., 2006; possibly one of these four is *Nephroselmis anterostigmatica*, which has been described recently (Nakayama *et al.*, 2007)]. A species

[4]Other classification systems exist, such as the one proposed by Cavalier-Smith (1993, 1998), which places *Nephroselmis* in the class Nephrophyceae within the infraphylum Prasinophytae; Nakayama *et al.* (2007) propose the new order Nephroselmidales and rename the class to Nephroselmidophyceae.

[5]The GenBank database (Benson *et al.*, 2005) uses family Pycnococcaceae.

[6]Three other freshwater species have been reported (*N. discoidea*, *N. ellipsoidea* and *N. hemisphaerica*), but these are considered unconfirmed in the present study. See Section 3.7 for a discussion of these species.

Table 1.2. Summary of the four orders of the class Prasinophyceae

Reformatted from Sym and Pienaar (1993)

<table>
<tr><th colspan="6">Mamiellales</th></tr>
<tr><td colspan="6">A-, uni- or biflagellate; backward swimmers; primitive;
Only two microtubular roots attached to one of the basal bodies;
Persistent interzonal spindle during mitosis</td></tr>
<tr><td colspan="3">Mamiellaceae
Scaled flagellates or non-flagellates</td><td colspan="3">Micromonadaceae
Naked flagellates</td></tr>
<tr><td colspan="3">Dolichomastix, Mamiella, Mantoniella, Bathycoccus</td><td colspan="3">Micromonas</td></tr>
<tr><th colspan="6">Pseudoscourfieldiales</th></tr>
<tr><td colspan="6">Biflagellate with flagellar (undulatory) movement;
Two flagellar scale layers: pentagonal under layer and rod-like/stellate outer layer;
Three microtubular roots; persistent interzonal spindle during mitosis</td></tr>
<tr><td colspan="3">Pseudoscourfieldiaceae
Same scale types on body and flagella</td><td colspan="3">Nephroselmidaceae
Rod-like scales of flagella replaced by stellate*
type on cell body; additional layers possible</td></tr>
<tr><td colspan="3">Pseudoscourfieldia</td><td colspan="3">Nephroselmis</td></tr>
<tr><th colspan="6">Chlorodendrales</th></tr>
<tr><td colspan="6">Quadriflagellate; ciliary (breast-stroke) movement; non-motile during division; advanced;
Four cruciately arranged roots (X-2-X-2); same flagellar scales as Pseudoscourfieldia;
Body covering thecate (derived from fused stellate scales); phycoplast; metacentric spindle</td></tr>
<tr><td colspan="6">Chlorodendraceae</td></tr>
<tr><td colspan="6">Scherffelia, Tetraselmis</td></tr>
<tr><th colspan="6">Pyramimonadales</th></tr>
<tr><td colspan="6">Quadriflagellate (motiles); four cruciately arranged roots;
Complex scaly covering (three body, two flagellar); transitional helix/coiled fibre;
Characteristic rhizoplast/nucleus/microbody/chloroplast association</td></tr>
<tr><td colspan="2">Pterospermataceae
Phycoma formers; flagellar
movement; backward swimmers;
Scale forms shared by
the Mamiellales and
the Pyramimonadaceae</td><td colspan="2">Pyramimonadaceae
Structurally complex;
4, 8 or 16 flagella;
MLS possible</td><td colspan="2">Mesostigmataceae†
Atypical features; MLS present;
compressed in longitudinal
axis; four cruciate roots; only
one layer of flagellar scales;
naviculoid and basket-like
body scales</td></tr>
<tr><td colspan="2">Pterosperma, Tasmanites</td><td colspan="2">Halosphaera, Pyramimonas,
Cymbomonas, Prasinopapilla</td><td colspan="2">Mesostigma†</td></tr>
</table>

* The stellate type here is replaced by Maltese cross or paper windmill scales in some species.

† Now considered to belong to the charophytes (Marin and Melkonian, 1999).

MLS = multilayered structure.

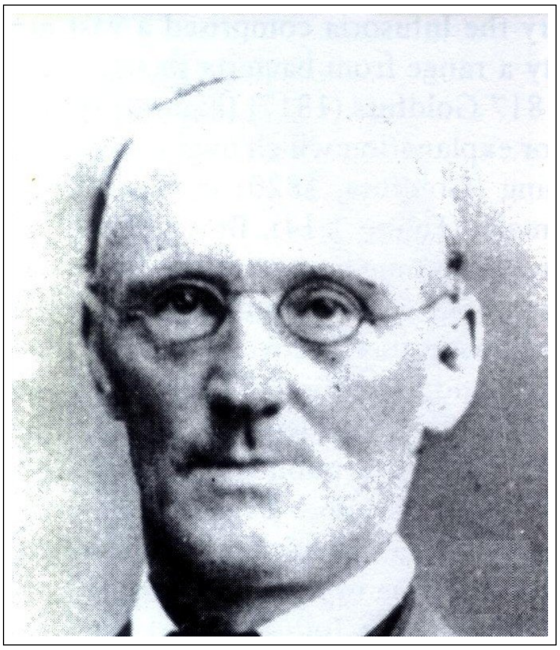

Figure 1.1. *Friedrich Ritter von Stein (1818–1885), reproduced from Leadbeater and McCready (2000: Figure 10). Stein's four illustrated volumes produced during his time at the German-speaking University of Prague are still held in high regard (Leadbeater and McCready, 2000).*

list for *Nephroselmis*, including confirmed and unconfirmed species, is provided in Table 1.3.

The original description of *Nephroselmis* by Stein (1878) (reproduced in the legend to Figure 1.2) consists of only a very brief description focusing on cell shape and movement, providing no morphological or ultrastructural details. Stein does provide a number of drawings of the cell. A subsequent description of the type species by Bütschli (1884) describes the cell shape, flagella and details of collection sites, and reports that there is only one species in the genus. The diagrams included in Bütschli (1884) are reproductions of Stein's originals. Bourrelly (1951) provides a more detailed morphological description of the type species, including details of movement and collection sites. Original drawings are included. A thorough and detailed study of members of the genus was undertaken by Manton *et al.* (1965), including the species which was to become known as *N. rotunda*. Fott (1971) reports several species of *Nephroselmis* and includes original drawings. Brief mention is made of *N. discoidea* and a drawing is provided. A detailed list of references is included in the emended description of the definitive investigation of the type species (Moestrup and Ettl, 1979). The independent work of two authors resulted in the formal recognition of the new combination *N. pyriformis* (Ettl, 1982; Moestrup, 1983, 1984b). Five new species of *Nephroselmis* have been reported in the last quarter of a century (Inouye and Pienaar, 1984; Inouye *et al.*, 1991; Young, 1991; Suda, 2003; Nakayama *et al.*, 2007). However, *N. viridis* (Inouye *et al.*, 1991) has not been formally described and the existence of *N. gaoae* (Tseng *et al.*, 1994) is questionable[7]. Suda (2003) includes the characteristics of the genus as reported by Inouye and Pienaar (1984). Nakayama *et al.*

[7] Morphological information from the original description was insufficient to provide a full data set for morphological cladistic analysis. See Section 3.7.3.

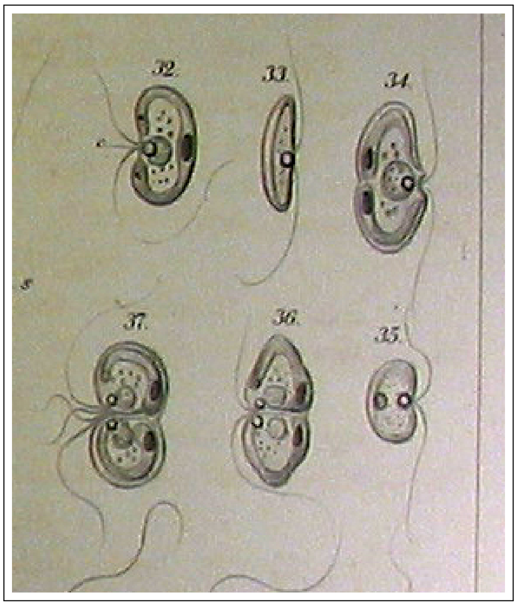

Figure 1.2. *Original drawings of* Nephroselmis olivacea *from Stein's description of the genus* Nephroselmis*, reproduced from Stein (1878: Plate 19). Sub-figure 32 shows the cup-shaped chloroplast, the nucleus with nucleolus and the ventral pyrenoid. The structure between the two flagella in this figure is a label line. Curiously, two eyespots are shown – one under each flagellum. The figure is redrawn with two eyespots in Bütschli (1884) and Moestrup and Ettl (1979). Possibly this cell was about to undergo division, as sub-figures 34, 36 and 37 show a dividing cell. Stein's original species description consisted of the following:* The animal moves in the direction of the longer body axis, usually swimming on the broad side, often turning around the longitudinal axis.

(2007) propose the creation of a new order (Nephroselmidales) within the renamed class Nephroselmidophyceae of Cavalier-Smith (1993). As this proposed classification system is very recent (2007) and has not been discussed in the literature, it will not be followed in the present study.

Only one attempt has been made to provide distinguishing characters for the genus. The proposal of Inouye and Pienaar (1984) is as follows:

1. A bean-shaped, flattened cell
2. Two heterodynamic, unequal flagella
3. A swimming action in which the short flagellum is directed forwards, with the long flagellum trailing.
4. A third layer of flagellar scales or flagellar pit scales.
5. Two to four layers of body scales, with the second layer of scales having a Maltese cross or paper windmill shape.
6. A flagellar root system which consists of only three microtubular roots (one of which is multilayered) and a rhizoplast.

The convoluted taxonomic history of the genus raises the question of whether all those species currently considered as belonging to the genus *Nephroselmis* form a monophyletic group – that they are all in fact sufficiently similar to each other as to be considered a genus.

1.4 Distribution

Distribution data for *Nephroselmis*, gathered from the literature and opportunistic sampling, are presented in Figure 1.3. Absence of data for particular regions does not necessarily infer the absence of the organism from that area, but rather the absence of sampling, or an inability to demonstrate the existence of an organism even when it is present. The genus appears to be cosmopolitan, although there is a paucity of sampling data from the tropics and South America particularly. *Nephroselmis* samples have also been recorded from the following marine locations: Kenton on Sea (South Africa), Hout Bay (South Africa), St James (South Africa), Inhaca Beach and Rock Pool (South Africa), Amanzimtoti (South Africa), Kewalo Yacht Club Basin (Hawaii) (SD Sym, pers. comm., 2006). *Nephroselmis* was not found in many samples taken from a variety of marine locations during the course of the present study[8].

1.5 Morphological and Ultrastructural Features

The following morphological and ultrastructural features are generally accepted as useful when investigating the relationship between algal species and are used extensively in the literature [for example, Moestrup and Ettl (1979); Inouye and Pienaar (1984); Sym and Pienaar (1993); Suda (2003); Nakayama *et al.* (2007)].

[8]Camp's Bay Beach, South Africa (GV Cron, March 2006); Nature's Valley Beach, South Africa (GV Cron, April 2006); Durban Beach, South Africa (SD Sym, May 2006); Mtimzini Beach, South Africa (B Maritz, June 2006); Lerai Forest (Ngorongoro Crater), Tanzania (TG Bell, July 2006) (freshwater); Mnemba Island Beach (West), Zanzibar (LH Bell, July 2006); Zanzibar Island (East), Zanzibar (TG Bell, July 2006); Cape Vidal Beach, South Africa (C Marangoni, September 2006) and Fish Hoek Beach, South Africa (KN van Wyk, January 2007).

Table 1.3. List of *Nephroselmis* species

Species	Authority	Reference
CONFIRMED SPECIES: Electron microscopy and species descriptions available		
*Nephroselmis anterostigmatica**	Nakayama, Suda, Kawachi & Inouye	Nakayama *et al.* (2007)
*Nephroselmis astigmatica**	Inouye & Pienaar	Inouye and Pienaar (1984)
*Nephroselmis olivacea**	Stein em. Moestrup & Ettl	Stein (1878); Moestrup and Ettl (1979)
*Nephroselmis pyriformis**	(Carter) Ettl	Carter (1937); Ettl (1982); Moestrup (1983)
*Nephroselmis rotunda**	(Carter) Fott	Carter (1937); Manton *et al.* (1965); Fott (1971)
*Nephroselmis spinosa**	Suda	Suda (2003)
Nephroselmis viridis sp. ined.*	Inouye, Suda & Pienaar	Young (1991)
UNCONFIRMED SPECIES: Dubious or absent microscopy and/or no detailed species descriptions		
Nephroselmis discoidea	Skuja	Skuja (1948); Ettl (1983)
Nephroselmis ellipsoidea	(Skvortzov) Bourrelly	Bourrelly (1972); Ettl (1983)
Nephroselmis hemisphaerica	(Skvortzov) Bourrelly	Bourrelly (1972); Ettl (1983)
Nephroselmis fissa	(Lackey) Inouye & Pienaar	Lackey (1940); Inouye and Pienaar (1984)
*Nephroselmis gaoae**	Tseng & Chen	Tseng *et al.* (1994)
Nephroselmis marina	Schiller	Schiller (1926)
Nephroselmis minuta	(Carter) Butcher	Carter (1937); Butcher (1959)
Nephroselmis olivana		Schiller (1926)
NEW		
Nephroselmis spp. (at least 4)		S Suda (pers. comm., 2006)

* Detailed ultrastructural studies exist (excluding the present study)

The taxonomic confusion which exists within the genus is illustrated by the following: The *Species Accounts* website[a] reports that *Nephroselmis* consists of the following species: *N. astigmatica*, *N. intermedia* [now officially described as *N. anterostigmatica*], *N. minuta*, *N. olivacea*, *N. pyriformis*, *N. spinosa* and *N. viridis*, whereas the *AlgaeBase* website (Guiry and Guiry, 2008) lists the following species, which include synonyms (although they are marked as "provisional"): *N. angulata* (Korshikov) Skuja [synonym for *N. olivacea*], *N. astigmatica* [Inouye and] Pienaar, *N. discoidea* f. *astigmata* Preisig [the only reference to this species], *N. discoidea* Skuja, *N. fissa* Lackey, *N. longifilis* (Butcher) Morris [now *N. pyriformis*], *N. marina* Schiller, *N. minuta* (N. Carter) Butcher, *N. olivacea* F. Stein, *N. pyriformis* (N. Carter) Ettl, *N. rotunda* (N. Carter) Fott, *N. spinosa* Suda and *N. violacea* Kufferath [now *Chroomonas violacea*; see Section 3.8.2].

[a] *http://www.speciesaccounts.org/Green%20algae%20and%20plants.htm*, accessed 27 June 2007

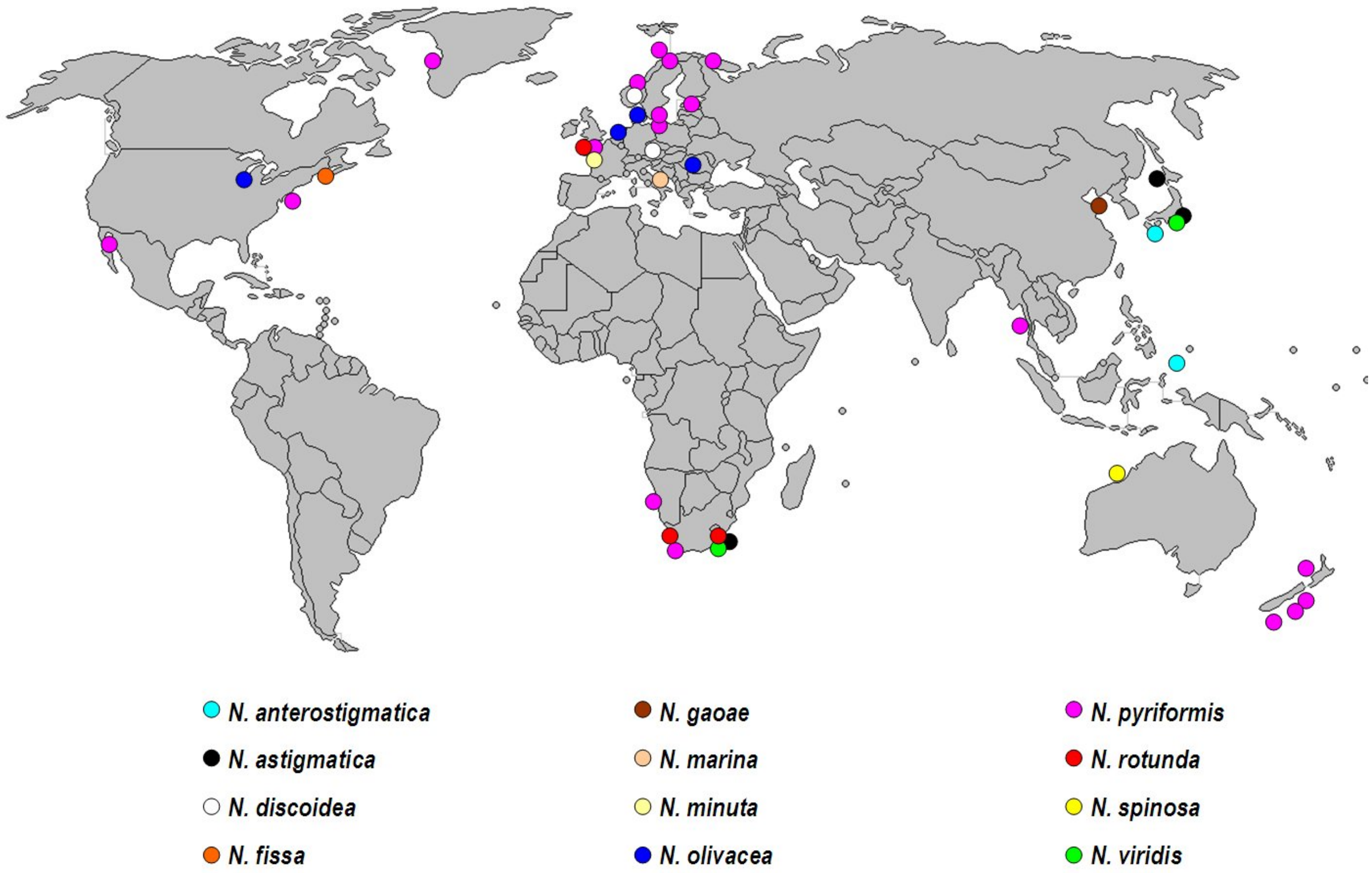

Figure 1.3. *Distribution map for* Nephroselmis *species. Locations and references for each datum point are provided in Table 1.4.*

Table 1.4. Locations and references for *Nephroselmis* distribution data presented in Figure 1.3

Sample	Locations	Reference
Nephroselmis anterostigmatica	Palau Islands (Republic of Palau); Saeki port, Oita Prefecture (Japan)	Nakayama *et al.* (2007)
Nephroselmis astigmatica	Durban, South Africa; Izu and Teshio, Japan	Inouye and Pienaar (1984)
Nephroselmis discoidea	Czechoslovakia (large ponds) and Sweden (lakes) (	Ettl (1983)
Nephroselmis fissa	Woods Hole, Cape Cod	Lackey (1940)
Nephroselmis gaoae	Qingdao, China	Tseng *et al.* (1994)
Nephroselmis marina	Adriatic Sea	Schiller (1926)
Nephroselmis minuta	Isle of Wight	Carter (1937)
Nephroselmis olivacea	Denmark; Grand River (Lake Michigan)	Moestrup and Ettl (1979)
Nephroselmis olivacea	Belgium; Kharkov, Ukraine	Butcher (1959)
Nephroselmis pyriformis	Isle of Wight	Carter (1937)
Nephroselmis pyriformis	Denmark; England; Finland; Norway; Mexico	Moestrup (1983)
Nephroselmis pyriformis	Godhavn, West Greenland; North Carolina, USA	Moestrup (1983)
Nephroselmis pyriformis	Phuket Island, Thailand; River Tamar (Cornwall / Devon)	Moestrup (1983)
Nephroselmis pyriformis	Wellington Harbour, New Zealand	Moestrup (1983)
Nephroselmis rotunda	Cornwall / Devon, UK	Butcher (1959)
Nephroselmis rotunda	Isle of Wight	Carter (1937)
Nephroselmis rotunda	Ryde and Yarmouth, Isle of Wight	Butcher (1959)
Nephroselmis spinosa	Port Hedland and Hamerin Pool, Western Australia	Suda (2003)
Nephroselmis viridis sp. ined.	Durban, South Africa; Japan	Young (1991)
Nephroselmis pyriformis	Collected from Fish Hoek via RN Pienaar, August 2006 Isolated by TG Bell, September 2006	Wits Internal Collection FH01
Nephroselmis pyriformis	Collected 60 nautical miles offshore at 23°S (Swakopmund) by DC Louw, 15 May 2006; Isolated by TG Bell, June 2006	Wits Internal Collection WW02
Nephroselmis rotunda	Collected from Langebaan Mouth and isolated by SD Sym, April 1989	Wits Internal Collection AA15
Nephroselmis rotunda	Collected from Palm Beach and isolated by SD Sym, May 1989	Wits Internal Collection BB2

1.5.1 Flagellar Apparatus

The flagellar apparatus of green algae is both biochemically and structurally complex and is potentially of great systematic value (Melkonian, 1984). Flagella are thought to be ancient structures, probably predating the acquisition of the chloroplast and mitochondrion, and this long evolutionary history may explain their structural complexity (Melkonian, 1984). Three major components together comprise the flagellar apparatus in green algae: (a) the flagellum proper, (b) the basal body and (c) the associated structures of the basal body (Melkonian, 1982).

1.5.1.1 The Flagellum

The flagellum consists of the flagellar membrane and its associated extracellular surface components, and the central axoneme (with a "9 + 2" arrangement of microtubule doublets) which is embedded in the flagellar matrix (Melkonian, 1984). Three regions may be distinguished along the length of a flagellum: the flagellar tip, the flagellar shaft and the transition region, which links the external region of the flagellum with the internal components (Melkonian, 1984). Evidence suggests that the "9 + 2" axoneme and the 9x3 microtubule arrangement of the basal bodies have arisen in eukaryotic cells only once (Moestrup, 2000).

The Flagellar Tip The flagellar tip is considered to be the area of the flagellum between the end of the peripheral doublets and the end of the flagellum (Melkonian, 1984). The flagellar tip may be an important character to consider when classifying green algae (Melkonian, 1984). The structure of the flagellar tip varies across green algal taxa and may be either pointed ("hair-point") or blunt (Inouye, 1993). The central pair of microtubules of hair-point flagellar tips extend towards the tip of the flagellum (at the membrane) while the peripheral doublets terminate distal to the membrane (Inouye, 1993). All scaly flagella have blunt tips (Melkonian, 1984), including those of *Nephroselmis*. Thin sections rather than whole mounts should be used to determine whether hair-point or blunt tips are present in a particular specimen (Melkonian, 1984). Special types of flagellar hairs (either tubular or non-tubular) may be associated with the flagellar tip region (Melkonian, 1984), although specialized flagellar tip scales are absent in species of *Nephroselmis* examined by Marin and Melkonian (1994).

The Flagellar Shaft The flagellar shaft comprises the surface scales, the membrane, the axoneme and the matrix (Melkonian, 1984). Flagellar scales are a distinctive and taxonomically useful feature within the prasinophytes, with some species such as *Nephroselmis olivacea* exhibiting several distinct scale layers (Melkonian, 1984). Hair-like structures, termed flagellar hairs or hair scales, may also be present on the surface of the flagellum. These hairs may be tubular (as in *Nephroselmis*) or non-tubular (Moestrup, 1982). The ultrastructure of flagellar hairs may be of phylogenetic value (Marin and Melkonian, 1994). The claim by Moestrup (1982) that prasinophytes are effectively isokont because there is no difference in the structure or distribution of flagellar hairs across flagella within any species of this group has been shown to be incorrect by Marin and Melkonian (1994), who report on the structure of several different types of hair scales. Flagellar hairs in green algae are attached to the B-tubule of doublets 4 and 8, the hairs therefore extending outwards perpendicular to the plane of flagellar beating (Melkonian, 1984; Inouye, 1993).

The Transition Region The transition region is considered to be that region of the flagellum between the basal body and the flagellar shaft itself (Moestrup, 1982). Six different transition region structures have been identified, with the prasinophytes possessing what is termed a "stellate pattern" (Moestrup, 1982). This pattern is created by filaments extending from each tubule of the outer axonemal doublet (Melkonian, 1984). The transition region often appears as an "'H"-shaped structure in longitudinal sections (Inouye, 1993). The filaments of the stellate pattern are arranged in a helix, with two or three full turns required to complete a full stellate pattern (Melkonian, 1984). The stellate structure may be single or bipartite in the prasinophytes (Sym and Pienaar, 1993). The position of the transitional plate (septum) differs between species of *Nephroselmis*: the plate is distal to the stellate structures in *N. olivacea*, whereas the plate occurs between the two stellate structures in *N. astigmatica* and *N. rotunda* (Moestrup, 1982; Melkonian, 1984; Sym and Pienaar, 1993). An additional transitional plate above the stellate structures has been reported in two strains of *N. olivacea* (Mattox and Stewart, 1977; Moestrup and Ettl, 1979). A "coiled fibre" structure on the inside of the peripheral doublet is absent in *N. olivacea* (Moestrup and Ettl, 1979; Moestrup, 1982) but may be present in *N. rotunda* (Manton *et al.*, 1965; Sym and Pienaar, 1993).

1.5.1.2 Basal Bodies

Basal bodies are cylinders of microtubule triplets, located inside the cell and proximal to the transition region of the flagellum, which are continuous with the microtubule doublets of the axoneme (Melkonian, 1984). The basal body gives rise to the axoneme of the flagellar proper and is continuous with it (Melkonian, 1984). Scaly green flagellates are considered to have long basal bodies, regardless of the actual size of the cell itself – no prasinophyte has a basal body length of less than 500nm (Melkonian, 1984). This finding led Melkonian (1984) to conclude that ancestral green algae had long basal bodies and therefore proportionately short transition regions. The length of basal bodies, therefore, is suggested as a useful systematic character (Melkonian, 1984). Basal bodies may contain a variety of specific inclusions (Moestrup, 1982). The basal bodies of *Nephroselmis rotunda* contain ribosomes (Manton *et al.*, 1965; Moestrup, 1982), whereas those of *Nephroselmis olivacea* do not (Moestrup, 1982). As mentioned in Table 1.1, the basal bodies of prasinophytes are considered to be parallel (or near-parallel) and are positioned in the cell parallel to the direction of motions (Sym and Pienaar, 1993). Exceptions to this can found in several genera, including *Nephroselmis*, in which the basal bodies are aligned between 45° and 120° relative to each other (Moestrup and Ettl, 1979; Inouye and Pienaar, 1984; Sym and Pienaar, 1993).

1.5.1.3 Associated Structures of the Basal Body

Any structures which are attached to the microtubule triplets of the basal body (such as connecting fibres or flagellar roots) are considered associated structures of the basal body (Melkonian, 1984). Connecting fibres and flagellar roots are fibrillar or microtubular structures which may be banded or plate-like (Melkonian, 1984). Connecting fibres interconnect basal bodies and are fibrillar in structure (Moestrup, 1982). A thick distal connecting fibre (previously termed a synistosome), which may be striated in some taxa, connects the distal ends of basal bodies 1 and 2 (Inouye, 1993; Sym and Pienaar, 1993).

Flagellar roots are attached to basal bodies and terminate elsewhere in the cell (Melkonian, 1984). Two types of roots are found in flagellated cells, namely "ascending" (Manton, 1966) or "superficial" microtubular roots, which extend from the basal bodies, run under the plasmalemma, and terminate in the cytoplasm, and "internal" or "deep" (Manton, 1966) roots ("rhizoplasts" (Norris, 1980) or System II fibres), which penetrate into the cell and come into contact with various organelles (Moestrup, 1982; Sym and Pienaar, 1993). In *Nephroselmis*, the long flagellum (the oldest) is numbered "1" and the short flagellum is numbered "2" (Moestrup, 2000). The roots associated with the basal body of the long flagellum are termed "1d" (the right root) and "1s" (the left root) (Inouye, 1993). Similarly, the roots associated basal body number 2 are termed "2d" and "2s" roots. Typically, each basal body has two associated microtubular roots (Melkonian, 1984), with a different number of microtubules present in each of the two roots (Sym and Pienaar, 1993). The root system of some biflagellates consists of only two roots in total, as no roots are associated with one of the basal bodies (Melkonian, 1984). Exceptions to this general rule are found in *Pseudoscourfieldia marina* (Moestrup and Throndsen, 1988) and *Nephroselmis* (Moestrup and Ettl, 1979; Inouye and Pienaar, 1984), where only three roots in total are found, consisting, in *Nephroselmis olivacea* for example (Moestrup and Ettl, 1979), of three, four and seven to eleven [twelve in *Nephroselmis astigmatica* (Inouye and Pienaar, 1984)] microtubules in roots 1d, 1s an 2d respectively (Moestrup and Ettl, 1979; Moestrup, 1982; Sym and Pienaar, 1993). Thus, *Pseudoscourfieldia* and *Nephroselmis* lack the 2s root (Sym and Pienaar, 1993). The four microtubular roots of green algae are typically arranged in a "cruciate" pattern, with the number of microtubules recorded as X-2-X-2 (Moestrup, 1978). The "X" indicates a variable number of microtubules in the "s" roots and the "2" indicates two microtubules occur in the "d" roots (Sym and Pienaar, 1993).

The single root of the second basal body in *Nephroselmis* (that is, the 2d root) is associated with the eyespot (Moestrup and Ettl, 1979; Melkonian and Robenek, 1984; Moestrup, 2000). This association is lacking in other prasinophytes, where the position of the eyespot may vary, even between species of the same genus (Moestrup, 2000). An association exists between the other root (the 2s root) of the second basal body and the eyespot in more advanced green algae (Moestrup, 2000).

System II fibres have been observed in association with the 1d root in *Nephroselmis olivacea* (Melkonian, 1984) as well as in other genera (Sym and Pienaar, 1993). A multilayer-like structure has been reported in association with the 2d root of *Nephroselmis olivacea* (Moestrup and Ettl, 1979) and *Nephroselmis astigmatica* (Inouye and Pienaar, 1984). System II fibres, containing the contractile protein centrin, extend into the cell to the nucleus (Sym and Pienaar, 1993).

1.5.2 Flagellar Scales

With the exception of the Mamiellales *sensu* Moestrup and Throndsen (1988), the flagella of almost all other prasinophytes are covered by an underlayer of small pentagonal scales (Sym and Pienaar, 1993). In the Chlorodendrales *sensu* Melkonian (1990), the underlayer scales are interspersed with small scales which resemble a human figure (Sym and Pienaar, 1993). These scales have been described previously as "rod" scales (Moestrup and Ettl, 1979) and "man" scales (Becker *et al.*, 1990). The only exception in the Chlorodendrales is *Nephroselmis rotunda*, in which small stellate scales replace the "rod" scales (Manton *et al.*, 1965). An additional layer of stellate scales comprising a small distal curved spine directed towards the flagellar tip and several proximal roots has been described in *Nephroselmis olivacea* (Moestrup and Ettl, 1979). Pit hairs are found in *Nephroselmis astigmatica*, *N. pyriformis* and *Pseudoscourfieldia marina* (Manton *et al.*, 1965; Manton, 1975; Inouye and Pienaar, 1984). Scales, restricted to the flagellar pit and termed "pit scales", may also be present, as in *Nephroselmis astigmatica* (Inouye and Pienaar, 1984).

Flagella hairs (hair scales or lateral hairs), present in almost all prasinophytes, are

Table 1.5. Flagellar hairs in *Nephroselmis* and closely-related species [Marin and Melkonian (1994)]

Species	Tip Hair	Pt-hair	T-hair
Nephroselmis	Absent	Immature flagellum 2	Both flagella
Pseudoscourfieldia marina	Flagellum 1	Immature flagellum 2	Both flagella
Mamiella gilva	Both flagella	Immature flagellum 2	Flagella 1
Mantoniella squamata	Flagellum 1	Immature flagellum 2	Flagella 1

found on the sides of the flagellum (Marin and Melkonian, 1994). Specialized hairs on the tip of the flagellum, termed "tip hairs", are absent in *Nephroselmis*, but are found on flagellum number 1 of *Mantoniella* and *Pseudoscourfieldia*. Two types are flagella hairs are recognized: T (*Tetraselmis*-type) hairs, which are 15 nm in diameter, between 0.5 and 1.3 μ m in length and consisting of a smooth tubular shaft, and Pt (*Pterosperma*-type) hairs, which are 30 nm in diameter and 1.5 to 5.4 μ m in length (Marin and Melkonian, 1994). Pt-hairs are only found on the shorter (number 2) immature flagellum in *Nephroselmis*, *Mantoniella*, *Mamiella* and *Pseudoscourfieldia* (Marin and Melkonian, 1994). T-hairs are found on both sides of both flagella in *Nephroselmis*, while Pt-hairs occur on one side of the short flagellum only. The flagellar hair types found in *Nephroselmis* and closely related species are summarized in Table 1.5.

1.5.3 Body Scales

With only a few exceptions, the cell body of all prasinophytes is covered by scales (Sym and Pienaar, 1993). These non-mineralized scales are composed of acidic polysaccharides with unusual 2-keto sugar acids (Becker *et al.*, 1994). The number of layers of scales ranges from one to five, with a unique morphology being found in each species (Sym and Pienaar, 1993). Apart from the Mamiellales *sensu* Moestrup and Throndsen (1988), small square underlayer scales are found in all scaly prasinophytes (Sym and Pienaar, 1993). A second layer of underlayer scales may also be present, as in *Pyramimonas* and *Nephroselmis* (Sym and Pienaar, 1993). In *Nephroselmis*, these resemble a Maltese cross and a paper windmill in several species. The remaining layers of body scales, termed intermediate and outer layers, show much variation in morphology, ranging from the spider web-like scales of *Cymbomonas*, *Pterosperma* and *Tasmanites* to the open-ended boxes of *Halosphaera* and *Pyramimonas*, and the tiered stellate scales and spines of *Nephroselmis* (Sym and Pienaar, 1993).

1.5.4 Chloroplast and Pyrenoid

With the exception of two species, prasinophytes possess a single parietal chloroplast, with most of the chloroplast material opposite the flagellar insertion point (Sym and Pienaar, 1993). The cup-shaped chloroplast, which has a double-membrane but lacks girdle lamellae, may or may not be lobed (Sym and Pienaar, 1993).

The pyrenoid is a non-membrane-bound region of the chloroplast, rich in the enzyme RuBisCO (ribulose-1,5-bisphosphate carboxylase/oxygenase), in which carbon dioxide fixation takes place (Raven *et al.*, 1992; Whatley, 1993). At least one pyrenoid is found in the chloroplast of all prasinophytes, with the exception of only two genera in which the pyrenoid is absent (Sym and Pienaar, 1993). Starch grains making up a starch sheath of variable size and shape surrounds the pyrenoid (Sym and Pienaar, 1993). The granular matrix of the pyrenoid may be penetrated by single or multiple thylakoids (Whatley, 1993). Thylakoid penetration of the pyrenoid and the structure of the surrounding starch sheath, both of which may be extensive in *Nephroselmis*, are considered to be of taxonomic importance (Sym and Pienaar, 1993). An unusual granular structure, termed a disc or a lens, located between the outer chloroplast surface and the pyrenoid, has been found in *Nephroselmis olivacea* (Moestrup and Ettl, 1979). This structure, which is divided into two layers, lacks thylakoids (Moestrup and Ettl, 1979). A similar structure has been observed in the undescribed species *Nephroselmis viridis* sp. ined. (Sym and Pienaar, 1993).

1.5.5 Eyespot (Stigma)

The eyespot is an area of orange or red pigmentation which is visible at the light microscope level and acts as a photoreceptive organelle which produces two photobehavioural responses: a photophobic (avoidance) response and a phototactic response (Melkonian and Robenek, 1984). Most prasinophytes possess an eyespot, which is always intraplastidial (Sym and Pienaar, 1993). Local specialization of the chloroplast and the plasmalemma make up the "eyespot apparatus", which consists of the eyespot proper (one or several layers of pigmented lipid globules together with specialized thylakoids) and the eyespot membranes (chloroplast envelope and plasmalemma) which cover the eyespot lipid globules (Melkonian and Robenek, 1984). The layer of lipid globules is located directly beneath the inner chloroplast envelope membrane. The outer chloroplast envelope membrane which covers the eyespot lipid globules is always attached to the plasmalemma. The plasmalemma covering the eyespot lipid globules is structurally specialized, consisting of a high density of characteristic intramembrane particles which are 8 nm to 12 nm in size (Melkonian and Robenek, 1984).

In cases where several eyespots occur in a single cell, they are located close to each other or along an axis which is parallel to the plane of the flagellar beat (Melkonian and Robenek, 1984). When eyespots are found on opposite sides of a cell, such cells are always preparing for division. The cross-sectional surface (perpendicular to the plane of the flagellar beat) of an eyespot may be convex, concave or straight. Concave surfaces are typically found in eyespots which consist of more than two globule layers, whereas convex surfaces are typically found in eyespots which consist of only one globule layer (Melkonian and Robenek, 1984). In *Nephroselmis olivacea*, which has a concave eyespot (Moestrup and Ettl, 1979) of approximately circular shape, globules of different sizes are found, but no tight hexagonal packing of these globules occurs (Melkonian and Robenek, 1984). In *Nephroselmis* species, variation in the electron density of eyespot globules occurs within one eyespot – peripheral globules are more electron-dense than central globules (Moestrup and Ettl, 1979; Moestrup, 1983; Melkonian and Robenek, 1984). The distance between the outer chloroplast envelope and the plasmalemma in *Nephroselmis* species is 30 nm to 40 nm (Melkonian and Robenek, 1984).

Tseng *et al.* (1994) mention that the eyespot of *Nephroselmis gaoae* contains rod-like structures and that this feature is sufficient to delineate this sample a new species and is unique among all algal groups. However, rod-like structures have subsequently been reported in the eyespots of two species of *Pyramimonas*: *P. chlorina* Sym and Pienaar (1997: Figure 38) and *P. formosa* Sym and Pienaar (1999: Figure 26).

The location of eyespots is traditionally referred to in relation to the position of the flagellar apparatus (Melkonian and Robenek, 1984). The eyespot position may be in the plane of the flagellar beat or may be displaced a certain number of degrees clockwise or anticlockwise (Melkonian and Robenek, 1984). The eyespot of *Nephroselmis olivacea*, *N.*

rotunda and *N. pyriformis* is located anteriorly under the short flagellum (Melkonian and Robenek, 1984). Different data were reported for *N. olivacea* and *N. angulata* (Melkonian and Robenek, 1984), despite these two samples being the same species (*Heteromastix angulata* = *N. angulata* = *N. olivacea*) (Moestrup and Ettl, 1979). The eyespot is located lateral to the flagellar insertion point and is associated with a unique microtubular flagellar root which is homologous to the two-stranded ("right") root of a X-2-X-2 flagellar root system (Melkonian and Robenek, 1984). The angle of displacement in *N. olivacea* and *N. rotunda* is reported to be between 20° and 30° clockwise (Melkonian and Robenek, 1984). The findings of Moestrup and Ettl (1979) with regard to the association of the eyespot apparatus with microtubular flagellar roots in *N. olivacea* are reported in Table 3 of Melkonian and Robenek (1984): *N. olivacea* does not possess an X-type root, the other root is 12-stranded and the direction and angle of displacement is 20° clockwise. In *Nephroselmis* species, the eyespot is not located in the cleavage plane of the cell (Melkonian and Robenek, 1984).

1.5.6 Golgi Apparatus

The Golgi apparatus in prasinophytes is composed of a variable number of dictyosomes and, with a few exceptions, is involved in scale production (Sym and Pienaar, 1993). The Golgi apparatus is typically located in the proximity of the basal body or the flagellar pit (Sym and Pienaar, 1993).

1.5.7 Mitochondrion

The single, highly reticulated mitochondrion of prasinophytes is typical of that found in green algae (Sym and Pienaar, 1993). A double unit membrane surrounds a lumen which is filled with a finely granular matrix. Typically, the mitochondrion is found lining the inner chloroplast membrane.

1.5.8 Nucleus

The double-membraned nucleus of prasinophytes is typically spherical to pyriform and located close to the basal apparatus, where present (Sym and Pienaar, 1993). A spherical nucleolus is always present. With only a few exceptions, the nucleus is attached to the system II fibres.

1.6 Motility Studies

Swimming in green algae is typically achieved via ciliary-type beating of the flagella, which is termed "breast-stroke" (Inouye and Hori, 1991). However, other groups of green flagellates instead exhibit an undulatory beating pattern (flagellar), starting at the base of the flagellum and extending to the tip. Two swimming patterns are known in algae, one being the normal forward motion pattern and the other being an avoidance response in which the cell changes direction and swims backwards. Flagellar beat and swimming patterns in algae have been used to infer evolutionary trends (Inouye and Hori, 1991). Swimming patterns which make use of both ciliary beats (for forward swimming) and flagellar beats (for forward and backward (avoidance) swimming) are more advanced than those which make use of flagellar beats only. Backwards swimming is more primitive than forward swimming, as all flagellates which are capable of swimming forwards are also capable of swimming backwards (Inouye and Hori, 1991). The diversity of swimming behaviours can be useful in determining phylogenetic relationships (Inouye and Hori, 1991; Sym *et al.*, 2000). The long (trailing) flagellum of the three species of *Nephroselmis* (*N. astigmatica*, *N.* aff. *rotunda* and *N. olivacea*) investigated by Inouye and Hori (1991) showed the typical flagellar beat pattern. The short flagellum of *N. astigmatica* exhibited the typical flagellar beat pattern, but in the other two species, this flagellum showed a ciliary beat pattern (Inouye and Hori, 1991). This is very unusual, as the occurrence of both flagellar and ciliary beat patterns in the same species has not been reported before. The typical flagellar beat pattern was shown during avoidance response in all three species (Inouye and Hori, 1991).

1.7 Cladistics

1.7.1 Cladistic Methodology

One of the purposes of cladistics is to determine which taxa in a group are more closely related to each other than to any other taxon within the group (Funk, 1995). The concept of relatedness in this sense refers to groups sharing uniquely derived characters (apomorphies) which are not present in the other taxa outside the group (Funk, 1995). Cladistic theory (phylogenetic systematics) is concerned primarily with finding monophyletic groups (clades) – that is, groups which share a common ancestor and all descendants of that common ancestor only (Wiley *et al.*, 1993; Funk, 1995). Cladistic methodology will be used to study relationships within the genus *Nephroselmis* and to investigate whether the genus is monophyletic.

Groups which are not monophyletic may be either paraphyletic (the group does not contain one or more descendants of the most recent common ancestor) or polyphyletic (members of the group share some derived character which is not found in other groups from the most recent common ancestor) (Farris, 1974; Oosterbroek, 1987; Wiley *et al.*, 1993). Cladograms are used to represent the "relatedness" graphically, via branching patterns (Funk, 1995). The three central tenets of cladistics, as detailed by Funk (1995), are the following: (1) Apomorphy: Uniquely derived evolutionary characters; synapomorphies are derived characters which are shared by more than one taxon; (2) Parsimony: The simplest explanation from a set of alternatives is the one which should be chosen – that is, the one which requires the least number of character changes and (3) Monophyletic groups.

Characters which are apomorphic are determined by including outgroups into cladistic analyses (Funk, 1995). Outgroups are typically groups which are most closely related to the study group (the ingroup) – that is, sister groups to the ingroup (Funk, 1995). Plesiomorphic characters ("ancestral") are ones which occur in the outgroup and in some taxa of the ingroup. Apomorphic characters are ones which occur in some taxa of the ingroup only and not in the outgroup (Funk, 1995). Corresponding characters in different taxa which are thought to have arisen as a result of the shared ancestry of the two taxa are termed homologous characters (Skelton and Smith, 2002). Such characters, which are thought to have arisen as a result of convergent evolution, are termed homoplasious characters (Skelton and Smith, 2002). These terms are applicable to both molecular and morphological characters.

The robustness of the cladograms that have been constructed is measured via various indices (Funk, 1995). The Consistency Index (CI) is a measure of the proportion of transformations which are not homoplasious (not repeated) (Skelton and Smith, 2002). It is calculated by dividing the minimum number of steps (character transformations) required by the actual number of steps observed (Farris, 1989; Skelton and Smith, 2002). A CI value of 1 indicates the absence of homoplasy (Farris, 1989; Skelton and Smith, 2002). The

Retention Index (RI) measures the degree of synapomorphy present in a character or set of characters on a cladogram (Skelton and Smith, 2002). That is, the retention index is "the fraction of apparent synapomorphy in the characters that is retained as synapomorphy on the tree". (Farris, 1989: 418). The Rescaled Consistency Index (RC) is calculated by multiplying the CI by the RI (Farris, 1989). The RC yields a value of 1 when a character change is considered to be a synapomorphy and a 0 when a synapomorphy is not necessarily implied (Skelton and Smith, 2002).

Characters can be weighted according to prior assumptions regarding the probability of a particular character transformation (*a priori* weighting) (Skelton and Smith, 2002). This method is not often used for molecular characters. *A posteriori* weighting involves reweighting characters according to their level of congruence with other characters (Skelton and Smith, 2002). Character data may also be reweighted successively according to various indices. This procedure assigns a lower weigh to characters which are considered homoplasious (that is, those that do not fit the three well) and a higher weight to characters which support the tree. Reweighting is typically continued until weights do not change between two consecutive analyses or until two identical topologies are found in successive analyses (Swofford and Begle, 1993). This type of reweighting algorithm, provided in *Hennig86*, is also available in *PAUP** (Farris, 1988; Swofford, 2003).,

Confidence limits can be placed on individual branches of a cladogram via the "bootstrapping" method (Funk, 1995). This involves drawing random samples (with replacement) of character information to build many "bootstrap" data sets. These are analysed to produce one or more trees. The level of support for a particular monophyletic group can be determined by the number of times that it appears among the trees from the sample data sets. Consensus trees are used when more than one equally parsimonious tree is produced (Funk, 1995). Two types of consensus trees are commonly used (Funk, 1995): Strict Consensus, in which only groups occurring in all equally parsimonious trees are included and Majority Rule Consensus, in which branching sequences occurring in the majority of the trees are included. In many studies, the true phylogeny is not known and accuracy predictions are based on statistical analyses, congruence studies and computer simulations (Poe and Wiens, 2000).

1.7.2 Morphological versus Molecular Data

Systematics involves the detection, description and explanation of the diversity of the biological world (Moritz and Hillis, 1996). Much debate has taken place regarding the use of molecular and morphological features for phylogenetic purposes and which approach is the better one (Hillis, 1987; Moritz and Hillis, 1996; Baker *et al.*, 1998; De Queiroz, 2000; Hillis and Wiens, 2000; Wiens, 2000). The key question to consider when evaluating the different approaches is whether variation appropriate to the questions posed will be exhibited by the characters used (Moritz and Hillis, 1996). Also worthy of consideration is whether the characters being studied have a clear and independent genetic basis (Moritz and Hillis, 1996). Molecular systematics can be particularly useful in scenarios where only limited morphological variation is present (Moritz and Hillis, 1996) or difficult to characterize.

Character data for a study is either qualitative or quantitative (Swofford *et al.*, 1996). Qualitative data can be either binary (typically used to indicate the presence or absence of a feature) or multistate. Multistate character states may be either ordered or unordered. Wagner Parsimony, which assumes that a transformation from one state to another implies a transformation through all intermediate states, can be applied to characters which are binary, ordered multistate or continuous (Swofford *et al.*, 1996). In contrast, Fitch

Parsimony permits character states to transform from one state to any other state. The characters used in cladistic analyses can be weighted according to prior assumptions regarding the probability of a particular character transformation (*a priori* weighting) (Skelton and Smith, 2002). This method is not often used for molecular characters. *A posteriori* weighting involves re-weighting characters according to their level of congruence with other characters.

Three steps are involved in the process of estimating a particular phylogeny: (1) character and taxon selection, (2) character coding and data collection and (3) finding optimal trees by various analytical processes (Poe and Wiens, 2000). The selection of characters to include in a phylogenetic study is critical as characters are the essential units of such a study (Freudenstein, 2005). An "internally-consistent, nonarbitrary, yet flexible" method of viewing characters is therefore important (Freudenstein, 2005: 965).

The understanding of organisms, as well as their traits and interactions, is increasingly being studied with the help of, and in the context of, phylogenetics (Wiens, 2000). Our historical knowledge and classification of organisms exists as a result of morphological phylogenetics (Wiens, 2000). Recent developments (since circa 1960) in molecular systematics will not unseat morphology in phylogenetic reconstructions (Wiens, 2000). Morphological data is important in phylogenetics as analysis of fossil records relies exclusively on this type of data . Additionally, the only existing records of many organisms are morphological ones (Wiens, 2000).

Morphological and molecular methods of phylogenetic analysis and reconstruction should be seen as complementary, with each having its own advantages and disadvantages (Hillis, 1987; Hillis and Wiens, 2000). The two methods can each address issues which cannot be addressed by the other (Hillis and Wiens, 2000).

The advantages of morphological data are as follows (Hillis and Wiens, 2000):

1. Much more thorough taxonomic sampling can be undertaken in morphological analyses. Molecular analyses rely on fresh material, thereby excluding the use of herbarium or museum specimens [but see for example Cron (2005)] and sampling many taxa can be expensive and time-consuming. Long branches in an estimated molecular tree may be subdivided by including additional taxa and this is one of the chief reasons for doing so.
2. Morphology is critical to alpha taxonomy – species descriptions are based on morphological data. Molecular analyses typically rely on such species descriptions to determine which species have been sampled.

The advantages of molecular data are as follows (Hillis and Wiens, 2000):

1. Molecular data provide a much larger number of observable characters for analysis and this is the most important advantage of this method (Hillis, 1987). Estimating phylogenetics relies on the existence of sufficient characters (Hillis *et al.*, 1994). Morphological studies typically include fewer than a hundred characters, whereas molecular studies may include tens of thousands. The number of useful characters for molecular phylogenetic analyses are limited by two assumptions:
   (a) Characters are independent of one another: that is, change in one character being analysed does not affect the probability of change in any other character being analysed.
   (b) Characters are heritable: that is, character variation passes (with rare mutation) from ancestor to descendants. In theory, therefore, the maximum number of characters which meet these assumptions is effectively the size of the entire genome, although large numbers of repeated sequences reduce this number.

2. A second advantage of molecular data is the fact that nucleotides are subject to a wide range of substitution rates.
3. The genetic basis of characters is also important: in molecular data it is known, whereas in morphological data it has to be assumed. This can be problematic for morphological analysis, as the independence of characters often cannot be determined.
4. The selection of characters for molecular studies is largely objective and straightforward. Decisions regarding alignment and the choice of the gene or region to be sequenced are the only potential areas of subjectivity. In contrast, characters used in morphological analyses may be quite arbitrary and details regarding the selection of particular characters is rarely provided.

It is important to note that it is likely that each morphological character included in a study is coded for by a different gene, or set of genes, and that tree reconstruction from molecular data may yield well-supported, but incorrect, answers to questions about species phylogeny if the evolution of the gene or genes examined differs from that of the species (Doyle, 1992; Hillis and Wiens, 2000).

Most incongruities between morphological and molecular trees are spurious and are often a result of the analyses performed (Omland, 1994; Hillis and Wiens, 2000). However, in some cases the reason for incongruity between the morphological and molecular analyses is not known (Baker *et al.*, 1998). Incongruity is often a result of undersampling of taxa, weak support for either or both of the estimates or as a result of different methods of analysis having being employed (Hillis and Wiens, 2000). Rooting molecular cladograms with only a single species makes estimates susceptible to long-branch problems (Hillis and Wiens, 2000). It has been shown that the conflicts between morphological and molecular studies of whales are a result of the position of the root – the unrooted topologies were the same (Hillis and Wiens, 2000). Conflicts between morphological and molecular phylogenies may also arise when the phylogenetic history of the gene is different from that of the species (Hillis and Wiens, 2000). Paralogy, lineage sorting and the lateral transfer of genes between unrelated species have been shown to be the cause of such differences (Doyle, 1992; De Queiroz, 1993).

Groups which are poorly-resolved morphologically also tend to be difficult to resolve via molecular analyses (Hillis and Wiens, 2000). A suggested reason for this is that these groups speciated rapidly and there has been insufficient time to accumulate long branches, either for morphological or molecular changes (Hillis and Wiens, 2000). In situations where both morphological and molecular data sets exist, they should be analysed via a combined analysis in a single matrix as well as separately, to allow for comparison of the results from each analysis (Hillis and Wiens, 2000).

Characters which are independent of each other are desirable when combining characters – this results in stronger support that each analysis on its own (Barrett *et al.*, 1991). When all characters are unweighted, a signal present in one data set may be obliterated when data sets are combined, particularly with regard to morphological and molecular data sets (Barrett *et al.*, 1991). However, it is not easy to support any approach in which unequal weights are assigned to characters (Barrett *et al.*, 1991).

Two approaches exist when considering the analysis of different data sets (Kluge and Wolf, 1993; De Queiroz, 1995). The first is termed taxonomic congruence and involves constructing a consensus tree from the trees obtained from the separate analyses (Kluge and Wolf, 1993; De Queiroz, 1995). The second involves combining the data sets into one and analysing the combined data set (De Queiroz, 1995). This approach is termed "total evidence" or "character congruence". The consensus approach enjoys support because it gives equal weight to each data set and is considered a more conservative estimate of a phylogeny (De Queiroz, 1993). However, the combined approach argues that the most parsimonious patterns of character change are not necessarily indicated by consensus trees and that such trees can contradict combined trees (De Queiroz, 1993). A strong argument in favour of separate (consensus) analysis is that estimates of phylogenies depend on a particular model of evolution (De Queiroz, 1995). Combining the data sets in one analysis assumes the same model of evolution for both data sets (De Queiroz, 1995). The combination of data sets which each reflect different accuracies of the true phylogeny has been proposed as another argument in support of consensus analyses (De Queiroz, 1995). Combined analyses make use of "total evidence" and avoids arbitrary decisions regarding consensus methods (De Queiroz, 1995). Additionally, the arbitrary weighting of individual trees in a consensus analysis is avoided in a combined analysis (De Queiroz, 1995). An approach in which both consensus and combined methods are used is termed "global consensus" (Levasseur and Lapointe, 2001). This approach allows for the comparison of the results of the methods individually as well as when combined. A detailed discussion of taxonomic congruence can be found in Kluge and Wolf (1993).

1.8 Species Concept

The goals of a species concept, according to Wheeler and Platnick (2000a: 143) are as follows:

- To recognize the kinds and numbers of distinct, self-perpetuating organisms on Earth, past and present.
- To identify end-products of diverse evolutionary processes.
- To discover the elements of phylogenetic analysis – that is, those groups of organisms among which there is a retrievable common history and which may not be divided into less inclusive units for which the same is true.
- To determine the least inclusive units usefully accorded formal recognition in a Linnaean classification, consistent with the goals of communicating and predicting the distribution of characters among organisms. In this sense, species names occupy a special place as the expression of taxonomists' least inclusive hypotheses preliminary to cladistic analysis.

The Biological Species Concept is defined by Mayr (1969: 26) as "groups of interbreeding natural populations that are reproductively isolated from other such groups". It has previously been accepted that evolutionary units are "biological species" and are reproductively discontinuous with other such units (Cracraft, 1983). An approach which considers the results of evolution rather than the processess which produce those results may be a better solution. The results of evolution are species, or "taxonomic entities, defined in terms of their evolutionary differentiation from other such forms" (Cracraft, 1983: 169). From this, "a species is the smallest diagnosable cluster of individual organsms within which there is a parental pattern of ancestry and descent" (Cracraft, 1983: 170). The Phylogenetic Species Concept has several advantages over the Biological Species Concept. The most important are the following, from Cracraft (1983):

- The diagnosable taxonomic units are equivalent to the evolutionary units.
- The incongruent pattern of geographic and/or clinal variation shown by different characters is removed, as species are defined by diagnostic characters.
- Subspecies are not considered as evolutionary units.

- Reproductive isolation data is not involved in species recognition.

Two commonly used variations of the Phylogenetic Species Concept are those proposed by Mishler and Theriot (2000), and Wheeler and Platnick (2000b). Mishler and Theriot (2000: 46) define their species concept as follows:

> *A species is the least inclusive taxon recognized in a formal phylogenetic classification. As with all hierarchical levels of taxa in such a classification, organisms are grouped into species because of evidence of monophyly. Taxa are ranked as species rather than at some higher level because they are the smallest monophyletic groups deemed worthy of formal recognition, because of the amount of support for their monophyly and/or because of their importance in biological processes operating on the lineage in questions.*

Wheeler and Platnick (2000b: 58) define their phylogenetic species concept as "the smallest aggregation of (sexual) populations or (asexual) lineages diagnosable by a unique combination of character states". The Phylogenetic Species Concept will be adopted in the present study. A combination of the preceeding systems will be used, incorporating both the concept of monophyly and that of unique combinations of character states.

1.9 Aims and Objectives

This study focuses on the taxonomy and phylogeny of the genus *Nephroselmis* Stein (1878), a ubiquitous group of largely marine, unicellular photosynthetic anisokont biflagellates, in the class Prasinophyceae of the phylum Chlorophyta. The purpose of this study is to clearly delineate and review the systematics of the genus by means of morphological, ultrastructural and molecular data and cladistic analyses, and to investigate evolutionary trends in *Nephroselmis*. The following questions are posed:

1.9.1 Circumscription and Review of *Nephroselmis*

1. What are the defining or delineating morphological characteristics of the genus?
2. Is there evidence to support moving some species [such as *Nephroselmis fissa* (Figure 3.12) and *Nephroselmis marina* (Figure 3.13)] from the genus *Nephroselmis* into some other, or a new, genus?
3. Are all the species currently considered to belong to the genus *Nephroselmis* correctly classified, in terms of morphological and molecular phylogenetic analyses? Is the genus *Nephroselmis* monophyletic?
4. Is there evidence to support the creation of subgenera within the genus *Nephroselmis*?
5. Should any of the species within the genus *Nephroselmis* be subsumed into one species?
6. Should the formal description of the genus be revised or amplified, and if so, how?

1.9.2 Evolutionary Trends in *Nephroselmis*

7. Which species of *Nephroselmis* is most likely to be ancestral (that is, a basal lineage) and which more recently diverged?
8. What inferences regarding habitat changes within the genus can be made?
9. Do the marine species group together separately, distinct from the freshwater species?
10. What hypotheses can be made regarding species relationships and evolutionary trends within the genus?

Chapter 2

Materials and Methods

2.1 Selection of Study Species

Seven species of *Nephroselmis* were obtained from three international culture collections (CCAP, MBIC and NIES; see Tables 2.1 and 2.2) for use in morphological and molecular cladistic analysis and ultrastructural study of the genus. The databases of many culture collections were searched during the years 2006 and 2007. The samples subsequently purchased for this study represent all identified strains which were available during this period[9]. Cultures were transported via express courier, shipping typically taking between 3 and 5 days, and sub-cultured into fresh growth medium (see Section 2.3.3) immediately upon arrival. Only one strain (population) of each species was purchased, in order to minimize the cost of the study and because of time constraints. The sample of *N. olivacea* supplied by CCAP was found not to be *Nephroselmis*. The sample of *N. pyriformis* supplied by CCAP was found to be a strain of *N. rotunda*. The strain of *N. olivacea* from NIES was unfortunately completely overrun by a chrysophyte alga before molecular work on it could be undertaken. Unidentified strains from culture collections were not included, as the cost of ordering and maintaining strains which may be duplicates was unjustified.

Cultures of *Nephroselmis* from the internal culture collection of the Phycology Research Section at the University of the Witwatersrand (designated 'Wits') were also examined (strains AA15, BB2, FH01 and WW02 in Table 2.2). Cultures were established from opportunistic sampling of inshore waters in South and East Africa and were examined. However, none of these samples yielded any additional species of *Nephroselmis* and none have been included in this study. Therefore, this study can be considered to be as representative of the genus *Nephroselmis* as is possible in the limited time available.

Two outgroup taxa were included in the morphological cladistic study and twelve in the molecular cladistic study (Tables 2.2 and 2.6). Outgroups were selected after examining previous molecular and taxonomic studies of the chlorophytes and prasinophytes (Sym and Pienaar, 1993; Nayakama *et al.*, 1998; Fawley *et al.*, 2000; Nakayama *et al.*, 2007), which informed the decision to root the molecular trees using *Prasinococcus*. Of the various outgroups which could be used, five readily available from the 'Wits' internal culture collection were selected (Table 2.2). *Pseudoscourfieldia* appears as the sister group to *Nephroselmis*, with *Tetraselmis* appearing in a sister clade in phylogenetic studies based

[9] A strain of *Nephroselmis minuta* (SCCAP K-0022) of suspected Finnish origin [as mentioned in an *rbc*L phylogenetic study of various Prasinophycean and Pedinophycean genera by Daugbjerg *et al.* (1995)] from the Scandanavian Culture Collection of Algae and Protozoa is no longer alive (N Larsen, pers. comm., 2007). The only sequences of *rbc*L data for *Nephroselmis* species available on GenBank are those submitted by Daugbjerg *et al.* (1995), for *N. minuta* and *N. olivacea*.

Table 2.1. Collections from which cultures of *Nephroselmis* species were obtained for use in this study

Abbreviation	Name and Website
CCAP	Culture Collection of Alga and Protozoa (Argyll, Scotland) *http://www.ccap.ac.uk*
MBIC	Marine Biotechnology Institute Culture Collection (Japan) *http://seasquirt.mbio.co.jp/mbic/index.php?page=mbichome*
NIES	National Institute for Environmental Studies (Japan) *http://www.nies.go.jp/biology/mcc/home.htm*

Table 2.2. Samples of *Nephroselmis* and outgroups which were maintained for use in this study

Species	Strain Reference(s)
Nephroselmis anterostigmatica	MBIC 11158
Nephroselmis astigmatica	NIES 252
Nephroselmis olivacea	CCAP 1960/4B§ NIES 483¶
Nephroselmis pyriformis	Wits FH01, Wits WW01
Nephroselmis rotunda	Wits AA15, Wits BB2 CCAP 1960/1 CCAP 1960/3†
Nephroselmis spinosa	NIES 935
Nephroselmis viridis sp. ined.	NIES 486
Dolichomastix tenuiformis	Wits
Halosphaera sp.	Wits Nam3
Pseudoscourfieldia sp.	Wits Fine1
Pyramimonas mucifera	Wits
Tetraselmis sp.	Wits NV25

§This sample was found not to be *Nephroselmis*.

¶An unidentified chrysophyte contaminated this culture before molecular work could be undertaken.

†Supplied as "*N. pyriformis*"; identified here as *N. rotunda* (see discussion).

on morphological and 18S data (Sym and Pienaar, 1993; Friedl, 1997; Nayakama *et al.*, 1998; Nakayama *et al.*, 2007). Morphological trees were rooted with both *Dolichomastix tenuilepis* and *Pseudoscourfieldia marina*. Selection of these two species was informed by consultation of the literature as above and from preliminary trees resulting from the molecular investigation. Additionally, outgroups possessing two flagella rather than four were selected for the morphological study to avoid difficulties in coding character data. Flagellar features, such as hair scale detail or the presence or absence of blunt-ends for example, would be more difficult to code when some samples possess two flagalla and others possess four.

2.2 Selection and Coding of Characters

Characters and character state data for *Nephroselmis* species were determined from direct observations using light and electron microscopy and were supplemented with data gleaned from the literature (Manton *et al.*, 1965; Fott, 1971; Moestrup and Ettl, 1979; Moestrup, 1983; Inouye and Pienaar, 1984; Suda and Watanabe, 1989; Marin and Melkonian, 1994; Young, 1991; Suda, 2003; Suda *et al.*, 2004; Nakayama *et al.*, 2007). Data for the outgroups (*Dolichomastix tenuilepis* and *Pseudoscourfieldia marina*) were extracted from published material (Manton, 1977; Moestrup and Throndsen, 1988; Throndsen and Zingone, 1997). Data relating to siphonaxanthin, lutein and pigmentation presence and type were extracted from Yoshii *et al.* (2005) and Yoshii (2006). The forty-six unordered morphological characters selected for the cladistic study are presented in Table 2.3. As characters are unordered, values for outgroups are not always necessarily zero. However, a value of zero was allocated to a character for at least one of the outgroups for most of the characters. Constant (invariant) characters were included for reference purposes, but were excluded from the analyses. Unfortunately, flagellar hair scale ultrastructure was not well-preserved in most of the whole mount preparations. Presence of T-hair and/or Pt-hair scales could be confirmed for most samples however. This character may not be useful at the species level, as intraspecific variation exists in flagellar hair ultrastructure in different populations of *Nephroselmis* (Marin and Melkonian, 1994; Nakayama *et al.*, 2007).

The character data matrix used for the morphological cladistic analysis (maximum parsimony heuristic search) is shown in Table 2.4. Missing data was coded with a "?" character and data which was not applicable was coded with a "-" character. The software package *PAUP** (Swofford, 2003) (see Section 2.5.3) which was used for the analysis treats both of these characters in the same way however – that is, as missing data. Character 46 (Sexual reproduction present/absent) was included for reference. As sexual reproduction has only been observed in *Nephroselmis olivacea* (Suda and Watanabe, 1989; Suda *et al.*, 2004), this character was coded as unknown for all other species. This could increase the number of possible trees from a maximum parsimony search. However, *PAUP** deals with missing data by assigning the character a state which would be most parsimonious given its placement on the tree. Only characters with no missing data affect the placement of taxa[10]. Character data, which was entered into a spreadsheet, was copied to the clipboard. The custom *morph* program (see Section 2.5.6) was then executed which formatted the character data from the clipboard into the Nexus format and created a data file on disk for input into *PAUP**. See Table 2.9 for details of the software programs used in this study. Character data was reweighted in *PAUP** according to the rescaled consistency index. This procedure assigns a lower weighting to characters which are homoplasious by *PAUP**.

[10] *http://paup.csit.fsu.edu/paupfaq/paupans.html.*

Table 2.3. The forty-six unordered morphological characters used in the cladistic study

No.	Character	States
1	Cell shape in lateral view	0 Conical, 1 Round, 2 Ovate, 3 Renal, 4 Triangular
2	Lateral symmetry around flagellar insertion	0 Symmetrical, 1 Asymmetrical
3	Number of starch grains	0 One, 1 Two, 2 Three
4	Starch grain shape	0 Oval, 1 Watch glass-shaped plates (bilenticular), 2 Triangular-shaped plates
5	Thylakoid penetration	0 Ventral, 1 Radial (pyrenoid penetrated by thylakoids from any direction, but typically left-right), 2 None
6	Number of flagella	0 Two
7	Short flagellum parking (settling behaviour)	0 Open (flagella held away from the cell), 1 Closed (flagella held against the cell)
8	Long flagellum parking (settling behaviour)	0 Open (flagella held away from the cell), 1 Closed (flagella held against the cell)
9	Number of body scale layers	0 One, 1 Two, 2 Three, 3 Four, 4 Five
10	Body scale layer 1 present/absent	0 Present, 1 Absent
11	Body scale layer 1 shape	0 Pentagonal, 1 Circular
12	Body scale layer 2 present/absent	0 Present, 1 Absent
13	Body scale layer 2 shape	0 Rod, 1 Small Stellate, 2 Maltese Cross, 3 Paper Windmill
14	Body scale layer 3 present/absent	0 Present, 1 Absent
15	Body scale layer 3 number of spines	0 Sixteen, 1 Eleven, 2 Thirty-three, 3 Thirteen
16	Body scale layer 3 spine polarity	0 Unipolar (one terminal spine, projection or arm)
17	Body scale layer 4 present/absent	0 Present, 1 Absent
18	Body scale layer 4 number of spines	0 Five, 1 Sixteen, 2 Twenty, 3 Twenty-six; 4 Twenty-four
19	Body scale layer 4 spine polarity	0 Unipolar (one terminal spine, projection or arm), 1 Bipolar (terminal spines, projections or arms at both ends of the scale), 2 Multipolar (many spines, projections or arms radiating from a central point)
20	Body scale layer 5 present/absent	0 Present, 1 Absent
21	Body scale layer 5 number of spines	0 Seventeen
22	Body scale layer 5 spine polarity	Unipolar (one terminal spine, projection or arm), 1 Bipolar (terminal spines, projections or arms at both ends of the scale), 2 Multipolar (many spines, projections or arms radiating from a central point)
23	Number of flagellar scale types	0 One, 1 Three, 2 Four
24	Flagellar scale 1 present/absent	0 Present, 1 Absent
25	Flagellar scale 1 shape	0 Pentagonal, 1 Elliptical
26	Flagellar scale 2 present/absent	0 Present, 1 Absent
27	Flagellar scale 2 shape	0 Rod, 1 Stellate
28	Flagellar scale 3 present/absent	0 Present, 1 Absent
29	Flagellar scale 3 shape	0 Curved Hook, 1 Stellate
30	Pit scales present/absent	0 Present, 1 Absent
31	Pit hairs present/absent	0 Present, 1 Absent
32	Flagellar hair point present/absent	0 Present, 1 Absent
33	Pt-hair scales on short flagellum present/absent	0 Present, 1 Absent
34	Pt-hair scales on long flagellum present/absent	0 Present, 1 Absent
35	T-hair scales on short flagellum present/absent	0 Present, 1 Absent
36	T-hair scales on long flagellum present/absent	0 Present, 1 Absent
37	Tip hair present/absent	0 Present, 1 Absent
38	Eyespot presence and position	0 Absent, 1 Present under short flagellum, 2 Present on ventral side of pyrenoid, 3 Present on anterior surface
39	Habitat	0 Marine, 1 Freshwater
40	Lens structure near pyrenoid present/absent	0 Present, 1 Absent
41	Keel present/absent	0 Present, 1 Absent
42	Flange present/absent	0 Present, 1 Absent
43	Siphonaxanthin pigment series present/absent	0 Present, 1 Absent
44	Siphonaxanthin pigment type	0 Type I, 1 Type II, 2 Type III, 3 Type IV, 4 Type V (caroteinoid types I to V)
45	Lutein content of total carotenoids	0 Less than 5%, 1 Greater than 5%
46	Sexual reproduction present/absent	0 Present; 1 Absent

Table 2.4. Character data matrix used in the morphological cladistic analysis of *Nephroselmis* and two outgroups

Species / Character Number	**1**	**2**	**3**	**4**	**5**	**6**	**7**	**8**	**9**	**10**	**11**	**12**	**13**	**14**	**15**	**16**	**17**	**18**	**19**	**20**	**21**	**22**	**23**
Nephroselmis anterostigmatica	2	1	0	0	0	0	1	0	4	0	0	0	3	0	1	0	0	1	0	0	0	0	1
Nephroselmis astigmatica	2	0	0	0	0	0	0	0	3	0	0	0	3	0	2	0	0	3	1	1	-	-	1
Nephroselmis olivacea	1	0	1	1	1	0	1	1	3	0	0	0	2	0	1	0	0	2	2	1	-	-	2
Nephroselmis pyriformis	1	1	0	0	1	0	1	0	1	0	0	0	1	1	-	-	1	-	-	1	-	-	1
Nephroselmis rotunda	1	0	0	0	1	0	1	1	2	0	0	0	1	0	1	0	1	-	-	1	-	-	1
Nephroselmis spinosa	3	0	2	2	2	0	0	0	3	0	0	0	2	0	1	0	0	0	0	1	-	-	1
Nephroselmis viridis sp. ined.	1	0	0	0	0	0	1	1	3	0	0	0	3	0	3	0	0	4	2	1	-	-	2
Pseudoscourfieldia marina	0	0	0	0	0	0	0	0	1	0	0	0	0	1	-	-	1	-	-	1	-	-	0
Dolichomastix	4	1	0	3	0	0	0	0	0	0	1	1	?	1	-	-	1	-	-	1	-	-	0

Species / Character Number	**24**	**25**	**26**	**27**	**28**	**29**	**30**	**31**	**32**	**33**	**34**	**35**	**36**	**37**	**38**	**39**	**40**	**41**	**42**	**43**	**44**	**45**	**46**
Nephroselmis anterostigmatica	0	0	0	0	1	-	1	1	1	1	1	0	0	1	3	0	1	1	0	0	0	0	?
Nephroselmis astigmatica	0	0	0	0	1	-	0	0	1	1	1	0	0	1	0	0	1	1	0	0	0	0	?
Nephroselmis olivacea	0	0	0	0	0	0	1	1	1	0	1	0	0	1	1	1	0	1	1	1	4	1	0
Nephroselmis pyriformis	0	0	0	0	1	-	1	0	1	0	1	0	0	1	1	0	1	1	0	0	0	0	?
Nephroselmis rotunda	0	0	0	1	1	-	1	1	1	0	1	0	0	1	1	0	1	1	1	0	1	0	?
Nephroselmis spinosa	0	0	0	0	1	-	1	1	1	0	1	0	0	1	1	0	1	0	1	0	3	1	?
Nephroselmis viridis sp. ined.	0	0	0	0	0	1	1	1	1	0	1	0	0	1	1	0	0	1	1	0	2	1	?
Pseudoscourfieldia marina	0	0	0	0	1	-	1	1	0	0	1	0	0	0	0	0	1	1	1	0	?	?	?
Dolichomastix	0	1	1	?	1	-	1	1	1	1	0	0	0	0	2	0	1	1	1	?	?	?	?

Missing data was coded with a "?" character and data which was not applicable was coded with a "-" character. These are both treated as missing data by the *PAUP** software program. Constant (invariant) characters were included for reference purposes, but were excluded from the analyses. The full list of characters and character states appears in Section 2.2.

2.3 Culturing Techniques

2.3.1 Growth Conditions and Culturing

All cultures of *Nephroselmis* and outgroups were maintained in walk-in growth rooms at the University of the Witwatersrand. The photoperiod was 18 hours light to 6 hours dark with an ambient temperature of 20°C. Light intensity was 27 μE.m^{-2}.s^{-1} (2200 lux). Samples were sub-cultured every three to four weeks into clean, autoclaved Erlenmeyer flasks or into capped test tubes. Back cultures were maintained by placing them into a darker location in the growth room [light intensity of 5 μE.m^{-2}.s^{-1} (400 lux)] or into a 12°C growth chamber. Freshwater samples were sub-cultured under sterile conditions inside a sterilized laminar flow bench to prevent contamination.

2.3.2 Cleaning Procedures

Erlenmeyer flasks and test tubes were washed and scrubbed with detergent in hot water, rinsed in an acid wash, cold water and distilled water, dried in a *P Selecta* oven at 150°C for 30 minutes and finally autoclaved for 40 minutes in a either a *Tomy SD-30N* or a *SA-300V* autoclave at a temperature of 120°C and a pressure of 1.1 kgf.cm^{-2}.

2.3.3 Growth Medium Preparation and Recipes

Seawater from 25 ℓ carboys was pre-filtered through two layers of fine cloth gauze (mesh size of 20 μm) and then through number 1 filter paper into clean, pre-autoclaved 2 ℓ medium bottles, which were then autoclaved again for 40 minutes as detailed in the previous section. The water was allowed to cool and growth medium (PES) was added (10 mℓ per ℓ). Freshwater medium was prepared by filling clean, pre-autoclaved 2 ℓ medium bottles with ultrapure Millipore water and autoclaving as above. Growth medium (PES, Soil Extract or BBM) was then added to the bottles under sterile conditions inside a sterilized laminar flow bench to prevent contamination. Media recipes are provided in Appendix B.

2.3.4 Sampling and Enrichment Procedure

Strains obtained from opportunistic sampling in the field (see Table 1.4 for locations) were enriched before examining them for species of *Nephroselmis*. 100 mℓ of the sample was placed into a clean Erlenmeyer flask and 50 mℓ of growth medium was added. Germanium Dioxide was added, to kill any diatoms which may be present (see Appendix C). The flask was placed into the growth room and the enrichment examined with inverted and compound microscopes every three days.

2.3.5 Isolating Procedure

Strains of *Nephroselmis* were isolated from enrichments or the internal culture collection via traditional cell isolation techniques (Andersen and Kawachi, 2005) as follows. A micropipette was created by stretching a Pasteur pipette over a flame and snapping it to produce a very fine isolating needle. A small drop of culture was placed onto a clean slide on the inverted microscope, along with two small drops of growth medium. The isolating needle was then attached to a thin plastic tube and placed into the drop of culture. A single cell of *Nephroselmis* sp. was then pulled into the isolating needle and deposited into a drop of growth medium. The cell was then transferred from the drop of medium to a well in a replidish and a culture allowed to establish. The well was examined under the inverted microscope at regular intervals and a sample was transferred to a clean, autoclaved Erlenmeyer flask containing growth medium when unialgal cultures were seen.

2.3.6 Preservation of Cultures

Cultures were preserved to ensure that molecular systematic work could be undertaken even if some cultures died. Large glass centrifuge tubes were half-filled with culture and centrifuged for 5 minutes at 1000 g and then for 10 minutes at 3000 g to produce a pellet. The supernatant was discarded and the pellet was suspended in a small amount of 70% alcohol. This mixture was then transferred to sterile 1.5 mℓ plastic Eppendorf tubes and stored in a freezer at -20°C. Unfortunately, the strain of *Nephroselmis olivacea* from NIES (NIES 483) was not preserved.

2.4 Microscopy Techniques and Micrographs

Light and electron microscopy were used to examine the morphology and ultrastructure of the samples in this study. Standard procedures were followed to prepare whole mounts and ultrathin sections of fixed material (see Appendix A). Light microscopy provided data relating to the cell shape and colour, chloroplast shape, flagellar length, flagellar parking (settling) behaviour, starch grain position and shape, and pyrenoid position and shape. Whole mounts were used to examine the external morphology of the cell, including body scale morphology and flagellar hair scale morphology. Ultrathin sections provided data relating to the internal cell ultrastructure and body and flagellar scale morphology. Black and white micrograph negatives (6.0 cm by 8.6 cm) were scanned in 16-bit greyscale at a resolution of 1200 DPI on an Epson Perfection V700 Photo scanner. Editing and cropping was done in Adobe Photoshop 7.0 running on Microsoft Windows XP Professional. Plates were produced with the open-source desktop publishing program *Scribus*, version 1.3.3.9 (*http://www.scribus.net*) under Windows XP (SP2) and version 1.3.3.11 under Kubuntu Linux. A Zeiss AxioPhot compound photomicroscope equipped with a 100x oil-immersion lens, digital camera (AxioCam HRc), video graphics printer (Sony UP-895CE) and traditional 35 mm film camera was used. Nomarski and phase contrast optics were available on this microscope. Images from fresh and fixed material were captured electronically via the digital camera using *AxioVision* Version 4 software, via the black and white video printer and onto 35 mm Tungsten slide film. Processed slides and video prints were scanned electronically on an Epson Perfection V700 Photo scanner.

2.5 Molecular Techniques

2.5.1 Selection of Genomic DNA Regions for Sequencing

The two Internal Transcribed Spacer (ITS) regions flanking the 5.8S gene have previously been used to infer specific-level phylogenies in a range of organisms (chlorophytes, angiosperms and metazoans) (for example: Coleman and Mai, 1997; Mai and Coleman, 1997; Coleman and Vacquier, 2002; Cron, 2005). The region has also been used in members of the Prasinophyceae, including *Pyramimonas* (SD Sym, pers. comm., 2006). Therefore, it was initially decided to use the ITS regions in this study. The forward and reverse universal eukaryotic primers of White *et al.* (1990) were used (see Table 2.5). The sequence data (not shown here) consisted of the ITS1 region (208 to 263 bases), the 5.8S gene (120 to 162 bases bases) and the ITS2 region (279 to 400 bases) – a total of 653 to 761 bases. The 5.8S gene sequence was confirmed by comparison with the same region for *Tetraselmis* from GenBank (Accession Numbers AY574382.1 and X65967.1), as no ITS or 5.8S data for *Nephroselmis* was available on GenBank. ITS sequences for the specimens sequenced have been submitted to GenBank; Accession Numbers for these sequences are provided in Table 2.6.

The sequences for the ITS1 and ITS2 regions obtained for *N. anterostigmatica*, *N. pyriformis*, *N. rotunda* and *Tetraselmis* sp. were found to be too variable to align with any confidence. When sequence alignment was forced manually over the 5.8S gene region, the ITS regions showed only very few invariant sites, both among the *Nephroselmis* samples and between them and the two *Tetraselmis* samples (the sequenced sample and the GenBank sample). The BLAST algorithm (Table 2.9) was used offline locally to search the *Nephroselmis* sequences for the 5.8S gene (from the *Tetraselmis* GenBank sample). This gene was found within all of the sequenced samples and details of its position in the sequence have been added to the GenBank entries for the samples in question. The ITS region was not sequenced for all samples in the study – once it was determined that the ITS region would not be informative, no further sequencing of this region was undertaken. However, the sequence data for the ITS regions which was obtained may be useful for future identification of these species.

The 18S gene region was then selected, as this region has also previously been used to infer specific-level phylogenies in a range of organisms, including the prasinophytes (Hamby *et al.*, 1988; Medlin *et al.*, 1988; Rowan and Powers, 1992; Steinkötter *et al.*, 1994; Nayakama *et al.*, 1998; Fawley *et al.*, 1999; Huss *et al.*, 1999; Fawley *et al.*, 2000; Moon-van der Staay *et al.*, 2000; Krienitz *et al.*, 2001; Moon-van der Staay *et al.*, 2001; Zingone *et al.*, 2002; Guillou *et al.*, 2004; Romari and Vaulot, 2004). As the entire 18S gene region is approximately 1800 bases long, internal primers would probably be required in order to obtain good sequence data for the entire region. Only the first 1000 bases of this region were selected because of cost and time constraints. Analysis of the first 1000 bases of 18S sequences of *Nephroselmis* and the various outgroups from GenBank indicated that approximately 138 parsimoniously informative sites are available. The forward universal eukaryotic primer of White *et al.* (1990) and a custom-designed reverse primer were used (Table 2.5). A custom reverse primer was required to terminate the sequence approximately 1000 bases into the 18S gene. This primer was designed by selecting a highly conserved region from aligned GenBank sequences of *Nephroselmis* and the various outgroups. GenBank Accession Numbers for the samples sequenced and the outgroups used are provided in Table 2.6.

2.5.2 DNA Extraction and Sequencing

DNA, which was extracted using one of three kits as detailed below, was concentrated for 30 to 60 minutes at 30°C under vacuum in an *Eppendorf Concentrator 5301* as required. The *GenElute™ Plant Genomic DNA Miniprep Kit* (Sigma G2N-10) was used to extract DNA for most samples. For this procedure, 10 mℓ of dense cell culture in growth medium was centrifuged for 5 minutes at 1000 *g* and then for 10 for minutes at 3000 *g* in glass centrifuge tubes. The supernatant was discarded and the pellet was resuspended in a small amount of the growth medium which remained in the centrifuge tube. The resuspended material was transferred to a 2 mℓ Eppendorf tube and five to ten autoclaved glass beads were added. The manufacturer's protocol was then followed, starting from the step in which the Lysis Buffer is added to the sample. The *Fungal/Bacterial DNA Kit™* (Zymo Research D6005)

Table 2.5. PCR primers used to sequence the ITS and 18S regions of *Nephroselmis* and selected outgroups

Region	Name	Sequence	Direction	Length	Tm (°C)	Product Size	Reference
ITS	ITS5	GGAAGTAAAAGTCGTAACAAGG	Forward	22	59.0	600	White *et al.* (1990)
ITS	ITS4	TCCTCCGCTTATTGATATGC	Reverse	20	58.4	600	White *et al.* (1990)
18S	NS1	GTAGTCATATGCTTGTCTC	Forward	19	55.9	900	White *et al.* (1990)
18S	B01R	GCTTTCGCAGAAGTTCGTCT	Reverse	20	60.4	900	This study

Table 2.6. Samples of *Nephroselmis* and selected outgroups from which ITS and/or 18S data were sequenced or obtained from GenBank for the molecular cladistic analysis

Sample	GenBank Accession Number ITS	18S	Strain
Nephroselmis anterostigmatica	EU334586*	EU330215*	MBIC 11158
	None	AB158372	Saeki-S
	None	AB158373	PM8-2
Nephroselmis astigmatica	None	EU330216*	NIES 252
		AB158374	
Nephroselmis olivacea	None	None	CCAP 1960/4B§
		None	NIES 483¶
		X74754	SAG 40.89
Nephroselmis pyriformis	EU334587*	EU330217*	FH01, WW02
	None	AB058378	MBIC10641
	None	AB058391	MBIC11099
	None	AB158376	UTEX LB2001
Nephroselmis rotunda	EU334589*	EU330218*	AA15, BB2
	EU334590*	EU330219*	CCAP 1960/1
	EU334591*	None	CCAP 1960/3†
Nephroselmis spinosa	None	EU330220*	NIES 935
		AB158375	SD959-3
Nephroselmis viridis sp. ined.	None	EU330221*	NIES 486
		AB214976	
Nephroselmis sp.	None	AB214975	MBIC11149
Dolichomastix tenuiformis	None	EU330214*	Wits
		AF509625	–
Halosphaera sp.	None	AB017125	Shizugawa
Mamiella sp.	None	AB017129	Shizugawa
Pseudoscourfieldia marina	None	EU330222*	Wits Fine1
		AF122888	K-0017
		AJ132619	K-0017
Prasinoderma coloniale	None	AB058379	MBIC10720
Pyramimonas mucifera	None	EU330223*	Wits
Pyramimonas olivacea		AB017122	Shizugawa
Pyramimonas parkeae		AB017124	Hachijo
Tetraselmis sp.	EU334592*	EU330224*	Wits NV25
Tetraslmis suecica	AY574382	None	–
Tetraselmis convolutae	None	U05039	NEPCC208
Tetraselmis kochiensis	None	AJ431370	–
Prasinococcus capsulatus	None	AB058384	MBIC11011

*Sequences submitted during the course of this study.
§This sample was found not to be *Nephroselmis*.
¶An unidentified chrysophyte contaminated this culture before molecular work could be completed.
†Supplied as "*N. pyriformis*"; identified here as *N. rotunda* (see discussion).

Table 2.7. Summary of PCR stages for the ITS and 18S regions of *Nephroselmis* and selected outgroups amplified in this study

	ITS		18S	
Step	**Temperature (°C)**	**Time (minutes)**	**Temperature (°C)**	**Time (minutes)**
Premelt	95	2	95	2
Denature	95	1	95	1
Anneal	54	1	51	1
Extend	72	1	72	1
Final Extension	72	5	72	5
Hold	4	∞	4	∞
Cycles	30		30	

was used for DNA extraction of two samples[11]. DNA from *Nephroselmis viridis* sp. ined. was extracted using the *DNeasy Plant Mini Kit (50)* (Qiagen 69104). The manufacturer's protocol was followed without modification for both of these kits.

PCR reactions were run in a *Hybaid PCR Sprint Temperature Cycling System.* Details of the reactions for the various regions of the genome which were examined (ITS and 18S) are given in Table 2.7. PCR product was obtained using either the *2X PCR Master Mix* (Fermentas K0171) or by mixing components on ice, as detailed in Table 2.8. Primer details are given in Table 2.5. PCR product was purified using the *DNA Clean & Concentrator*™*-5* kit (Zymo Research D4003 and D4013).

Sequencing was performed off-site by *Inqaba Biotechnical Industries Pty. Ltd.*, South Africa[12], using an Applied Biosystems 3130xl genetic analyser (Applied Biosystems, Foster City, CA) and ABI Big Dye Terminator Cycle Sequencing kit version 3.1 (Applied Biosystems, Foster City, CA). Electropherograms of the sequences generated were inspected with *Chromas* software (version 1.45; Technelysium Pty. Ltd., Helensvale, Queensland, Australia).

PCR reactions were undertaken using the *2X PCR Master Mix* (Fermentas K0171) and run on ABI 9700 PCR machines. PCR clean-up was undertaken using *DNA Clean & Concentrator*™ kits (Zymo Research D4003 and D4013). Final forward and reverse sequence data were provided as trace files (chromatograms).

A 1% agarose electrophoresis minigel[13] was used to visualize extracted DNA (5 $\mu\ell$ each of DNA and loading buffer), PCR product (5 $\mu\ell$ each) and purified DNA (2 $\mu\ell$ each). Ethidium Bromide was used as a dye and Bromophenol Blue (Tetrabromophenolsulfonephthalein) as a loading buffer and indicator. Minigels were run at 75 V in a *FOTO/Force*® *250 Fotodyne* kit, viewed on a *Tec* ultraviolet light box and photographed with a *Polaroid Gelcam.*

[11] A small supply of this kit was available and was used in order to determine if it was suitable for the extraction of DNA from microalgae. As similar results were obtained from the two different kits used, it was not considered problematic that DNA for all samples was not extracted using the same kit.

[12] *http://www.inqababiotec.co.za*

[13] 0.3 g UniLAB Agar in 30 mℓ TAE Buffer. Buffer recipe provided in Section C.6 on page 102.

Table 2.8. Summary of PCR components used in the amplification of the two DNA regions (ITS and 18S) of *Nephroselmis* and selected outgroups examined in this study

Component	Quantity ($\mu\ell$) 2X PCR Master Mix Fermentas K0171	TrueStart™ *Taq* Fermentas EP0611	GoTaq® Promega M7911
dH_2O	23	36.6	31.75
Buffer (10x)	25	5	10
dNTPs (10 mM)	25	1	1
$MgCl_2$ (25 mM)	25	5	5
Taq DNA Polymerase	25	0.4	0.5
Forward Primer (10 mM)	0.5	0.5	0.5
Reverse Primer (10 mM)	0.5	0.5	0.5
Template DNA*	1	1	1
Total	**50**	**50**	**50**

*$3\mu\ell$ was used for weaker samples; water volume was not adjusted in these cases

2.5.3 Editing and Analysis

The computer software packages and programs used in the editing and analysis of the data are listed in Table 2.9; references for each package are provided there. Trace files were examined using *Chromas Lite* (Technelysium Pty. Ltd.). Forward and reverse sequences from trace files were combined, checked and edited using *Sequencher* (Gene Codes Corporation, Michigan). A complete dataset was prepared by importing sequence data from *Sequencher* and sequences from GenBank (Benson *et al.*, 2005) into *MEGA4* (Tamura *et al.*, 2007). Multiple sequence alignment using *ClustalW* (Thompson *et al.*, 1994) with default parameters was executed on this dataset from within *MEGA4*. *Muscle* (Edgar, 2004b,a) was also used for multiple sequence alignment on the same dataset. GenBank sequences in the aligned dataset were truncated at 960 bases. All sequences were then further trimmed at both ends to eliminate missing data. All gaps were removed from all sequences and an analysis of the alignments resulting from different *ClustalW* parameters was undertaken. The custom *penaltytest* program (see Section 2.5.6) was used to execute a *ClustalW* alignment on the dataset with different gap-opening and gap-extension parameters for slow pairwise alignment and multiple sequence alignment. The program then converted the data file into Nexus format using the *ReadSeq* (Gilbert, 2001) program and executed a maximum parsimony heuristic search and bootstrap analysis in *PAUP**, with the output being logged to a file. The custom *penaltyparser* program (see Section 2.5.6) was used to analyse the log file from *penalytester*. A selection of 18 different parameter combinations was selected from values around the defaults. Parameters which yielded a higher consistency index (CI), better bootstrap support and fewer collapsed nodes were selected. The full dataset was aligned with the selected parameters with *ClustalW* and edited manually in *MEGA4*. *MEGA4* FASTA sequence data was converted to Nexus format with *SeqVerter* (GeneStudio, Inc.) and analysed with *PAUP** (Swofford, 2003). Accelerated transformation (ACCTRAN) character-state optimization, the tree-bisection-reconnection (TBR) branch-swapping algorithm and ten random stepwise additions were selected in *PAUP**. Gaps were treated as missing data. A maximum likelihood heuristic search was performed on the data set in *PAUP**.

The *water* (Smith and Waterman, 1981), *needle* (Needleman and Wunsch, 1970) and *fuzznuc* (a searching algorithm) programs from the EMBOSS suite (Rice *et al.*, 2000) were used to analyse sequence data, as detailed in Section 2.5.6. The BLAST algorithm (Altschul *et al.*, 1990) was used offline locally to search for nucleotide matches in sequences.

2.5.4 Combined Analysis

The morphological and molecular data sets were combined and analysed in *PAUP**. The full morphological data set was used (seven ingroup species and two outgroup species) and the corresponding molecular data which was sequenced for these species only. A partition homogeneity test (also termed an incongruence length difference test) (Farris *et al.*, 1995) was conducted on the data in *PAUP**. Uninformative characters were excluded from the analysis (Cunningham, 1997a,b; Lee, 2001). A heuristic search (as detailed previously) was then performed on the combined data set.

2.5.5 Indel Coding

Insertions or deletions (indels) in the alignment were coded using two methods. The first made use of the *GapCoder* software program, which is an implementation of the simple gap coding method of Simmons and Ochoterena (2000). The second method was a custom *seqindelcode* program (see Section 2.5.6) which coded indels based on the species groupings specified by the user. Typically there would be at least two groups – one containing the ingroup taxa and one containing the outgroup taxa. Howeverever, it may sometimes be useful to split the outgroup taxa into two or more groups. Indel coding was performed with an ingroup group and an outgroup group, as well as an ingroup group and two outgroup groups, which were selected based on their relationship to the ingroup. Indel-coded characters as prepared by each of the two methods separately were appended to the genomic sequence data for each sequence and analyses in *PAUP** performed.

2.5.6 Custom *Python* Programs

Various small programs were written in the *Python* programming language[14] (version 2.5) to assist with various analyses of sequence data during the course of the study. Code was edited and printed with *Notepad++*[15]. Details of the individual programs are provided in Appendix D.

[14] *http://www.python.org*
[15] *http://notepad-plus.sourceforge.net*

Table 2.9. Computer software packages used

Package	Version	Reference	Function
BioEdit	7.0.9.0	Hall (1999)	Sequence viewing and manipulation
BLAST	2.2.17	Altschul *et al.* (1990) NCBI	Sequence aligning and searching
ClustalW	1.83	Thompson *et al.* (1994)	Sequence aligning
Chromas Lite	2.01	Technelysium Pty. Ltd.	Chromatogram viewing
EMBOSS	2.10.0 Win-0.8	Rice *et al.* (2000)	Various analyses
GapCoder		Young and Healy (2003)	Indel coding
MEGA4	4	Tamura *et al.* (2007)	Sequence viewing, manipulation and tree printing
MUSCLE	3.6	Edgar (2004a) Edgar (2004b)	Sequence aligning
PAUP*	4.0b10	Swofford (2003)	Phylogenetic analyses
PHYLIP	3.67	Felsenstein (2007)	Phylogenetic analyses
ReadSeq	2.1.24	(Gilbert, 2001)	File format conversion
Sequencher	4.1.2	Gene Codes Corporation, Michigan	Sequence editing and aligning
SeqVerter	2.0.3.4	GeneStudio, Inc.	File format conversion
TreeView	1.6.6	Page (1996)	Tree viewing

All software was used on a Windows XP (SP2) computer, except *Sequencher*, which was used on an Apple Macintosh computer running OS 9.2.

Chapter 3

Results

3.1 Sources of Raw Data

The following synopsis is the result of data obtained from the morphological, ultrastructural and molecular analyses of the genus. Light and electron microscopy were used to examine the morphology and ultrastructure of the samples in this study (see Section 2.4). Light microscopy provided data relating to the cell shape and colour, chloroplast shape, flagellar length, flagellar parking (settling) behaviour, starch grain position and shape, and pyrenoid position and shape. Whole mounts were used to examine the external morphology of the cell, including body scale morphology and flagellar hair scale morphology. Ultrathin sections provided data relating to the internal cell ultrastructure and body and flagellar scale morphology. DNA was extracted from samples, sequenced, edited and aligned, as described in Section 2.5. All of these data were supplemented with data available in the literature, as referenced.

3.2 Synopsis of the Genus *Nephroselmis* Stein

Nephroselmis Stein

Reference: Stein (1878)

Nephroselmis cells are approximately bean-shaped or kidney-shaped (reniform) in lateral view. The two heterodynamic, anisokont, blunt-ended, scaly flagella arise laterally from a small depression where the hilum is located on a typical bean or kidney. The side of the cell from which the flagella arise is termed the ventral surface, with the opposite side being the dorsal surface (see Figure 3.1). The short flagellum is typically recurved around the side of the cell considered to be anterior and the long flagellum trails beyond the side of the cell considered to be posterior. The left and right surfaces of the cell follow from the previous definitions. The distance from the ventral to the dorsal surface is considered to be the height of the cell. The distance from the anterior to the posterior surface is considered to be length of the cell, and the distance from the left to the right surfaces is considered to be the width of the cell.

The internal structure of *Nephroselmis* is remarkably well-conserved across species. The chloroplast is typically shaped approximately like a cup or a viking boat, extending anteriorly and posteriorly from the ventral surface to the dorsal surface. Starch grains are deposited internally in the cell in such a way that they are surrounded by the chloroplast. The pyrenoid is typically located on the ventral side of the starch grain. The nucleus is

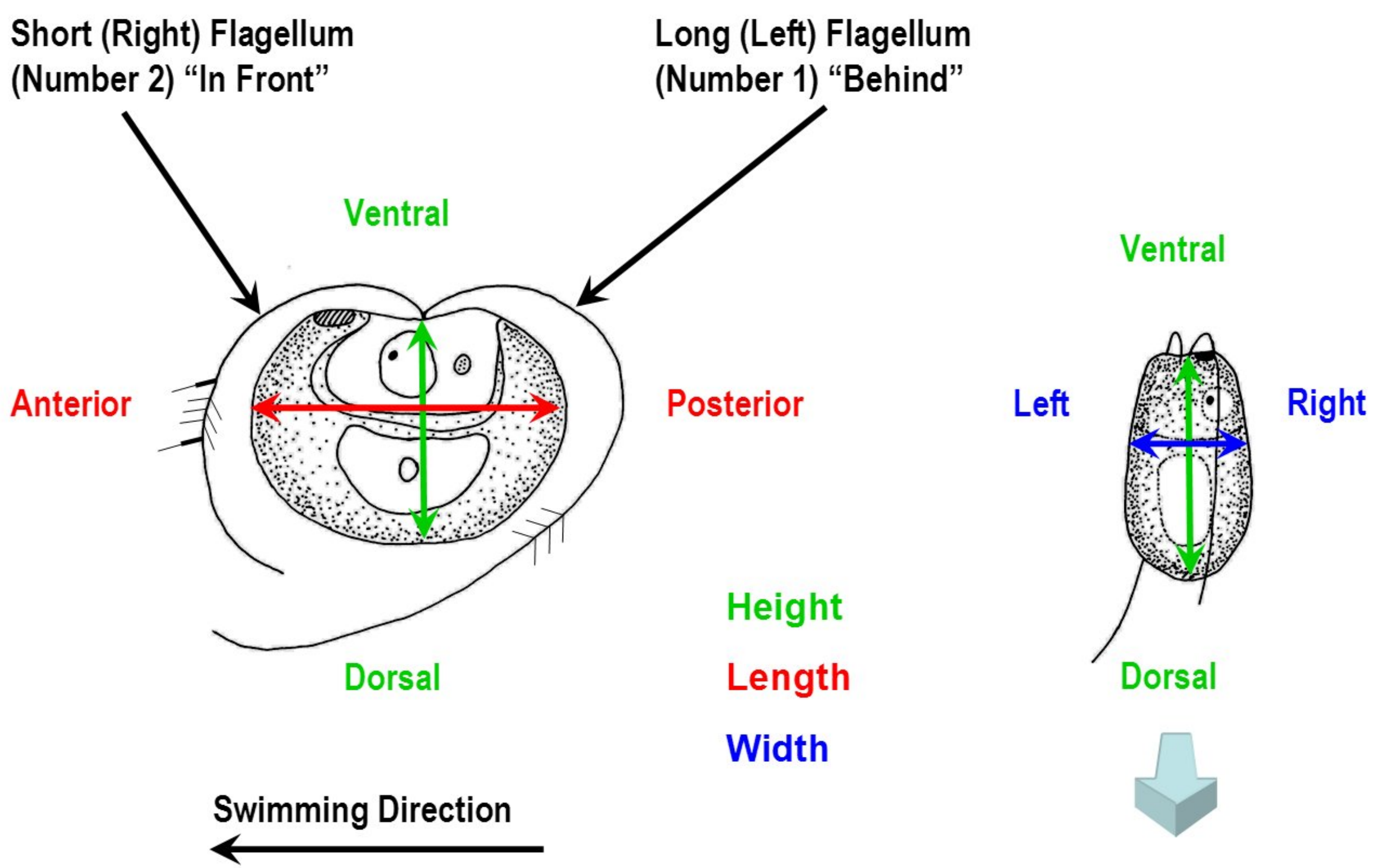

Figure 3.1. *Illustration of the cell orientation terminology [after Suda (2003)].*

located towards the ventral surface on the right side of the cell, with the Golgi apparatus occupying an equivalent position on the left of the cell. The lobes of the mitochondrion are reticulate, but are typically found adjacent to the ventral surface of the chloroplast. The intraplastidial eyespot, when present[16], is composed of approximately circular lipid globules and is located on the ventral surface of the cell, below the short flagellum, except in the recently-described species *Nephroselmis anterostigmatica*, where it is located on the anterior surface of the cell. One or more large circular lipid globules are often located in the region of the nucleus and Golgi apparatus. Refractile granules or inclusions may also be present.

Flagella enter the cell laterally at approximately 90° to each other. The long flagellum, which extends posteriorly, is termed flagellum number 1. The short flagellum, which extends anteriorly, is termed flagellum number 2. When viewed from the ventral surface, flagellum number 1 is located on the right of the cell and orientated posteriorly and flagellum number 2 on the left, orientated anteriorly. Two roots extend superficially into the cell from the basal body of flagellum number 1: the 1s (left) root and the 1d (right) root. Only one root, the 2d (right) root, extends superficially into the cell from the basal body of flagellum number 2. The 2s (left) root is absent in *Nephroselmis*. A rhizoplast (system II fibre) of contractile centrin extends dorsally into the cell from the basal bodies, passing adjacent to the nucleus and typically terminating in the proximity of the chloroplast. A microbody is often found in this region.

The cell and flagellar surfaces of all members of the genus are each covered by at least two layers of non-mineralised organic scales (Plates 1 and 2). Scale morphology is one of the principle features used to distinguish species. Small (30 nm) approximately square underlayer scales are found on the body surface of all species. Body scale morphology differs among the species from the second layer of scales upwards. Additional layers of complex body scales (termed third, fourth and fifth layer body scales) are found in all members of the genus except *N. pyriformis*. Fourth layer body scales are absent in *N. rotunda*. The flagella too are covered by an underlayer of small (30 nm) scales which closely resemble those found on the body, but are more pentagonal in shape. The second layer of flagella scales are small (30 nm), indistinct structures which have previously been termed "rod" or "man" scales (Becker *et al.*, 1990) They are found in all but one species – small stellate scales are found in this position in *N. rotunda*. A third type of scale, termed a hair scale, is also found on the flagellar surface. Short, simple T-hair scales are found on both sides of both flagella. Longer, more complex Pt-hair scales may be found on one side of the short flagellum only.

3.3 Checklist of Morphological Features

To aid in the identification and affinity of unidentified species, a checklist of morphological features of known *Nephroselmis* species is provided in Table 3.1

3.4 Key to the Genus *Nephroselmis* Stein (Prasinophyceae, Chlorophyta)

A key to the seven confirmed species of *Nephroselmis* (see Section 3.6) appears below. The terms "asymmetrical" and "symmetrical" refer to the cell symmetry around the flagellar insertion point, as described in Section 2.2.

[16]Absent in *Nephroselmis astigmatica*.

Table 3.1. Checklist of morphological features for the seven confirmed *Nephroselmis* species

Feature	Ant	Ast	Oli	Pyr	Rot	Spi	Vir
Eyespot present	•		•	•	•	•	•
Eyespot under short flagellum			•	•	•	•	•
Lens structure near pyrenoid			•				•
Spine scales						•	
Triangular starch grains						•	
Keel						•	
Asymmetrical shape	•			•			
Two watch-shaped starch grains			•				
Freshwater habit			•				
Pit scales		•					
Third layer body scales	•	•	•		•	•	•
Fourth layer body scales	•	•	•			•	•
Fifth layer body scales	•						

Ant = *N. anterostigmatica*, Ast = *N. astigmatica*, Oli = *N. olivacea*, Pyr = *N. pyriformis*
Rot = *N. rotunda*, Spi = *N. spinosa* and Vir = *N. viridis*.

1a. Eyespot absent .... *Nephroselmis astigmatica*
1b. Eyespot present .... 2.
2a. Third layer of body scales absent .... *Nephroselmis pyriformis*
2b. Third layer of body scales present .... 3.
3a. Large (± 1 μm) spine scales present .... *Nephroselmis spinosa*
3b. Spine scales absent .... 4.
4a. Fourth layer of body scales absent .... *Nephroselmis rotunda*
4b. Fourth layer of body scales present .... 5.
5a. Eyespot anterior; cells asymmetrical .... *Nephroselmis anterostigmatica*
5b. Eyespot not anterior; cells symmetrical .... 6.
6a. Third layer of flagellar scales curved spines with hooks .... *Nephroselmis olivacea*
6b. Third layer of flagellar scales stellate .... *Nephroselmis viridis* sp. ined.

3.5 Scale Formulae

In order to record the detailed structure of scales, a scale formula was constructed. This formula reflects the total number of spines, the number and position of any terminal (polar) spines, the number of tiers (layers) of spines and the number of scales in each tier. The formula is as follows:

```
Total:  Terminal1 + Terminal2; Number of Tiers / Scales per Tier
```

For example, the scale formula for the fourth layer of body scales of *N. astigmatica* is:

```
26:  1+1; 6/4
```

This indicates that there are 26 spines in total, two terminal (polar) spines (one at each end of the scale, as shown by the “1 + 1”), and 6 tiers of spines with 4 spines in each tier.

Table 3.2. Scale formulae for the third, fourth and fifth layer body scales of the seven confirmed species of *Nephroselmis*.

Species	Third layer body scales	Fourth layer body scales	Fifth layer body scales
N. anterostigmatica	11: 1; 2/5	16: 1; 3/5	17: 1+1; 3/5
N. astigmatica	33: 1; 4/8	26: 1+1; 6/4	–
N. olivacea	11: 1; 2/5	20: 0; ?	–
N. pyriformis	–	–	–
N. rotunda	11: 1; 2/5;	–	–
N. spinosa	11: 1; 2/5;	5: 1; 1/4	–
N. viridis	13: 1; 2/6;	24: 0; 3/8	–

"-" indicates that the body scale layer is absent.
"?" indicates that the body scale layer formula is unknown.

A value of "1" for the "Terminal" spines indicates a unipolar spine; a value of "1+1" in this position indicates bipolar spines and a value of "0" in this position indicates multipolar spines (many spines, projections or arms radiating from a central point, as described in Section 2.2). Scale formulae for the third, fourth and fifth layer body scales of the seven confirmed species of *Nephroselmis* are provided in Table 3.2. Data for scale formulae was obtained from the results of the present study, as well as from the literature (Moestrup and Ettl, 1979; Inouye and Pienaar, 1984; Suda, 2003; Nakayama *et al.*, 2007). Tier detail of *N. olivacea* fourth layer body scales could not be determined from microscopy or the literature.

3.6 Confirmed Species

Seven species of *Nephroselmis* can be confirmed as a result of this study. Detailed electron microscopic work for these seven species is available in the literature and the existence of these species has been confirmed by morphological and molecular investigations from fresh samples in this study. The description which follows for each species is a composite of the data obtained in this study, supplemented by data in the literature, as referenced.

3.6.1 *Nephroselmis anterostigmatica* Nakayama, Suda, Kawachi and Inouye

References: Nakayama *et al.* (2003, 2007)
Source: MBIC 11158
Figure: 3.2
Plates: 3 and 4

Cell length 4.19 μm ± 0.28 μm, cell height 4.47 μm ± 0.85 μm and cell width 3.15 μm ± 0.10 μm. In lateral view, the cell is approximately oval or ovate in shape and is asymmetrical around the flagellar insertion point. One oval starch grain is typically present. The chloroplast lobes in some samples is bifurcated, extending ventrally and anteriorly on the right side of the cell only, and dorsally and posteriorly on the left side of the cell only. Thylakoid penetration of the pyrenoid is ventral. A single eyespot is present on the anterior face of the cell, which is atypical of the genus. A groove runs along the ventral surface for the length of the cell, creating cytoplasmic protrusions on the ventral surface of the cell, termed the flanges. The pigment siphonaxanthin is present. The short flagellum exhibits closed flagellar parking behaviour, while the long flagellum shows open parking behaviour. Three flagellar scale types are present (two flagellar scale layers and flagellar hair scales). Underlayer flagellar scales are pentagonal in shape and second layer flagellar scales are rod-shaped. Third layer flagellar scales, pit scales and pit hairs are absent. The flagella are blunt-ended (flagellar hair point absent) and lack a tip hair. Pt-hair scales are absent from both flagella, while T-hair scales are present on both flagella. The scale morphology of this species is complex, with five layers of body scales being present. Underlayer scales are square and second layer body scales resemble a paper windmill. 11 spines are found on the stellate, unipolar third layer body scales. The fourth layer body scales are stellate unipolar scales with 16 spines. The fifth layer body scales are bipolar with 17 spines and are similar in structure to the fourth layer body scales of *N. anterostigmatica*. Marine, known from Japan (Saeki port, Oita Prefecture) and the Republic of Palau (Palau Island).

Notes This species, the most recently-described, was initially known as *Nephroselmis intermedia* sp. ined., from two entries on the GenBank database (Accession Numbers AB158372 and AB158373) (Nakayama *et al.*, 2003). Recently, a morphological and molecular study of this species was published, along with a formal species description (Nakayama *et al.*, 2007). Only this species and *N. pyriformis* show parking behaviour which differs between flagella (Plate 3: Figure 1; Plate 9: Figure 1). This is the only species in the genus in which the eyespot (when present) is located in a position other than under the short flagellum (Plate 3: Figures 1, 2 and 3). *N. anterostigmatica* is also the only species of *Nephroselmis* presently known to have as many as five body scale layers. Nakayama *et al.* (2007) report that the fifth layer of body scales were not present in all samples and that they were not able to confirm the arrangement of the fourth and fifth body scale "layers". For the purposes of this study, the fifth "type" of body scale is considered as the fifth "layer". Fifth layer body scales were not seen in the samples examined in this study.

3.6.2 *Nephroselmis astigmatica* Inouye and Pienaar

Reference: Inouye and Pienaar (1984)
Source: NIES 252
Figure: 3.3
Plates: 5 to 7

Cell length 7.68 μm $\pm$ 1.08 μm, cell height 8.76 μm $\pm$ 1.35 μm and cell width 6.40 μm $\pm$ 1.06 μm. The cell is approximately oval or ovate, and symmetrical around the flagellar insert point, in lateral view. One oval starch grain is typically present. The cup-shaped chloroplast extends anteriorly and posteriorly from the ventral surface to the dorsal surface. Thylakoid penetration of the pyrenoid is ventral. The eyespot is absent. A groove runs along the ventral surface for the length of the cell, creating cytoplasmic protrusions on the ventral surface of the cell, termed the flanges. The pigment siphonaxanthin is present. Both flagella exhibit open parking behaviour. Three flagellar scale types are present (two flagellar scale layers and flagellar hair scales). Underlayer flagellar scales are pentagonal in shape and second layer flagellar scales are rod-shaped. Third layer flagellar scales are absent. Pit scales are present in only this species of *Nephroselmis*. Pit hairs are present. The flagella are blunt-ended (flagellar hair point absent) and lack a tip hair. Pt-hair scales are absent from both flagella, while T-hair scales are present on both flagella. The body scale morphology of this species is the most complex in the genus, with four layers of body

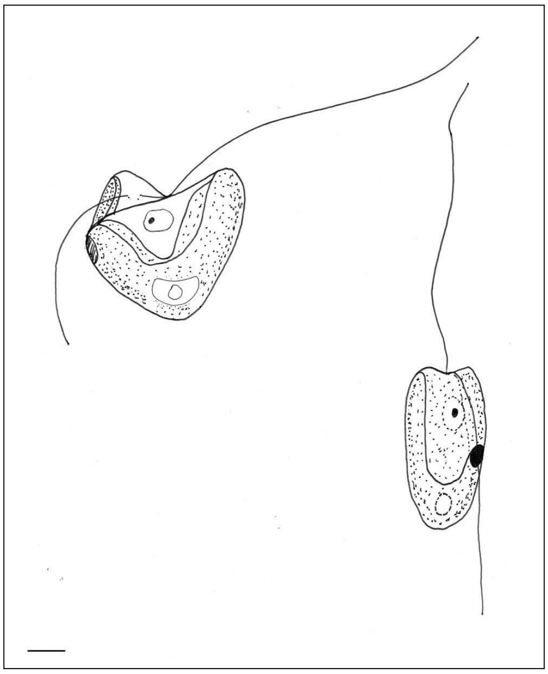

Figure 3.2. Nephroselmis anterostigmatica *drawn from fresh material. Left cell in lateral view with anterior cell face to the left of the image. Right cell in left-right view with anterior surface facing the reader. Chloroplast indicated by stippling effect. Nucleus present in ventral portion of the cell indicated by circular shape with dark nucleolus. Starch grains and pyrenoid are shown in the dorsal portion of the cell. Note the asymmetrical cell shape and the eyespot located on the anterior face of the cell. Scale bar = 1* μm.

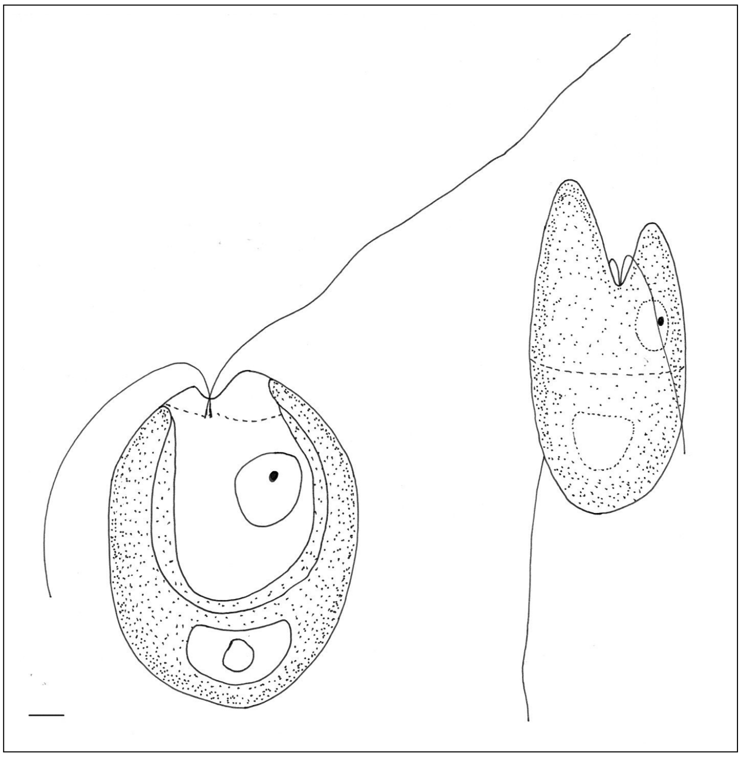

Figure 3.3. Nephroselmis astigmatica *drawn from fresh material. Left cell in lateral view with anterior cell face to the left of the image. Right cell in left-right view with anterior surface facing the reader. Chloroplast indicated by stippling effect. Nucleus present in ventral portion of the cell indicated by circular shape with dark nucleolus. Starch grains and pyrenoid are shown in the dorsal portion of the cell. Note the absence of an eyespot and the prominent flange shown in the right cell. Scale bar = 1 μm.*

scales being present. Underlayer scales are square and second layer body scales resemble a paper windmill. 12 spines are found on the stellate, unipolar third layer body scales, which resemble an eastern temple or a Christmas fir tree. The fourth layer body scales are particularly elaborate bipolar scales with 26 spines. Marine, known from Japan (Izu and Teshio) and South Africa (Durban).

Notes This is the only species of *Nephroselmis* which lacks an eyespot (Plate 5: Figures 1 to 4). It is also the only species in the genus in which pit scales are found (Plate 7: Figure 1). Pit hair scales are found in *N. astigmatica* and *N. pyriformis* only (Plate 7: Figure 1 Inset; Plate 10: Figures 7 and 8).

3.6.3 *Nephroselmis olivacea* Stein em. Moestrup *et* Ettl

Synonyms: *Sennia commutata* Pascher, *Nephroselmis commutata* Stein, *Heteromastix angulata* Korschikoff, *Nephroselmis angulata* (Korschikoff) Skuja
References: Stein (1878); Butcher (1959); Moestrup and Ettl (1979)
Source: NIES 483
Figure: 3.4
Plate: 8

Cell length 8.17 μm $\pm$ 0.75 μm and cell height 6.91 μm $\pm$ 0.24 μm. Cell width is unknown. The cell is round in shape and symmetrical around the flagellar insertion point in lateral view. Two starch grains are present, which are plate-like or watch-glass-shaped. The cup-shaped chloroplast extends anteriorly and posteriorly from the ventral surface to the dorsal surface. Thylakoid penetration of the pyrenoid is radial. A single eyespot is present under the short flagellum. A lens or disc-like structure is present between the pyrenoid and the plasmalemma on the dorsal side of the cell. The pigment siphonaxanthin is absent. Sexual reproduction has been shown to occur. Both flagella exhibit closed parking behaviour. Four flagellar scale types are present (three flagellar scale layers and flagellar hair scales). Underlayer flagellar scales are pentagonal in shape and second layer flagellar scales are rod-shaped. Third layer flagellar scales consist of a root-like structure with curved spines. Pit scales and pit hairs are absent. The flagella are blunt-ended (flagellar hair point absent) and lack a tip hair. Pt-hair scales are found on the short flagellum only. T-hair scales are found on both flagella. Four body scale layers are present. Underlayer scales are square and second layer body scales resemble a Maltese cross. 11 spines are found on the stellate, unipolar third layer body scales. The fourth layer body scales are multipolar scales with 20 spines. Freshwater, known from Belgium, Denmark, Ukraine (Kharkov) and the United States of America (Grand River, Lake Michigan).

Notes *N. olivacea* is the type species and only known freshwater species in the genus *Nephroselmis*. It is also the only species in which sexual reproduction has been described. The pigment siphonaxanthin, absent in *N. olivacea*, is found in all other members of *Nephroselmis*. *N. olivacea* is one of only two species of *Nephroselmis* in which third layer flagellar scales are found, the other being *N. viridis* [not seen; Moestrup and Ettl (1979); Young (1991)]. The lens or disc-like structure in the region of the pyrenoid is also found in these two species only [not seen; Moestrup and Ettl (1979); Young (1991)].

3.6.4 *Nephroselmis pyriformis* (Carter) Ettl

Synonyms: *Bipedinomonas pyriformis* Carter, *Anisomonas longifilis* Butcher, *Nephroselmis longifilis* (Butcher) Norris, *Anisonema longifilis* (Butcher) Norris, *Heteromastix longifilis* (Butcher) Rayns
Source: Wits FH01, Wits WW02
References: Carter (1937); Parke and Dixon (1964); Ettl (1983); Moestrup (1983, 1984b)
Figure: 3.5
Plates: 9 and 10

Cell length 4.22 μm $\pm$ 0.75 μm, cell height 4.26 μm $\pm$ 0.59 μm and cell width 2.85 μm $\pm$ 0.38 μm. In lateral view, the cell is approximately oval or ovate in shape and is asymmetrical around the flagellar insertion point. One oval starch grain is typically present. The cup-shaped chloroplast extends anteriorly and posteriorly from the ventral surface to the dorsal surface. Thylakoid penetration of the pyrenoid is radial. A single eyespot is present under the short flagellum. A groove runs along the ventral surface for the length of the cell, creating cytoplasmic protrusions on the ventral surface of the cell, termed the flanges. The pigment siphonaxanthin is present. The short flagellum exhibits closed flagellar parking behaviour, while the long flagellum shows open parking behaviour. Three flagellar scale types are present (two flagellar scale layers and flagellar hair scales). Underlayer flagellar scales are pentagonal in shape and second layer flagellar scales are rod-shaped. Third layer flagellar scales are absent. Pit scales are absent. Pit hairs are present. The flagella are blunt-ended (flagellar hair point absent) and lack a tip hair. Pt-hair scales

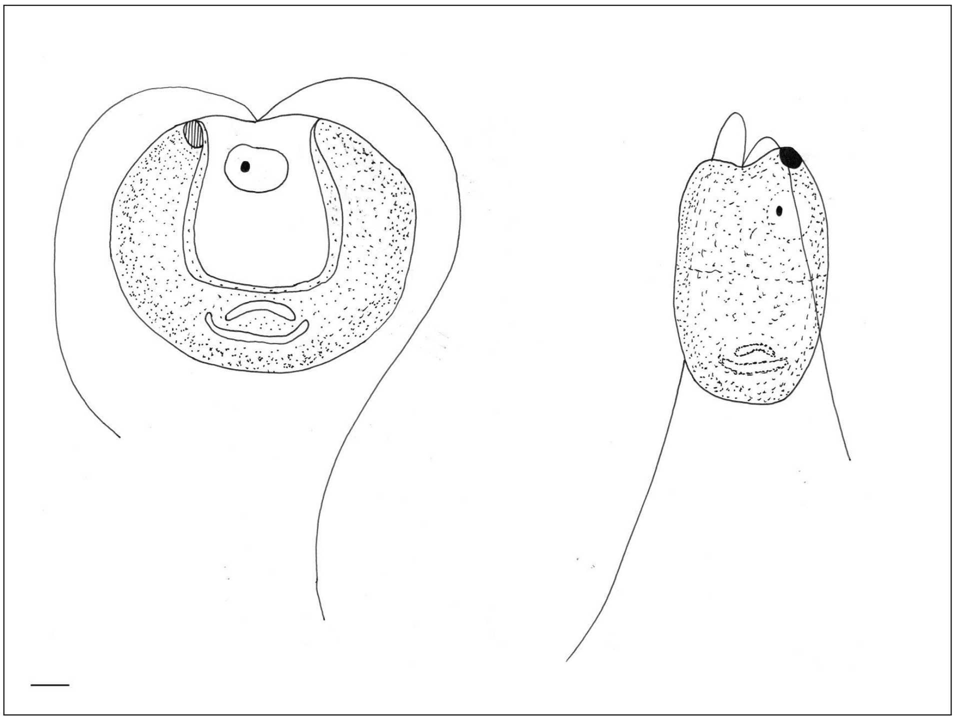

Figure 3.4. Nephroselmis olivacea *drawn from fresh material and Moestrup and Ettl (1979). Left cell in lateral view with anterior cell face to the left of the image. Right cell in left-right view with anterior surface facing the reader. Chloroplast indicated by stippling effect. Nucleus present in ventral portion of the cell indicated by circular shape with dark nucleolus. Note the characteristic plate-shaped starch grains in the dorsal portion of the cell and the eyespot located under the short flagellum. Scale bar = 1 μm.*

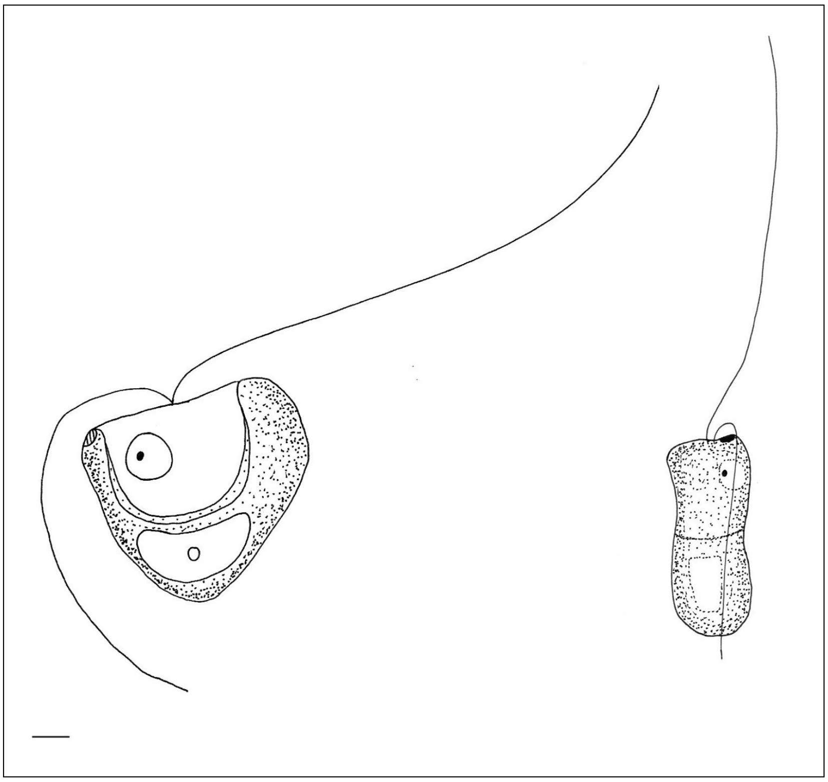

Figure 3.5. Nephroselmis pyriformis *drawn from fresh material. Left cell in lateral view with anterior cell face to the left of the image. Right cell in left-right view with anterior surface facing the reader. Chloroplast indicated by stippling effect. Nucleus present in ventral portion of the cell indicated by circular shape with dark nucleolus. Starch grains and pyrenoid are shown in the dorsal portion of the cell. Note the asymmetrical cell shape and the eyespot located under the short flagellum. The flange present in this species is not as prominent as that seen in* N. astigmatica. *Scale bar = 1 μm.*

are found on the short flagellum only. T-hair scales are found on both flagella. Only two layers of body scales are present. Underlayer scales are square and second layer body scales are small and stellate. Marine, known from Denmark, Finland, Mexico, Namibia (offshore Swakopmund), New Zealand (Wellington Harbour), Norway, South Africa (Fish Hoek), Thailand (Phuket Island), the United Kingdom (Cornwall, Devon and the Isle of Wight), the United States of America (North Carolina) and West Greenland (Godhavn).

Notes Nakayama *et al.* (2007) report that tip hairs are present in *Nephroselmis pyriformis*, citing Moestrup (1983) and Marin and Melkonian (1994), as well as their own paper, for the morphological features of *N. pyriformis* on which they report. Tip hairs were not present in the strains of *N. pyriformis* examined in the present study and are considered to be absent, as reported by Marin and Melkonian (1994).

3.6.5 *Nephroselmis rotunda* (Carter) Fott

Synonyms: *Bipedinomonas rotunda* Carter, *Heteromastix rotunda* (Carter) Manton
References: Carter (1937); Manton *et al.* (1965); Fott (1971)
Source: CCAP 1960/1, CCAP 1960/3 and Wits BB2

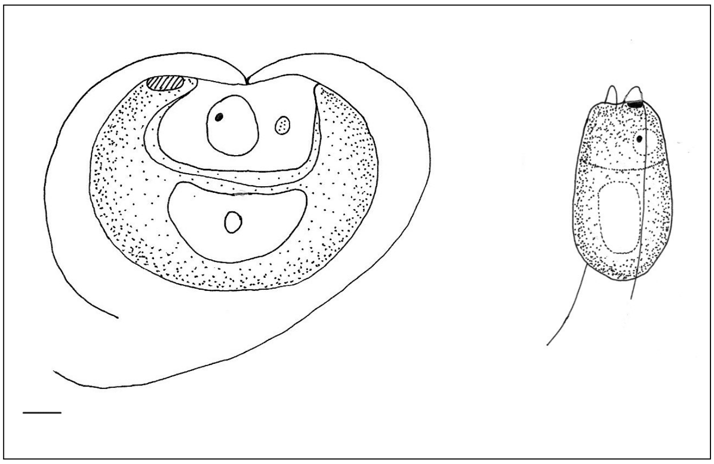

Figure 3.6. Nephroselmis rotunda *drawn from fresh material. Left cell in lateral view with anterior cell face to the left of the image. Right cell in left-right view with anterior surface facing the reader. Chloroplast indicated by stippling effect. Nucleus present in ventral portion of the cell indicated by circular shape with dark nucleolus. Starch grains and pyrenoid are shown in the dorsal portion of the cell. Note the round cell shape and the eyespot located under the short flagellum. A lipid globule is shown in the ventral portion of the cell. Scale bar = 1 μm.*

Figure: 3.6
Plates: 11 to 18

Cell length 5.00 μm ± 0.83 μm, cell height 4.54 μm ± 0.70 μm and cell width 3.18 μm ± 0.76 μm. The cell is round in shape and symmetrical around the flagellar insertion point in lateral view. One oval starch grain is typically present. The cup-shaped chloroplast extends anteriorly and posteriorly from the ventral surface to the dorsal surface. Thylakoid penetration of the pyrenoid is radial. A single eyespot is present under the short flagellum. The pigment siphonaxanthin is present. Large circular lipid globules are often present in the ventral half of the cell. Both flagella exhibit closed parking behavior. Three flagellar scale types are present (two flagellar scale layers and flagellar hair scales). Underlayer flagellar scales are pentagonal in shape and second layer flagellar scales are stellate. Third layer flagellar scales, pit scales and pit hairs are absent. The flagella are blunt-ended (flagellar hair point absent) and lack a tip hair. Pt-hair scales are absent from both flagella, while T-hair scales are present on both flagella. Three body scale layers are present. Underlayer scales are square and second layer body scales are small and stellate. 11 spines are found on the stellate, unipolar third layer body scales, which are particularly large. They may be absent in some cultures. Stellate body scales of intermediate size may sometimes be found in the flagellar pit region. Marine, known from South Africa (Langebaan Mouth and Palm Beach) and the United Kingdom (Cornwall, Devon, the Isle of Wight, Ryde and Yarmouth).

Notes This is the only species of *Nephroselmis* in which the second layer of flagellar scales are stellate rather than rod-shaped (Plate 16: Figure 5; Plate 18: Figure 6). Third layer body scales were absent from all cells in some cultures.

3.6.6 *Nephroselmis spinosa* Suda

Reference: Suda (2003)
Source: NIES 935
Figure: 3.7
Plates: 19 to 21

Cell length 8.64 μm $\pm$ 1.53 μm, cell height: 6.30 μm $\pm$ 0.71 μm and cell width 3.23 μm $\pm$ 0.59 μm. The cell is reniform (bean-shaped) in lateral view, resembling a flattened circle and is symmetrical around the flagellar insertion point. Three starch grains (plates) are arranged in a triangular formation in left-right view. The cup-shaped chloroplast extends anteriorly and posteriorly from the ventral surface to the dorsal surface. Thylakoid penetration of the pyrenoid is absent. A single eyespot is present under the short flagellum. The dorsal surface of the cell is tapered into a sharp keel in left-right view. The pigment siphonaxanthin is present. Both flagella exhibit open parking behaviour. Three flagellar scale types are present (two flagellar scale layers and flagellar hair scales). Underlayer flagellar scales are pentagonal in shape and second layer flagellar scales are rod-shaped. Third layer flagellar scales, pit scales and pit hairs are absent. The flagella are blunt-ended (flagellar hair point absent) and lack a tip hair. Pt-hair scales are absent from both flagella, while T-hair scales are present on both flagella. Four body scale layers are present. Underlayer scales are square and second layer body scales resemble a Maltese cross. 11 spines are found on the stellate, unipolar third layer body scales. The unipolar fourth layer body scales are immense ($\pm$ 1 μm) needle-like spines, consisting of five projections. The longest of these extends away from the cell surface and terminates in a small hook. The remaining four projections are arranged at the base of the spine and resemble four supporting feet. Marine, known from Western Australia (Port Hedland and Hamerin Pool).

Notes Several unique features characterise this species: the triangular-shaped starch grain (Plate 19: Figures 7 to 11; Plate 20: Figures 6 to 8), the absence of thylakoid penetration of the pyrenoid and the dorsal keel (Plate 19: Figures 7 to 11; Plate 20: Figures 6 and 8). The large needle-like spines of the outer body scale layers are unmistakable (Plate 20: Figures 3 and 4).

3.6.7 *Nephroselmis viridis* Inouye, Suda *et* Pienaar sp. ined.

References: Inouye *et al.* (1991); Young (1991)
Source: NIES 486
Figure: 3.8
Plates: 22 and 23

Cell length 5.93 μm $\pm$ 0.43 μm and cell height 5.64 μm $\pm$ 0.34 μm. Cell width is unknown. The cell is round in shape and symmetrical around the flagellar insertion point in lateral view. One oval starch grain is typically present. The cup-shaped chloroplast extends anteriorly and posteriorly from the ventral surface to the dorsal surface. Thylakoid penetration of the pyrenoid is ventral. A single eyespot is present under the short flagellum. A lens or disc-like structure is present between the pyrenoid and the plasmalemma on the dorsal side of the cell. The pigment siphonaxanthin is present. Both flagella exhibit closed flagellar parking behaviour. Four flagellar scale types are present (three flagellar scale layers and flagellar hair scales). Underlayer flagellar scales are pentagonal in shape and second layer flagellar scales are rod-shaped. Third layer flagellar scales are stellate. Pit

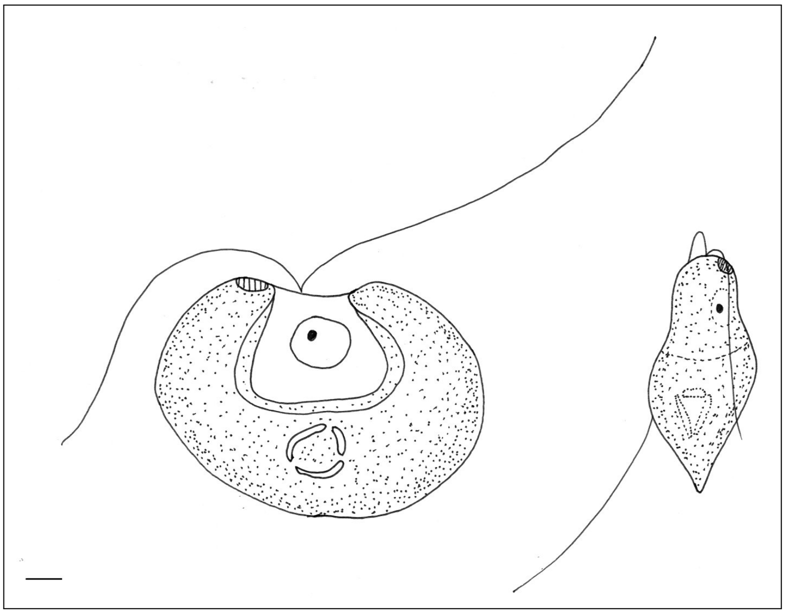

Figure 3.7. Nephroselmis spinosa *drawn from fresh material. Left cell in lateral view with anterior cell face to the left of the image. Right cell in left-right view with anterior surface facing the reader. Chloroplast indicated by stippling effect. Nucleus present in ventral portion of the cell indicated by circular shape with dark nucleolus. Note the characteristic triangular arrangement of the starch grains and the pointed keel at the dorsal surface. The eyespot is located under the short flagellum. Scale bar = 1 μm.*

scales and pit hairs are absent. The flagella are blunt-ended (flagellar hair point absent) and lack a tip hair. Pt-hair scales are found on the short flagellum only. T-hair scales are found on both flagella. Four body scale layers are present. Underlayer scales are square and second layer body scales resemble a paper windmill. 13 spines are found on the stellate, unipolar third layer body scales. The fourth layer body scales are multipolar scales with 26 spines. Marine, known from South Africa (Durban) and Japan.

Notes This species has not been officially described, although the name *N. viridis* is in general use. *N. viridis* is one of only two species of *Nephroselmis* in which third layer flagellar scales are found, the other being *N. olivacea* [not seen; Moestrup and Ettl (1979); Young (1991)]. The lens or disc-like structure in the region of the pyrenoid is also found in these two species only [not seen; Moestrup and Ettl (1979); Young (1991)].

3.7 Inadequately Known Species

The following species are considered unconfirmed, as an extensive search of the literature and the Internet yielded only original species descriptions with light microscopic drawings, or reproductions of these in other papers. The only exception is *N. gaoae*, which is inadequately known, as the quality of the micrographs provided did not allow for a detailed description of the morphology and ultrastructure of this species. None of these species are available from any culture collections, although some have been available previously. None of these species were included in the present study.

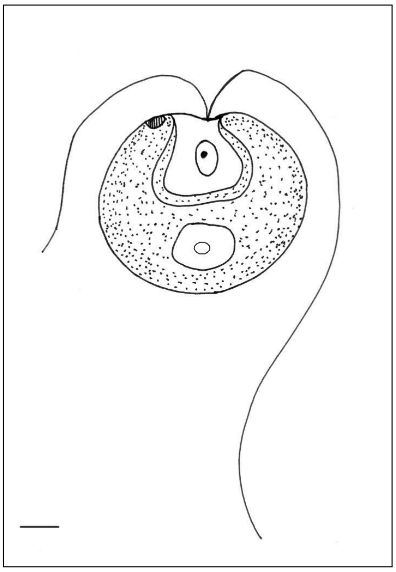

Figure 3.8. Nephroselmis viridis *sp. ined. drawn from fresh material. Left cell in lateral view with anterior cell face to the left of the image. Left-right view of the cell was not seen in any of the material examined and is not included in Young (1991). Chloroplast indicated by stippling effect. Nucleus present in ventral portion of the cell indicated by circular shape with dark nucleolus. Starch grains and pyrenoid are shown in the dorsal portion of the cell. The eyespot is located under the short flagellum. Scale bar = 1 μm.*

3.7.1 *Nephroselmis discoidea* Skuja

References: Skuja (1948); Fott (1971); Ettl (1983)
Source: Not available in any culture collections.
Figures: 3.9, 3.10 and 3.11

This species is considered to be freshwater, as it has been recorded from lakes and ponds in Czechoslovakia and Sweden (Ettl, 1983). However, Fott (1971) considers *N. discoidea* and *N. olivacea* to be identical, as they often occur together and are morphologically the same (Figure 3.9). As no electron microscopy of this species has been reported, the scale morphology of *N. discoidea* is unknown.

It is interesting to note that Ettl, one of the two authors responsible for the detailed morphological and ultrastructural investigation of *N. olivacea* (Moestrup and Ettl, 1979), reports on *N. discoidea* (Ettl, 1983). This implies, in contradiction to the suggestion of (Fott, 1971), that *N. discoidea* is <u>not</u> identical to *N. olivacea.* It is also possible though that Ettl simply included the species without necessarily having investigated it in detail (the images in Ettl (1983) are redrawn from Skuja (1948); see Figure 3.10), as it would appear that it was considered at the time to be a valid species of *Nephroselmis.* The cell at the bottom of Figure 3.10 is presumably undergoing cell division, as two eyespots are present, and the chloroplast and pyrenoid appear to have divided. The flagella of *Nephroselmis* species typically arise from a small depression, so the presence of a small papilla from which the flagella arise in the top cell is atypical, as is the location of the eyespot in the same cell.

The single micrograph of an unidentified freshwater species of *Nephroselmis* included

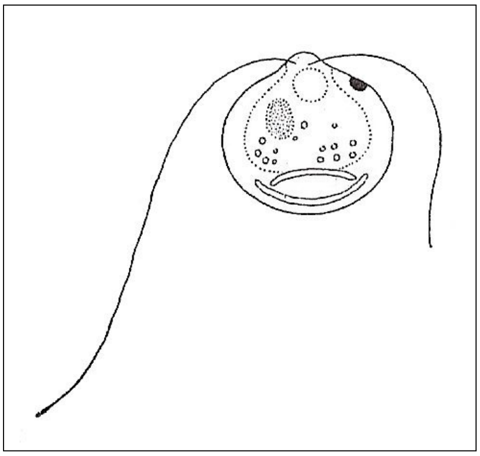

Figure 3.9. Nephroselmis discoidea*, reproduced from Fott (1971: Figure 3c). Note the similarity to* N. olivacea*, particularly with respect to the number of starch grains and their shape.*

in Manton *et al.* (1965) is reproduced here as Figure 3.11. Three layers of scales are visible on both the body and the flagellum. The scales of the outer (third) body and flagellum layers are stellate in shape. These third layer body scales are different from those found in the freshwater species *N. olivacea* (Plate 8: Figure 6), and from those found in *N. viridis* (Plate 23: Figure 4), a marine species which is closely related to *N. olivacea.* They are, however, similar in size and shape to the outer (third) layer body scales found in *N. rotunda* (Plate 16: Figures 1 to 4), which is also marine. Third layer flagellar scales are found in *N. olivacea* and *N. viridis* only. The unidentified species is not *N. olivacea*, and as it seems likely that *N. discoidea* and *N. olivacea* are identical, it follows that the unidentified species cannot be *N. discoidea*, as suggested by Young (1991). The identity of this freshwater species remains unresolved, but it is very likely that it is closely related to *N. olivacea* and *N. viridis.*

3.7.2 *Nephroselmis fissa* Lackey

Reference: Lackey (1940)
Source: Not available in any culture collections.
Figure: 3.12

Original description from Lackey (1940):

> *Length 28 µm. Width 25 µm. This form is almost circular in outline, or a little broader than long. A median depression divides it into right and left halves. It is greatly flattened, hardly exceeding 8 µm in thickness. The membrane is firm and smooth. A massive bright green cup shaped chloroplast is present and there is a large basal ring shaped pyrenoid enclosed in a shell. Two subequal flagella are present but they arise separately in the right and left halves. Two stigmas are similarly located near the flagellar bases. No reproduction observed. Swimming movements not seen, since all specimens found were quiescent. The organism was never common. A few individuals would appear in an occasional sample, in the sediment from traps as a rule but on occasion it was found in centrifuged material. The medium division and the location and separation of*

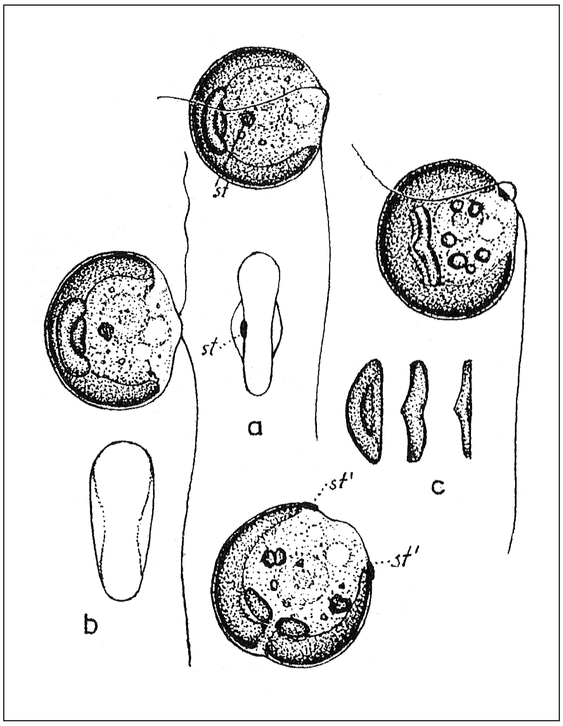

Figure 3.10. Nephroselmis discoidea, *reproduced from Ettl (1983: Figure 114), after Skuja (1948). Sub-figures labeled by Ettl (1983) as follows: (a) apical view, (b) narrow side, (c) starch grains; st = stigma.*

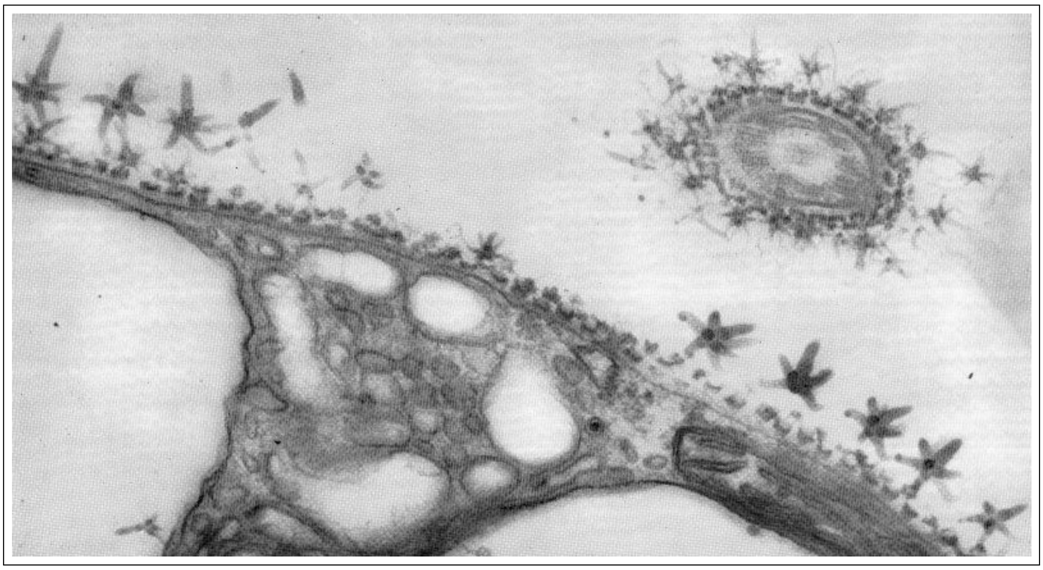

Figure 3.11. *Unidentified freshwater* Nephroselmis, *reproduced from Manton* et al. *(1965: Figure 43). Original caption from Manton* et al. *(1965):* Unidentified species of *Heteromastix* [...] isolated from fresh water at [...] Windermere [...] showing general agreement with other named taxa in scale structure and scale arrangement on body surface and flagellar surface [...].

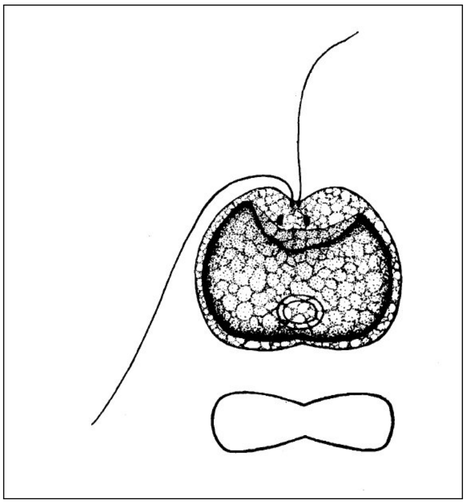

Figure 3.12. *The only drawings provided in the original description of* Nephroselmis fissa*, reproduced from Lackey (1940: Figure 9). Two eyespots are shown near the flagellar insertion point in the top diagram. The outline diagram at the bottom is labeled by Lackey as a cross-section.*

> *the flagella and stigmas are strikingly suggestive of a dividing* Pedinomonas*, near* P. rotunda *as described by Korschikoff from muddy pools in the Charkow region.* Pedinomonas *was never seen, however, and this organism occurred with sufficient frequency to indicate it was the normal vegetative state; also the organism would live several days in moist chambers, and move about, but never divide.* Heteromastix angulata *Korschikoff is common in Scioto River (Ohio) plankton; it has subequal flagella, is roughly hexagonal in outline and commonly lacks a stigma. The flagella of this marine form are almost equal, and it is not angulate. Class Chlorophyceae, Order Volvocales, Family Polyblepharidaceae.*

The cell dimensions provided for this species considerably exceed those of any other recorded species of *Nephroselmis*. No other species of *Nephroselmis* are recorded as having two stigmata (Figure 3.12). Lackey describes the specimen as a new species, yet mentions characters as being "strikingly suggestive" of a different group. *Nephroselmis olivacea* (*Heteromastix angulata*) has a distinct stigma, which makes the author's comments that this organism "commonly lacks a stigma" questionable. This also possibly raises a question regarding whether *N. fissa* possess two stigmata. No reference is provided for the samples examined by Korschikoff "from muddy pools in the Charkow area". The species description for *N. fissa* is briefly emended by Inouye and Pienaar (1984), who also mention that it is possibly not a member of the genus *Nephroselmis*. The details provided by Lackey are unsufficient to confirm the idenity of the species examined.

3.7.3 *Nephroselmis gaoae* Tseng and Chen

Reference: Tseng *et al.* (1994)
Source: Tseng *et al.* (1994) report that this species was sent to the ASIO Algal Culture Collection as specimen 84008 and was maintained there as culture number 1050. It is no longer available from any culture collections.

This species, which was recorded from Qingdao in China, exists in only one reference (Tseng *et al.*, 1994). It possesses a single chloroplast, a large circular or elliptical pyrenoid with a large starch sheath. Thylakoid penetration of the pyrenoid is radial (see Tseng *et al.*, 1994: Plate 1: Figure 4). The stigma is large. As noted previously, Tseng *et al.* (1994) consider the eyespot structure of *N. gaoae* to be unique among all algal groups, as it is composed of rod-like structures. However, rod-like structures have been reported in the eyespots of two species of *Pyramimonas*: *P. chlorina* Sym and Pienaar (1997: Figure 38) and *P. formosa* Sym and Pienaar (1999: Figure 26) (see page 23). Three layers of body scales and two layers of flagellar scales are present. The second layer of body scales are stellate. Preliminary morphological studies suggest that this species is closely related to *N. rotunda* (see Section 3.9 for discussion), but morphological information from the original description was insufficient to provide a full data set for the morphological cladistic analysis. This species was not included in the present study.

3.7.4 *Nephroselmis marina* Schiller

Synonym: *Sennia marina* (Schiller) Skuja
Reference: Schiller (1926) Source: Not available in any culture collections.
Figure: 3.13

Translation of the original description by Schiller (1926):

> *Cell shape irregular, kidney- or bean-shaped, laterally somewhat compressed, ventral side significantly bent, dorsal half smaller, groove situated closer to the front end, so not exactly on the equatorial plane, unsymmetrical toward the median, slightly spreading over to the other side, central-median is pronounced to form a short, downward gullet. Skin layer soft, without any differentiation. Cell metabolic. Two chromatophores, yellow in color, bent, hollow, slightly flapped. Length 6 – 8 µm, Width 4 – 6 µm. Two flagella, unequal in length, divergent, the longer one toward the back, the shorter one toward the front. Stigma, pyrenoid, vacuoles and trichocytes cannot be seen. Did not observe division. Vegetation Time: Spring, Summer. Habitat: Southern Adriatic, 0 – 10 m. Sociological Behaviour: Spread, Retreating, Grouped.* Nephroselmis marina *differs from* Nephroselmis olivacea *Stein (which is better known thanks to the work of Pascher) in that its two halves are unequal in size, it is laterally somewhat compressed and flagella differ significantly in length. These differences are significant, but I would not consider them significant enough to declare a new species. Therefore we can add a new marine specimen to Boehmen [Bohemia] and Stein's* N. olivana.

This is an anomalous species within the genus. Making mention that the differences are not sufficient to "declare a new species" within a new species description is somewhat confusing. No data describing cell thickness is provided. The cell possesses two chloroplasts, does not possess an eyespot or a pyrenoid, and is capable of metaboly[17] (Inouye and Pienaar, 1984; Suda, 2003). All of these characters are atypical of the genus *Nephroselmis*. Suggestions have been made that *N. marina* should be moved to some other genus (Moestrup, 1983; Inouye and Pienaar, 1984; Suda, 2003). It is interesting to note that, while *N. olivacea* is considered to be the only freshwater species in the genus, Stein's description mentions its habitat as the Southern Adriatic Sea, which is part of the Mediterranean Sea. However,

[17] The ability of a cell to change its shape.

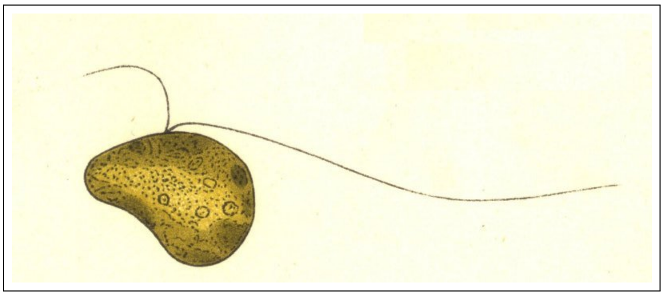

Figure 3.13. *The only drawing provided in the original description of* Nephroselmis marina, *reproduced from Schiller (1926: Plate 3: Figure 13).*

seven major rivers join the Adriatic Sea, so it is possible that the sample of *N. olivacea* which Stein encountered had washed downstream into the sea. The mention of "*N. olivana*" is surely a typographical error. No other references to this specific epithet can be found, despite extensive searching of the literature and the Internet. It is worth noting that the name "olivana" is a combination of "<u>oliva</u>cea" and "mari<u>na</u>", which further supports the suggestion that this name may well be the result a typographical error.

3.7.5 *Nephroselmis minuta* Carter

Synonym: *Heteromastix minuta* Carter
Reference: Carter (1937)
Source: No longer available from any culture collections (see Notes).
Figure: 3.14

Original description from Carter (1937):

> *Cells very small, naked, sub-elliptical, with truncated apical end; basal chloroplast with large pyrenoid; stigma located toward the front of the cell on the side; two subequal flagella. Approximate dimensions: 3 by 3.5 by 1.5 µm. Habitat: [...] very occasional in all zones [of the small brackish pool at Bembridge, Isle of Wight], usually from October to February. This organism differs from* Heteromastix angulata *Korschikoff [...] in its much smaller dimensions and more rounded cells. The stigma is further of quite a normal red colour, whereas in* H. angulata *it is said to be rather unusual in colour. The flagella are quite similar to those or Korschikoff's form. The presence of a small granular body in the middle of the living cell is a variable feature [...]. The chromatophore is similar to that of* Bipedinomonas *spp. in form and colour, and there is a basal pyrenoid. Division stages have been observed. At an early stage the pyrenoid divides and a second stigma arises in very much the same way as described for* Bipedinomonas *[...]. In some dividing individuals a conspicuous beak of colourless protoplasm is to be seen at the anterior end, which may show a distinctly bifid appearance although the rest of the protoplast may not yet show any sign of fission [...].*

Notes Carter's description mentions that *Nephroselmis minuta* cells are "naked". If this is correct, the organism would not be a member of the prasinophytes, as all other members possess scales. However, Carter undertook her work during the first half of the 20^{th} century

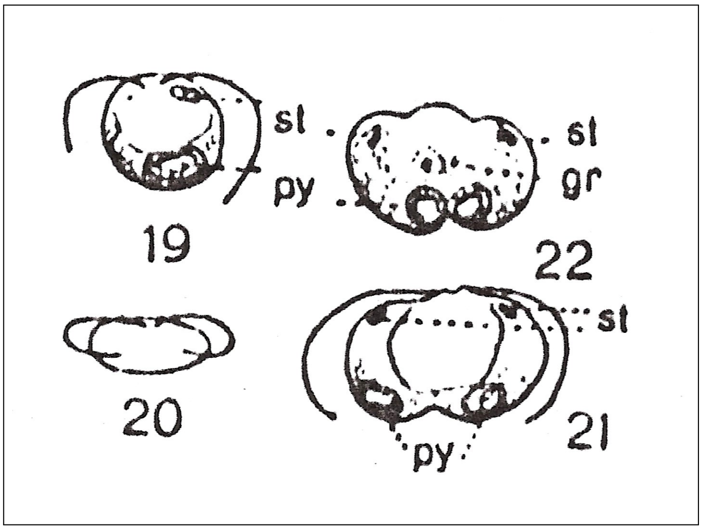

Figure 3.14. Nephroselmis minuta*, reproduced from Carter (1937: Plate 1);* gr = *starch grain;* py = *pyrenoid;* st = *stigma.*

and had access only to light microscopes. Prasinophyte scales are not visible under the light microscope. The term "naked" as used by Carter would indicate the absence of any type of periplast material. A strain of *Nephroselmis minuta* (SCCAP K-0022) of suspected Finnish origin [as mentioned in an *rbc*L phylogenetic study of various Prasinophycean and Pedinophycean genera by Daugbjerg *et al.* (1995)] from the Scandanavian Culture Collection of Algae and Protozoa is no longer alive (N Larsen, pers. comm., 2007). The only sequences of *rbc*L data for *Nephroselmis* species available on GenBank are those submitted by Daugbjerg *et al.* (1995), for *N. minuta* and *N. olivacea*.

3.7.6 Spurious Species

References to the following two freshwater species are found in Bourrelly (1972) and Ettl (1983) and their identity could not be confirmed. The original descriptions by Skvortzov could not be traced.

Nephroselmis ellipsoidea (Skvortzov) Bourrelly (Figure 3.15)
= *Klebsimastix ellipsoidea* Skvortzov
= *Klebsiella ellipsoidea* Skvortzov

Nephroselmis hemisphaerica (Skvortzov) Bourrelly (Figure 3.16)
= *Klebsimastix hemisphaerica* Skvortzov
= *Klebsiella hemisphaerica* Skvortzov

3.8 Species No Longer Belonging To *Nephroselmis*

There are two instances in which a species previously considered to be a member of *Nephroselmis* has been moved to another genus:

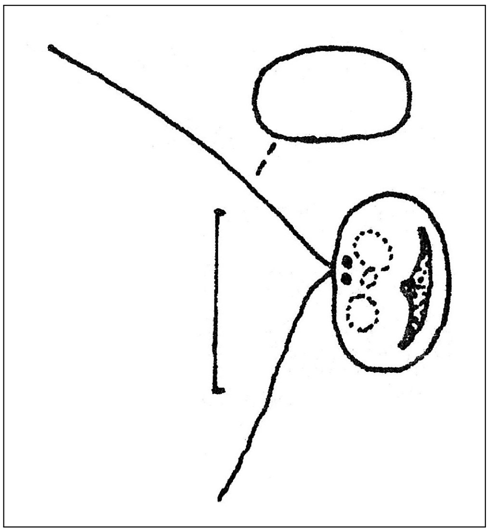

Figure 3.15. Nephroselmis ellipsoidea*, reproduced from Bourrelly (1972: Plate 135: Figure 2). No size measurement is provided for the scale bar, nor are any details of the internal structures given. It would appear that two eyespots are present at the flagellar insertion point. The identity of this species remains uncertain.*

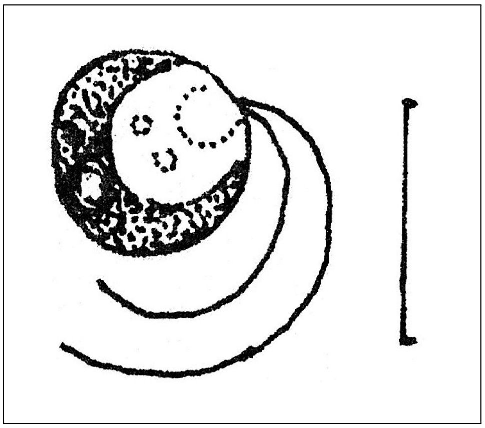

Figure 3.16. Nephroselmis hemisphaerica*, reproduced from Bourrelly (1972: Plate 135: Figure 3). No size measurement is provided for the scale bar, nor are any details of the internal structures given. The cup-shaped chloroplast and the position of what appears to be a pyrenoid towards the dorsal surface of the cell are suggestive, but not definitive, of* Nephroselmis*. The position of the flagella is atypical of* Nephroselmis*. The identity of this species remains uncertain.*

3.8.1 *Mamiella gilva* (Parke & Rayns) Moestrup

References: Parke and Rayns (1964); Moestrup (1984a)

Nephroselmis gilva Parke & Rayns is now the only member of the genus *Mamiella*.

3.8.2 *Chroomonas violacea* (Kufferath) Compère

References: Kufferath (1942); Compère (1987)

This species is reported as *Nephroselmis violacea* Kufferath on the AlgaeBase website (Guiry and Guiry, 2008). The text from Compère (1987) is as follows, translated from the original French via *http://babel.altavista.com*:

> *This species has purple [chloroplasts] and a furrow equipped with lines of trichocystes; it thus does not belong to the [genus]* Nephroselmis *Stein (Prasinophyceae). The shape of the cell, the longitudinal provision of the furrow and the lines of trichocystes rather classify it in the [genus]* Chroomonas *[...].*

3.9 Cladistic Analysis of Morphological Data

Thirty-seven unordered characters (binary and multistate), examined for seven *Nephroselmis* species and two outgroups (*Dolichomastix tenuilepis* and *Pseudoscourfieldia marina*), were included in the morphological cladistic analysis. The maximum parsimony heuristic search (all characters unweighted) yielded two equally most parsimonious (EMP) trees (Figures 3.17A and 3.17B; consensus tree in Figure 3.17C). These EMP trees each had a length of 72, consistency index (CI) of 0.83, retention index (RI) of 0.63 and rescaled consistency index (RC) of 0.52. Of the 46 characters, 9 were constant and excluded, 19 were parsimony-informative and 18 were parsimony-uninformative. A 1000-replicate bootstrap analysis reported weak support for many nodes (Figure 3.17), but strong support for the genus and the clade with *N. olivacea* and *N. viridis*. The position of *Nephroselmis rotunda* differed between the two EMP trees: *N. pyriformis* appeared as sister to *N. rotunda* in the first tree (Figure 3.17A), but *N. rotunda* appeared in a clade with *N. pyriformis* in the second tree (Figure 3.17B). This difference resulted in the resolution for these two species collapsing in the consensus tree (Figure 3.17C).

A maximum parsimony heuristic search after reweighting the characters in *PAUP** (reweighting with maximum fit on the rescaled consistency index) produced only one tree, for which bootstrap support was strong for two nodes and greater than 65% for all nodes within *Nephroselmis* (Figure 3.18). Bootstrap support for *Nephroselmis* was strong at 93%. The topology of the tree after reweighting is the same as that of the first of the two EMP trees in the unweighted analysis. The number of parsimony-informative sites remained at 19 after reweighting. No difference in the results of the analyses was found when the DELTRAN character-state optimization was used instead of the ACCTRAN method. Character weights after reweighting are given in Table 3.3. Nine characters were reweighted to values other than 1. Of these nine, three were reweighted to 0: Character 2 (Lateral symmetry around flagellar insertion), Character 31 (Pit hairs present/absent) and Character 38 (Eyespot presence and position).

Inclusion of *Nephroselmis gaoae* in the analysis using morphological data extracted from Tseng *et al.* (1994), revealed that this species grouped with *N. rotunda* (not shown here). Morphological data for this species was incomplete however, as only one published

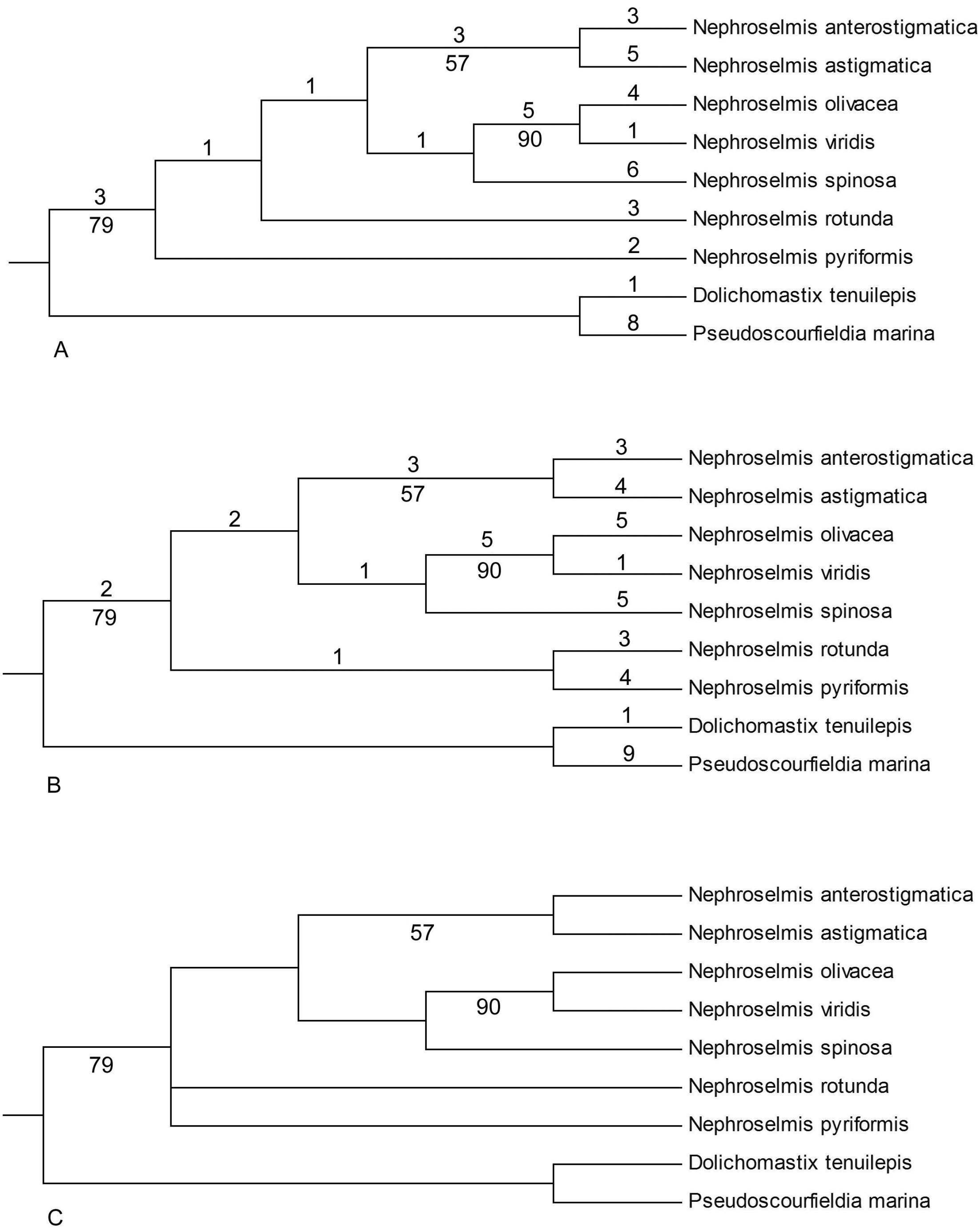

Figure 3.17. *Results from a maximum parsimony heuristic search on unweighted morphological data for seven confirmed species of* Nephroselmis *and two outgroups. Trees were rooted with* Dolichomastix tenuilepis *and* Pseudoscourfieldia marina*. Constant characters were excluded. Minimum branch lengths are shown above the line and bootstrap values above 50% from 1000 replicates below the line.* ***[A]*** *Tree one and* ***[B]*** *tree two of two equally most parsimonious trees, and* ***[C]*** *strict consensus of the two EMP trees. For all three trees, length is 72, consistency index (CI) is 0.83, retention index (RI) is 0.63 and rescaled consistency index (RC) is 0.52.*

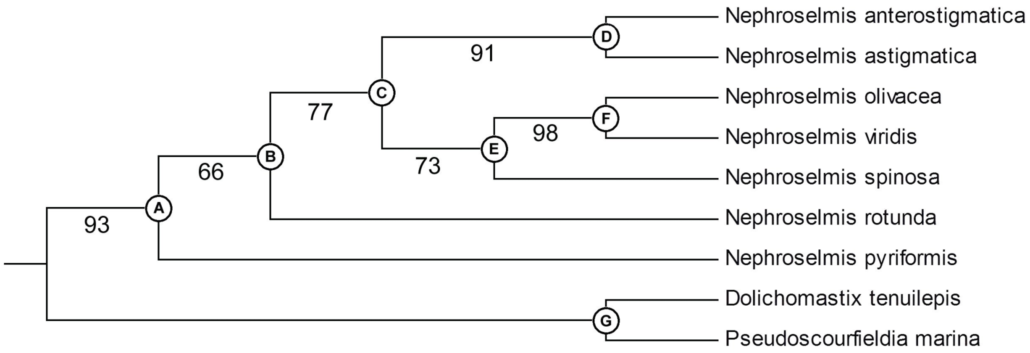

Figure 3.18. *Single most parsimonious tree from a heuristic search on reweighted morphological data for seven confirmed species of* Nephroselmis *and two outgroups. The tree was rooted with* Dolichomastix tenuilepis *and* Pseudoscourfieldia marina. *Bootstrap values above 50% from 1000 replicates below the line.*

reference exists and the organism was not available from any culture collection. In order to minimize missing data, it was excluded from the final analyses.

The results of the unweighted and weighted morphological cladistic analysis (Figures 3.17 and 3.18) show that *Nephroselmis* is monophyletic, with strong bootstrap support (79% for unweighted and 93% for reweighted) for the genus. The topology of the reweighted tree (Figure 3.18) is the same as the first of the two unweighted trees (Figure 3.17A). The position of *N. rotunda* and *N. pyriformis* is the only difference between the two unweighted trees (Figures 3.17A and 3.17B) – in the consensus of these two trees (Figure 3.17C), the node supporting *N. rotunda* and *N. pyriformis* has collapsed. Bootstrap support for the clade containing *N. anterostigmatica* and *N. astigmatica* (Clade D in Figure 3.18) is weak in the unweighted analysis (57%), but is strong in the reweighted analysis (91%). Clade F in Figure 3.18, containing *N. olivacea* and *N. viridis*, is robust, showing strong bootstrap support in both the unweighted and reweighted analyses. Fairly strong bootstrap support is also present for the clades containing *N. olivacea*, *N. viridis* and *N. spinosa* (Clade E in Figure 3.18) and the clade which includes all *Nephroselmis* species except *N. pyriformis* and *N. rotunda* (Clade C in Figure 3.18). Moderate support (66%) exists in the reweighted analysis for the clade containing all species of *Nephroselmis* excluding *N. pyriformis* (Clade B in Figure 3.18); this was the node which collapsed in the consensus tree (Figure 3.17C).

3.9.1 Character Performance and Character Change List

Table 3.3 shows character diagnostics for the two unweighted trees, the one reweighted tree, and the reweighted character values mentioned previously. Constant characters were excluded. Characters with an RI value of "0/0" in Table 3.3 indicate that character states are autapomorphic; those with an RI value of "1" are synapomorphic (with no homoplasy). A CI value of "1" for multistate characters indicates that the character state was derived only once. Character changes from the reweighted analysis, mapped onto the reweighted tree, are shown in Figure 3.19. This figure shows that there are 29 non-homoplasious apomorphies and 8 homoplasious apomorphies (characters 2, 5, 7, 8, 13, 31, 33 and 42), giving a total of 37 characters. 9 characters are constant (excluded).

Table 3.4 lists the autapomorphies for each species of *Nephroselmis*, as determined from Figure 3.19. The synapomorphic characters which support the various clades (as shown in Figure 3.18) are provided in Figure 3.20.

Table 3.3. Morphological character diagnostics for the two unweighted and one reweighted tree, and reweighted character values, for the seven confirmed *Nephroselmis* species and two outgroups

Character	Tree 1			Tree 2			RW			RWV
	TS	**CI**	**RI**	**TS**	**CI**	**RI**	**TS**	**CI**	**RI**	
1 (shap)	4	1	1	4	1	1	4	1	1	1
2 (symm)	3	0.33	0	3	0.33	0	3	0.33	0	**0**
3 (#stgrn)	2	1	0/0	2	1	0/0	2	1	0/0	1
4 (stgrnshp)	3	1	0/0	3	1	0/0	3	1	0/0	1
5 (thyl)	4	0.50	0	3	0.67	0.50	4	0.50	0	**0.33**
7 (shflpark)	3	0.33	0.33	3	0.33	0.33	3	0.33	0.33	**0.11**
8 (lnflpark)	2	0.50	0.50	2	0.50	0.50	2	0.50	0.50	**0.25**
9 (#bodysc)	4	1	1	4	1	1	4	1	1	1
11 (bl1sh)	1	1	0/0	1	1	0/0	1	1	0/0	1
12 (bl2pa)	1	1	0/0	1	1	0/0	1	1	0/0	1
13 (bl2sh)	4	0.75	0.50	4	0.75	0.50	4	0.75	0.50	**0.38**
14 (bl3pa)	1	1	1	2	0.50	0.50	1	1	1	1
15 (bl3#sp)	2	1	0/0	2	1	0/0	2	1	0/0	1
17 (bl4pa)	1	1	1	1	1	1	1	1	1	1
18 (bl4#sp)	4	1	0/0	4	1	0/0	4	1	0/0	1
19 (bl4pol)	2	1	1	2	1	1	2	1	1	1
20 (bl5pa)	1	1	0/0	1	1	0/0	1	1	0/0	1
23 (#flagsc)	2	1	1	2	1	1	2	1	1	1
25 (fl1)	1	1	0/0	1	1	0/0	1	1	0/0	1
26 (fl2pa)	1	1	0/0	1	1	0/0	1	1	0/0	1
27 (fl2)	1	1	0/0	1	1	0/0	1	1	0/0	1
28 (fl3pa)	1	1	1	1	1	1	1	1	1	1
29 (fl3)	1	1	0/0	1	1	0/0	1	1	0/0	1
30 (pitsc)	1	1	0/0	1	1	0/0	1	1	0/0	1
31 (pithr)	2	0.50	0	2	0.50	0	2	0.50	0	**0**
32 (flhairpt)	1	1	0/0	1	1	0/0	1	1	0/0	1
33 (ptshort)	2	0.50	0.50	2	0.50	0.50	2	0.50	0.50	**0.25**
34 (ptlong)	1	1	0/0	1	1	0/0	1	1	0/0	1
37 (tiphr)	1	1	1	1	1	1	1	1	1	1
38 (eye)	4	0.75	0	4	0.75	0	4	0.75	0	**0**
39 (hab)	1	1	0/0	1	1	0/0	1	1	0/0	1
40 (lens)	1	1	1	1	1	1	1	1	1	1
41 (keel)	1	1	0/0	1	1	0/0	1	1	0/0	1
42 (flange)	2	0.50	0.50	2	0.50	0.50	2	0.50	0.50	**0.25**
43 (sxser)	1	1	0/0	1	1	0/0	1	1	0/0	1
44 (sxtype)	4	1	0/0	4	1	0/0	4	1	0/0	1
45 (lutein)	1	1	1	1	1	1	1	1	1	1

TS = Tree Steps. CI = Consistency Index. RI = Retention Index; RI values of "0/0" indicate that the character is uninformative (autapomorphic). RW = Reweighted Tree. RWV = Character Values for Reweighted Tree; Values other than "1" indicated in bold. All fractional values rounded to two decimal places. Character labels: (1) Cell shape in lateral view, (2) Lateral symmetry around flagellar insertion, (3) Number of starch grains, (4) Starch grain shape, (5) Thylakoid penetration, (7) Short flagellum parking, (8) Long flagellum parking, (9) Number of body scale layers, (11) Body scale layer 1 shape, (12) Body scale layer 2 present/absent, (13) Body scale layer 2 shape, (14) Body scale layer 3 present/absent, (15) Body scale layer 3 number of spines, (17) Body scale layer 4 present/absent, (18) Body scale layer 4 number of spines, (19) Body scale layer 4 spine polarity, (20) Body scale layer 5 present/absent, (23) Number of flagellar scale types, (25) Flagellar scale 1 shape, (26) Flagellar scale 2 present/absent, (27) Flagellar scale 2 shape, (28) Flagellar scale 3 present/absent, (29) Flagellar scale 3 shape, (30) Pit scales present/absent, (31) Pit hairs present/absent, (32) Flagellar hair point present/absent, (33) Pt-hair scales on short flagellum present/absent, (34) Pt-hair scales on long flagellum present/absent, (37) Tip hair present/absent, (38) Eyespot presence and position, (39) Habitat, (40) Lens structure near pyrenoid present/absent, (41) Keel present/absent, (42) Flange present/absent, (43) Siphonaxanthin pigment series present/absent, (44) Siphonaxanthin pigment type, (45) Lutein content of total carotenoids. The detailed character list is provided in Table 2.3.

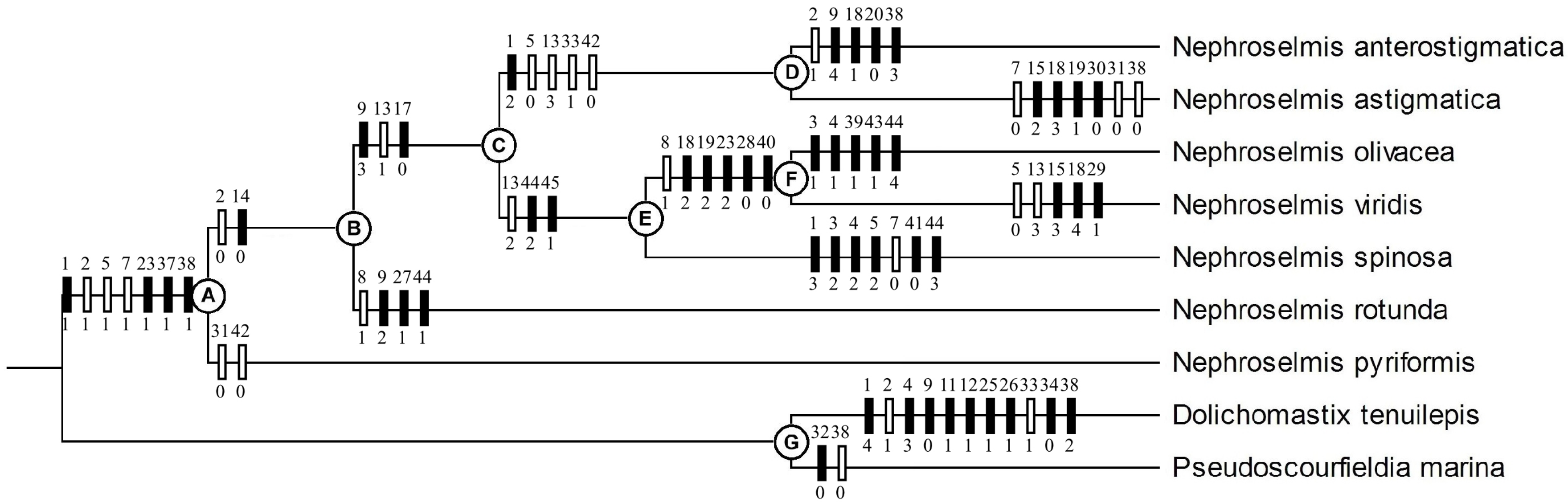

Figure 3.19. *Reweighted morphological tree showing character changes for each character. Filled bars indicate non-homoplasious apomorphies; unfilled bars indicate homoplasious apomorphies with parallelism or reversal. Non-homoplasious apomorphies on terminal branches are autapomorphies for that species (see Table 3.4). Character numbers are shown above the bar; character state values below the bar. The detailed list of characters and character states appears in Table 2.3.*

Table 3.4. Autapomorphies for each species of *Nephroselmis*, as determined from Figure 3.19

Species	Autapomorphic Character and State
N. anterostigmatica	9, 4: Five body scale layers 18, 1: 16 spines on fourth layer body scales 20, 0: Fifth body scale layer present 38, 3: Eyespot present on anterior cell surface
N. astigmatica	15, 2: 33 spines on third body scale layer 18, 3: 26 spines on fourth body scale layer 19, 1: Fourth body scale layer bipolar 30, 0: Pit scales present 38, 0: Eyespot absent
N. olivacea	3, 1: Two starch grains present 4, 1: Starch grains watch-glass-shaped 39, 1: Habitat freshwater 43, 1: Siphonaxanthin absent 44, 4: Siphonaxanthin Type V
N. pyriformis	2, 1: Asymmetrical cell shape* 31, 0: Pit hairs present* 42, 0: Flange present*
N. rotunda	9, 2: Three body scale layers 27, 1: Flagellar scale 2 shape stellate 44, 1: Siphonaxanthin Type II
N. spinosa	1, 3: Cell shape reniform 3, 2: Three starch grains 4, 2: Triangular starch grains 5, 2: No thylakoid penetration 41, 0: Keel present 44, 3: Siphonaxanthin Type IV
N. viridis	15, 3: 13 spines on third body scale layer 18, 4: 24 spines on fourth body scale layer 29, 1: Flagellar scale layer 3 stellate

*Homoplasious; no non-homoplasious autapomorphies were present for this species.

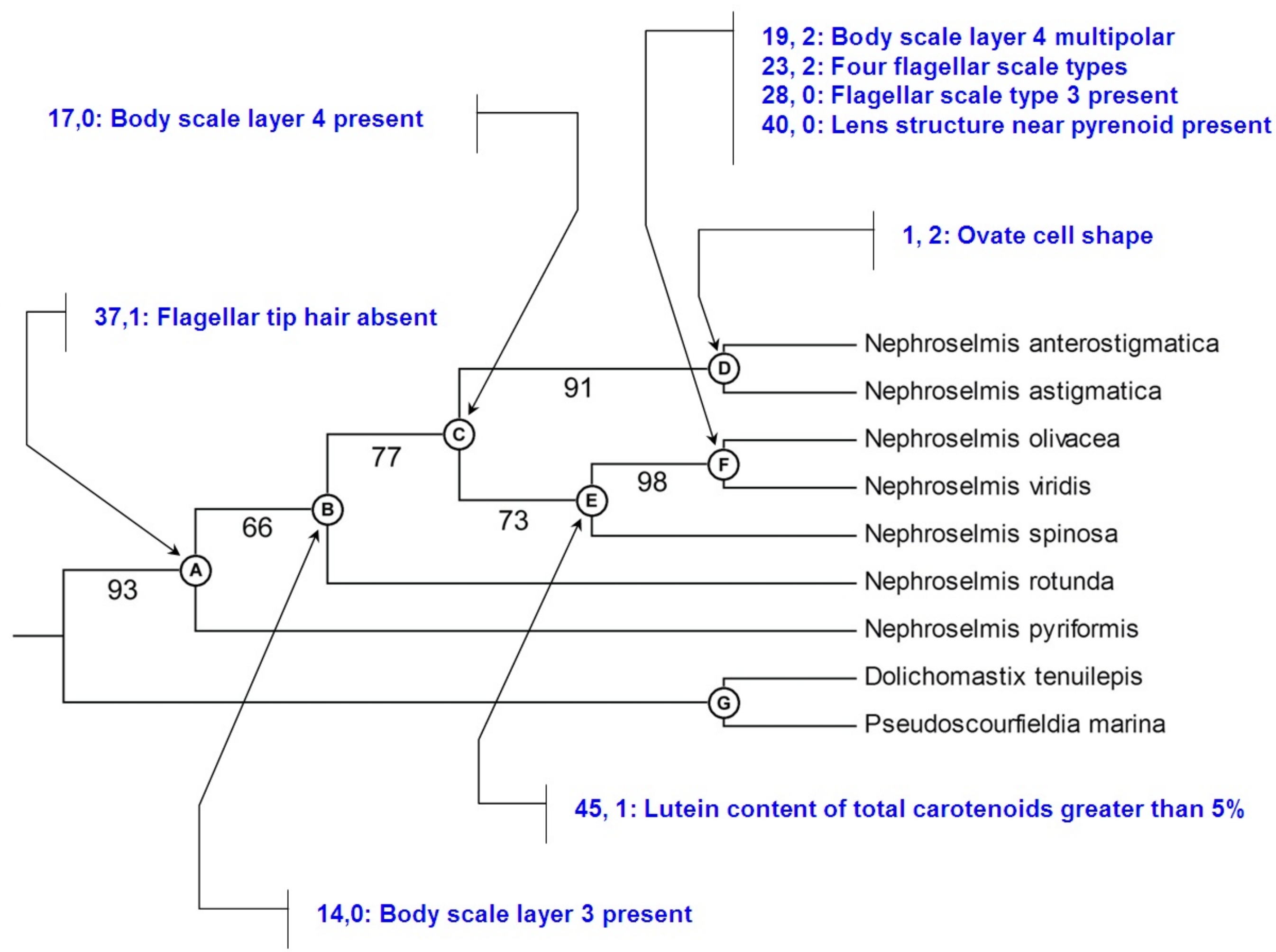

Figure 3.20. *Non-homoplasious synapomorphic characters which support the various nodes found in* Nephroselmis, *as determined from Figure 3.19, mapped onto the reweighted morphological tree (Figure 3.18). Note that synapomorphies which do not change in the descendent taxa are shown. The detailed character list is provided in Table 2.3.*

3.10 Cladistic Analysis of Molecular Data

3.10.1 Sequence Characteristics

Lengths of the trimmed and aligned sequences of the portion of the 18S gene investigated in this study ranged from 826 to 858 bases, with an average length of 850 bases (Table 3.5). A gap-opening penalty of 13 and gap-extension penalty of 5 for *ClustalW* slow pairwise and multiple sequence alignment was used, as determined by the analysis detailed in Section 2.5.3. The aligned sequence data used in the molecular analysis is provided for reference in Appendix E.

3.10.2 Sequence Analysis

Maximum parsimony heuristic searches in *PAUP** yielded one most parsimonious tree (Figure 3.21), with a length of 652, CI of 0.57, RI of 0.75 and RC of 0.43. The tree was rooted with *Prasinococcus capsulatus*. Of the 868 characters, 602 were constant and excluded, 57 were variable and parsimony-uninformative and 209 were parsimony-informative. A tree with the same topology and statistics was obtained when the DELTRAN rather than the ACCTRAN character-state optimization method was used in *PAUP**. The two methods of indel coding (using *GapCoder* and *seqindelcode*) used did not result in better trees. The results for both methods were generally similar, with nodes within the *Nephroselmis* group collapsing (not shown here). It was decided not to include the indel coded data in the final analyses. At least one indel was present in 82 of the 868 positions in the final aligned seqeuence (see Appendix E).

3.10.3 An anomolous insertion in *Nephroselmis viridis* sp. ined.

An insertion of 437 bases, starting at base 329, was found in the sequence data for *Nephroselmis viridis* sp. ined. Sequence data for *Nephroselmis* excluding the GenBank sequences, was preliminarily aligned with *ClustalW*. This resulted in a "right-aligned" alignment – the additional 437 bases of *N. viridis* occurred on their own on the left of the alignment. When the same dataset was aligned with *Muscle*, the additional 437 bases of *N. viridis* occurred on their own in the middle of the alignment. The same result was obtained with *ClustalW* and *Muscle* when the full dataset, including all GenBank sequences, was aligned. The alignment in which the additional bases occurred on the left was not good and was disregarded. The alignment in which the additional bases occurred in the middle of the sequence was considered a better alignment and is the one which was used. In order to continue with the analysis, the additional 437 bases of *N. viridis* were deleted from the alignment. The sequence with the insertion deleted was used for all subsequent analysis and reporting. The insertion sequence is provided for reference in Appendeix E.

The dataset consisting of the sequenced samples and the untrimmed GenBank sequences was searched using the custom *seqscanner* program (see Section 2.5.6) and the BLAST algorithm to determine if the insertion could be found elsewhere in the 18S gene. The BLAST algorithm found matches as detailed in Table 3.6. The *seqscanner* program found similar results. These matches were very short (11 to 13 bases long) and were considered insignificant. The inserted sequence was also entered into the BLAST program on the GenBank website (Benson *et al.*, 2005). This search returned two matches of between 80 and 200 bases and many matches of between 50 and 80 bases across a range of organisms. As the search sequence was 437 bases long, these matches were also not considered significant. The source of the 437-base insertion is therefore unknown at present. Insertions have been found in *Pyramimonas* and various euglenophytes (SD Sym, pers. comm., 2008).

Table 3.5. Lengths of sequences used in the partial 18S cladistic study of *Nephroselmis* and outgroups

Species	**Accession Number**	**Length**
Nephroselmis anterostigmatica MBIC 11158	EU330215*	854
Nephroselmis anterostigmatica	AB158372	855
Nephroselmis anterostigmatica	AB158373	854
Nephroselmis astigmatica NIES 252	EU330216*	840
Nephroselmis astigmatica	AB158374	856
Nephroselmis olivacea	X74754	853
Nephroselmis pyriformis WW02	EU330217*	852
Nephroselmis pyriformis	AB058378	852
Nephroselmis pyriformis	AB058391	852
Nephroselmis pyriformis	AB158376	852
Pseudoscourfieldia marina	X75565	852
Nephroselmis rotunda CCAP 1960/3	EU330219*	856
Nephroselmis rotunda BB2	EU330218*	849
Nephroselmis MBIC11149	AB214975	856
Nephroselmis spinosa NIES 935	EU330220*	843
Nephroselmis spinosa	AB158375	857
Nephroselmis viridis sp. ined. NIES 486	EU330221*	836 (1273)†
Nephroselmis viridis sp. ined.	AB214976	854
Pseudoscourfieldia marina Wits Fine1	EU330222*	826
Pseudoscourfieldia marina	AF122888	848
Pseudoscourfieldia marina	AJ132619	848
Dolichomastix tenuiformis Wits	EU330214*	848
Dolichomastix tenuiformis	AF509625	848
Mamiella sp.	AB017129	840
Pyramimonas mucifera Wits	EU330223*	855
Pyramimonas olivacea	AB017122	856
Pyramimonas parkeae	AB017124	854
Tetraselmis sp. Wits NV25	EU330224*	855
Tetraselmis convolutae	U05039	858
Tetraselmis kochiensis	AJ431370	853
Halosphaera sp.	AB017125	854
Prasinoderma coloniale	AB058379	841
Prasinococcus capsulatus	AB058384	845

See Table 2.6 on page 40 for further details of these samples.
*Sequences submitted to GenBank during the course of this study.
†An insertion of 437 bases was found in this sequence.

Table 3.6. BLAST matches for the 437-base insertion found in *Nephroselmis viridis* sp. ined.

Sample	Reversed and Complimented?	Sequence	Length
Nephroselmis pyriformis WW02	Yes	ATTGTACTCATTC	13
Tetraselmis sp. Wits NV25	Yes	ATTGTACTCATTC	13
Tetraselmis convolutae GenBank	Yes	ATTGTACTCATTC	13
Tetraselmis kochiensis GenBank	Yes	ATTGTACTCATTC	13
Dolichomastix tenuiformis Wits	Yes	GAAACGCCCGAG	12
Nephroselmis spinosa GenBank	No	GCCGAAAGGTT	11
Nephroselmis olivacea GenBank	No	GCCGAAAGGTT	11
Nephroselmis astigmatica GenBank	No	GCCGAAAGGTT	11
Nephroselmis viridis sp. ined. GenBank	No	GCCGAAAGGTT	11

3.10.4 Phylogenetic Relationships

Nephroselmis is monophyletic with strong bootstrap support (94%) for the genus (Figure 3.21). All of the GenBank samples of *Nephroselmis* which were included were located in clades with the corresponding species sequenced in this study. All of the outgroup taxa included from GenBank were located in clades with the corresponding species sequenced in this study, with the exception of *Pseudoscourfieldia* as discussed below. The sister clade to *Nephroselmis* contains four genera: *Dolichomastix*, *Mamiella*, *Pseudoscourfieldia* and *Tetraselmis* (Figure 3.21).

Moderate to very strong bootstrap support exists for most clades within *Nephroselmis*. The clade containing the various *N. rotunda* samples (Figure 3.21) has the weakest bootstrap support (57% and 59%). However, the clade containing *N. rotunda* and *N. spinosa* has 100% bootstrap support. The sample designated "MBIC 11149" in Figure 3.21 is an unidentified sample from GenBank which is positioned within the *N. rotunda* clade. However, the branch length for this sample is very long (13), which suggests that it may not be *N. rotunda*. Its position within the *N. rotunda* clade indicates that it is has a very close affinity to *N. rotunda* though. The topology of the tree did not change when "MBIC 11149" was removed from the data set and branch lengths within the clade changed only slightly (not shown here). However, bootstrap support for the *N. rotunda* clade increased to 95% when the "MBIC 11149" sample was removed (not shown).

3.10.5 Identification of taxa aided by sequence data and cladistic analysis

The identification of a number of strains of *Nephroselmis* and various outgroup species was corrected or facilitated by the molecular cladistic analysis. The strain of *Nephroselmis* designated "BB2" (see Tables 2.2 and 2.6) was identified as *Nephroselmis rotunda*, based on morphological features, including scale morphology. The strain named *N. pyriformis* received from the CCAP culture collection was determined to be the same as the strain of *N. rotunda* received from the same institution, as both their morphology and ITS sequences were identical (not shown here). Small stellate underlayer scales were found in both samples and the cells shared a similar size and shape. Large outer-layer stellate scales were not found in either of these samples however, which suggested that they might not be *N. rotunda*. After comparing the sequence data of all sequences and GenBank samples with the *seqcomp* program (see Section 2.5.6), it was determined that the high similarity between *N. rotunda* BB2 and the two samples from CCAP meant that these two samples were *N. rotunda* rather than a new species. Greater differences were seen in the sequences of different populations of the same species (such as *N. pyriformis*) than was seen between the CCAP samples and *N. rotunda* BB2 (not shown here). It is possible that the CCAP strains have lost their ability to produce outer layer scales, a condition which has been reported previously in *N. olivacea* (Moestrup and Ettl, 1979). CCAP has been notified that their sample designed *N. pyriformis* (CCAP 1960/3) has been misidentified and that it is *N. rotunda*. Their database and website have been updated accordingly. This misidentification was also noted by Nakayama *et al.* (2007).

The strain labeled *Pseudoscourfieldia marina* within the *Nephroselmis pyriformis* clade in Figure 3.21 is a sample from GenBank (Accession Number X75565, Culture Collection CCMP717) that has been misidentified (Fawley *et al.*, 1999; Marin and Melkonian, 1999; Fawley *et al.*, 2000; Watanabe *et al.*, 2000; Friedl and O'Kelly, 2002). The position of this sample within the *N. pyriformis* clade confirms the reports of the previous authors that it is *N. pyriformis* rather than *P. marina*.

The sample designated "*Pseudoscourfieldia marina* Wits" (Figure 3.21) included in this

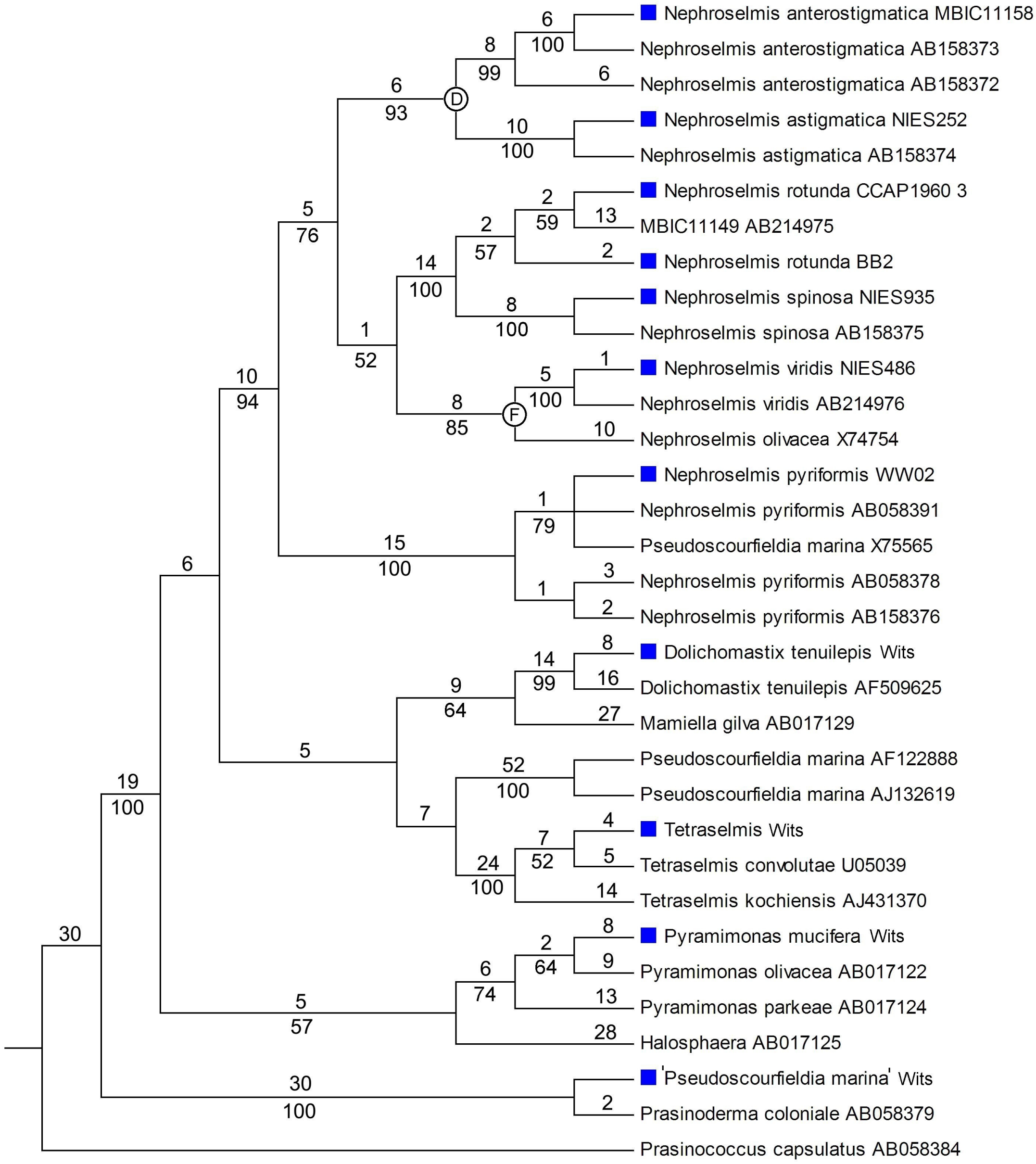

Figure 3.21. *Single most parsimonious tree from a heuristic search of partial 18S data for seven confirmed species of* Nephroselmis *and selected outgroups in the Prasinophyceae. Samples marked with a square were sequenced in this study; sequence data for other samples from GenBank. The tree, which was rooted with* Prasinococcus capsulatus, *has a length of 652, a consistency index (CI) of 0.57, a retention index (RI) of 0.75 and a rescaled consistency index (RC) of 0.43. Minimum branch lengths are shown above the line and bootstrap values above 50% from 1000 replicates below the line.*

study is problematic. This sample did not group with the two GenBank samples of *Pseudoscourfieldia* in preliminary alignments of the sequence data. A BLAST search of its sequence on the GenBank database returned matches with several samples of *Prasinoderma*. This sample groups with a *Prasinoderma* sequence from GenBank rather than with the *Pseudoscourfieldia* samples from GenBank (Figure 3.21). The sequence for an additional sample of *Prasinoderma* was obtained from GenBank (Accession Number AB183633). This sample showed a 99.6% to 99.9% similarity to the sequenced "*Pseudoscourfieldia*" and the GenBank *Prasinoderma* samples included in the present study, using the custom *seqcomp* program.

The sample of "*Pseudoscourfieldia*" sequenced in this study has previously shown a strong affinity with *Pycnococcus* based on preliminary 18S molecular data (SD Sym, pers. comm., 2007). Sequences of *Pycnococcus* from GenBank (Accession Numbers AB058377 and AF122889) were added to the data set and realigned with *ClustalW* and analysed in *PAUP** as before. *Pycnococcus* grouped with the two GenBank *Pseudoscourfieldia* samples (not shown here) [see also Fawley *et al.* (1999)]. Therefore, it can be concluded that "*Pseudoscourfieldia marina*" Wits is probably misidentified and it is likely that it is related to *Prasinoderma*, as shown in Figure 3.21.

3.11 Comparison of Morphological and Molecular Analyses

The reweighted morphological analysis (Figure 3.18) and the partial 18S molecular analysis (Figure 3.21) have similar topologies. The clade (Clade D) containing *N. anterostigmatica* and *N. astigmatica* occurs in both analyses, as does the clade containing *N. olivacea* and *N. viridis* (Clade F). *N. spinosa* appears as sister to Clade F and *N. pyriformis* appears in a basal position in both analyses. The position of *N. rotunda* differs between the analyses. In the reweighted morphological analysis, *N. rotunda* appears as sister to *N. pyriformis*, whereas the partial 18S molecular analysis places *N. rotunda* as sister to *N. spinosa*. In the partial 18S molecular analysis, the weakest bootstrap support for a clade within *Nephroselmis* occurs for the clade containing *N. rotunda*. As mentioned previously, bootstrap support for this clade increased to 95% when the "MBIC 11149" sample was removed from the data set (not shown).

3.12 Cladistic Analysis of Combined Data

A p-value of 0.15 was returned by the partition homogeneity test (Farris *et al.*, 1995) in *PAUP** on the two data sets, indicating that the morphological and molecular data are congruent (Cunningham, 1997a) and may be combined. Uninformative characters were excluded from these analyses (Cunningham, 1997a,b). The heuristic search performed on the combined data set (again with uninformative characters excluded) produced one tree (Figure 3.22). Of the 46 morphological characters, 27 were excluded, leaving 19 characters. Of the 868 molecular characters, 795 were excluded, leaving 73 characters. Therefore, a total of 92 characters of the combined 914 characters were included in the analysis; 822 characters in total were excluded. The tree obtained from the combined analysis (Figure 3.22) shows moderate to very strong bootstrap support for all nodes and agrees well with the trees obtained from the separate reweighted morphological and partial 18S molecular analyses.

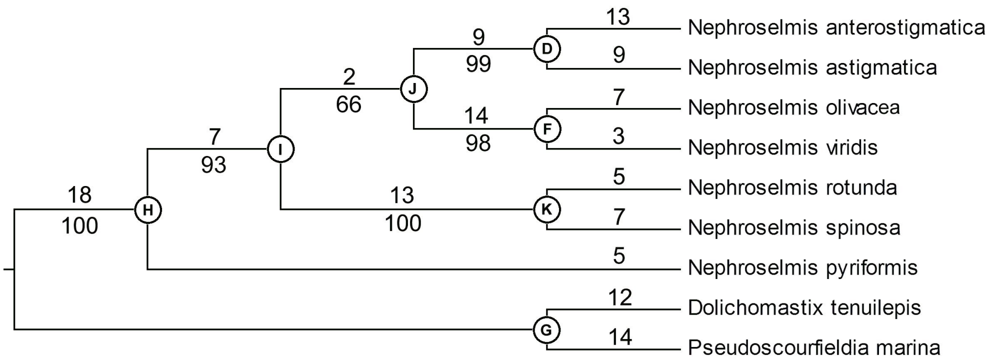

Figure 3.22. *Single most parsimonious tree from heuristic search of the combined unweighted morphological and partial 18S molecular data sets for seven confirmed species of* Nephroselmis *and two outgroups. The tree was rooted with* Dolichomastix tenuilepis *and* Pseudoscourfielda marina*. Tree length is 179, consistency index (CI) is 0.68, retention index (RI) is 0.57 and rescaled consistency index (RC) is 0.39. Minimum branch lengths are shown above the line and bootstrap values above 50% from 1000 replicates below the line.*

Chapter 4

Discussion

4.1 Generic Concept

The results of the three cladistic analyses undertaken (unweighted and reweighted morphological, partial 18S molecular and combined; termed "the three cladistic analyses") show that *Nephroselmis* is monophyletic with strong bootstrap support for various clades within the genus (Figures 3.18, 3.21 and 3.22). Seven species of *Nephroselmis* have been confirmed as distinct entities: *N. anterostigmatica*, *N. astigmatica*, *N. olivacea*, *N. pyriformis*, *N. rotunda*, *N. spinosa* and *N. viridis*.

The word "Nephroselmis" is derived from the Greek roots "nephr" or "nephro", meaning "kidney", and "selmis" or "selme", meaning "rowing seat" (Guiry and Guiry, 2008). The reference to "kidney" ("bean-shaped" or "reniform") has typically been used when describing the shape of the cell in lateral view (for example, Inouye and Pienaar, 1984; Sym and Pienaar, 1993; Tseng *et al.*, 1994). Specific mention of the cell shape is excluded from more recent reports however (for example, Suda, 2003; Nakayama *et al.*, 2007). The morphological cladistic analyses undertaken in the present study show that a reniform cell shape (Character 1) occurs in only one of the seven species of *Nephroselmis* (*N. spinosa*). The other species of *Nephroselmis* are either round or ovate in shape.

Only one synapomorphic character (Character 37) defines the genus *Nephroselmis* in the present study (Figure 3.20). However, several other characters (Characters 1, 23 and 38) support the definition of the genus. The term "synapomorphy" is used here to refer to a (non-homoplasious) apomorphy which is shared by all the members of a clade, without any subsequent changes in any descendant taxa. It is for this reason that *Nephroselmis* is supported by only one synapomorphy. Characters 1, 23 and 38 each show subsequent changes in descendant taxa (although no reversals or parallelisms), and are therefore not considered to be true synapomorphies. These characters are, however, considered to be useful in supporting the description of the genus *Nephroselmis*.

At least three autapomorphies are found in six of the seven species of *Nephroselmis* (Table 3.4). *N. pyriformis*, the only species lacking autapomorphies, shares three homoplasious apomorphies with *N. anterostigmatica* and *N. astigmatica* (Clade D in Figure 3.19). A flange and pit hairs are present in *N. pyriformis* and *N. astigmatica*, with *N. pyriformis* and *N. anterostigmatica* both showing cell asymmetry. Whether this homoplasy in *N. pyriformis* is a result of convergence or a loss of the characters in all other species is not known. In the present study, *N. pyriformis* is located in a basal position (Figures 3.18, 3.21 and 3.22), whereas the results from a maximum likelihood analysis of the entire 18S gene region place *N. anterostigmatica* and *N. astigmatica* (Clade D in Figures 3.18, 3.21 and 3.22) in a basal position (Nakayama *et al.*, 2007). *N. pyriformis* would not be recognized as a species according to the Phylogenetic Species Concept of Wheeler and Platnick (2000b) (see Section 1.8), which requires that a lineage be diagnosable by a unique combination of character states.

The morphological cladistic analyses included in the present study allow for the following suite of defining morpholoigical characters to be proposed for the genus *Nephroselmis*, modified from Inouye and Pienaar (1984). One feature ("Flagellar pit scales") mentioned by Inouye and Pienaar (1984) has been removed, as this character is not diagnostic for *Nephroselmis*, being found in *N. astigmatica* only.

1. An approximately round to ovate cell in lateral view, flattened in the left-right plane.
2. Two heterodynamic, unequal, blunt-ended, scaly flagella.
3. Two or three flagellar scale layers, in addition to flagellar hair scales.
4. Two to five[18] layers of non-mineralised[19] organic body scales, with the second layer of scales having a Maltese cross, paper windmill or stellate shape.
5. A swimming action in which the short flagellum is directed forwards, with the long flagellum trailing.
6. A flagellar root system which consists of (only) three microtubular roots (one of which is multilayered) and a rhizoplast.
7. A single, intraplastidial eyespot, typically located under the short flagellum (located on the anterior surface in *N. anterostigmatica* and absent in *N. astigmatica*).

Other organisms previously classified as *Nephroselmis*, such as *N. fissa* and *N. marina* for example (see Section 3.7), may need to be moved out of the genus once more detailed morphological and molecular studies have been undertaken. The morphological data presently available for *N. fissa* (the original light microscopy description and line drawings by Lackey (1940) only) is insufficient to confirm its affiliation with *Nephroselmis*. Cell dimensions greatly exceed those of other *Nephroselmis* species and the presence of two eyespots strongly suggests that this organism is not a member of *Nephroselmis*. It is not known, however, if Lackey (1940) observed dividing cells and concluded from this that the organism possesses two eyespots. *N. marina* possess two chloroplasts and lacks both an eyespot and a pyrenoid. Despite its apparent superficial similarity to *Nephroselmis* with regards to cell shape and flagellar orientation, it is not possible to confirm that this organism is a member of *Nephroselmis*. The identity of *N. minuta* remains unresolved due to a lack of both published ultrastructural data and live cultures. Detailed morphological, ultrastructural and molecular studies of *N. fissa*, *N. marina* and *N. minuta* are required in order to adequately identify them. As none of these organisms are available from any culture collection at present, such studies cannot be undertaken. Organisms fitting the general description of each of these species may become available in culture collections in the future.

4.2 Anomalies found in the Literature

Sym and Pienaar (1993: Figure 6) show that stellate third layer flagellar scales are found in all species of *Nephroselmis* except *N. pyriformis*. However, third layer flagellar scales are found in only two species of *Nephroselmis*: small spines with curved hooks are present in *N. olivacea* (Moestrup and Ettl, 1979) and small stellate scales are present in *N. viridis* (Young, 1991). Several morphological features are shared between these two species, as discussed below.

[18] Nakayama *et al.* (2007).
[19] Melkonian (1990).

Throndsen (1997: Plate 11) shows that the chloroplast of *N. pyriformis* is located on the anterior surface of the cell. The results of the present study indicate that the chloroplast of this species is located in the typical generic position – that is, lining the dorsal surface of the cell (see Figure 3.5 and Plate 9: Figures 1 and 2).

Yoshii *et al.* (2005) and Yoshii (2006) included three unidentified species of *Nephroselmis* in their 18S analyses. Their sample designated "sp. 1" (MBIC 11158) has recently been described as *Nephroselmis astigmatica* (Nakayama *et al.*, 2007). This is the same strain that was maintained and used in the present study. Their sample designated "sp. 2" (MBIC 11149) is included in the partial 18S molecular analysis of the present study (GenBank sequence) and is possibly *N. rotunda*, as discussed in Section 4.2. Their sample designated "sp. 3" (NIES 486) has subsequently been identified as *Nephroselmis viridis* sp. ined. by the NIES culture collection and is included in the partial 18S molecular analysis of the present study (GenBank sequence).

A difference found in the present study for *N. pyriformis*, as reported under the "Notes" heading in Section 3.6, is that tip hairs, reported as present in Nakayama *et al.* (2007), were not present in the strains of *N. pyriformis* examined in this study (Plate 10: Figure 1). In fact, the absence of tip hairs (Character 37), is the only true synapomorphy (that is, a (non-homoplasious) apomorphy, shared by all members of a clade, which does not subsequently change in descendant taxa, as discussed previously) for *Nephroselmis*, as shown in Figure 3.20.

4.3 Evolutionary Trends and Relationships in *Nephroselmis*

The partial 18S molecular tree obtained (Figure 3.21) agrees well with three previous phylogenetical analyses of some members of *Nephroselmis* based on the 18S gene (Yoshii *et al.*, 2005; Yoshii, 2006; Nakayama *et al.*, 2007). *Nephroselmis pyriformis* appears in a basal position in all three cladistic analyses undertaken in the present study. This early divergence is supported by the generally plesiomorphic features found in this species. Such features include the absence of third, fourth and fifth layer body scales, and the presence of only small, simple stellate scales in the second body scale layer (Plate 10: Figures 3 and 4).

The *N. anterostigmatica* / *N. astigmatica* clade (Clade D in Figures 3.18, 3.21 and 3.22) and the *N. olivacea* / *N. viridis* clade (Clade F in Figures 3.18, 3.21 and 3.22) are both very robust as they show strong bootstrap support in all three cladistic analyses. *N. anterostigmatica* and *N. astigmatica* appeared together in a clade in a maximum likelihood analysis of the entire 18S gene; *N. viridis* was not included in this particular study however (Nakayama *et al.*, 2007). *N. anterostigmatica* and *N. astigmatica* (Clade D) are the only species in the genus exhibiting modifications in eyespot presence or position: *N. astigmatica* lacks an eyespot, whereas the eyespot of *N. anterostigmatica* is located on the anterior surface of the cell, in contrast to all other members of the genus, in which the eyespot is located under the short flagellum, towards the ventral surface. Evidence of movement in the position of the eyespot, possibly linked to a loss of settling behaviour, has been recorded in *Pyramimonas* (Pienaar and Sym, 2002). The scale morphology of these two species is similar in that the scales are complex and intricate. Outer-layer body scales, where present, in other members of the genus are either spines, stellate or ophiuroid (Moestrup and Ettl, 1979) and are unipolar or multipolar. The outer-layer body scales of *N. anterostigmatica* (fifth layer) and *N. astigmatica* (fourth layer) (Clade D) are bipolar and similar in structure. Apomorphies for Clade D are an ovate cell shape, bipolar outer-layer body scales (fourth or fifth layer) and atypical eyespots.

The sister relationship of *N. olivacea* and *N. viridis* (Clade F) is supported by the apomorphies of scale morphology, multipolar body scales, the presence of a disc or lens structure in the region of the pyrenoid and the presence of a third type (layer) of flagellar scales. *N. olivacea*, the only known freshwater species, shows a strong affinity to *N. viridis*. This implies a possible habitat change in an ancestor of these two species, as discussed below.

The positions of *N. rotunda* and *N. spinosa* are less well-defined than those of Clades D and F, as the placement of these species differs between the three analyses (Figures 3.18, 3.21 and 3.22). In the reweighted morphological analysis (Figure 3.18), *N. rotunda* appears as sister to *N. pyriformis*, with *N. spinosa* as sister to Clade F. A clear grouping of the species according to the number of layers of body scales in the reweighted morphological analysis exists – *N. pyriformis* in a basal position lacks third, fourth and fifth layer body scales, *N. rotunda* as sister to *N. pyriformis* lacks fourth and fifth layer body scales, and the remaining species possess either four or five layers of body scales. The partial 18S molecular analysis places *N. rotunda* and *N. spinosa* in a clade together, sister to Clade F (*N. viridis* and *N. olivacea*) (Figure 3.21). This is a problematic grouping, as there are no morphological features which support this arrangement. The combined analysis also places *N. rotunda* and *N. spinosa* in a clade together, but sister to Clade J, comprising both Clades D and F (Figure 3.22). *N. pyriformis* occurs in a basal position in the combined analysis.

The relationships between *Nephroselmis* species found by Nakayama *et al.* (2007) (using maximum likelihood analyses) are similar to the present study. However, *N. rotunda* and *N. viridis* were not included in their study. The present study does agree with their results though, by showing strong affinity between *N. olivacea* and *N. spinosa*, and between *N. anterostigmatica* and *N. astigmatica*. In contrast to the present study however, their results reveal that *N. pyriformis* is not placed basally. Rather, the *N. anterostigmatica* and *N. astigmatica* clade diverged earliest, whereas the present study indicates that *N. pyriformis* diverged earliest. The absence of *N. rotunda* and *N. viridis* from their study could be the reason that *N. olivacea* and *N. spinosa* appear as sister species. In the present study, the position of *N. rotunda* is problematic as it appears in different positions in the different analyses (see Figures 3.18, 3.21 and 3.22).

The results of the three cladistic analyses in the present study suggest an increase in the number of body scales and the complexity of these scales in the genus are derived characters. The fewest number of body scale layers are found in *N. pyriformis*, which occurs in a basal position. Three body scale layers are found in *N. rotunda*. The remaining members of the genus possess four layers of body scales. The third and fourth layer body scales of *N. spinosa* are unipolar and simple. Those of *N. olivacea* and *N. viridis* (Clade F in Figures 3.18, 3.21 and 3.22) are multipolar ophiuroid scales of greater complexity than *N. spinosa*. The third and fourth layer body scales of *N. anterostigmatica* and *N. astigmatica* (Clade D in Figures 3.18, 3.21 and 3.22) are bipolar and show the greatest complexity.

4.4 Marine and Freshwater Species

In all three cladistic analyses, the type species of the genus, *N. olivacea*, does not appear in a basal position in the genus. *N. olivacea* occurs in a clade (Clade F in Figures 3.18, 3.21 and 3.22) with *N. viridis* in all three cladistic analyses. This implies that *N. olivacea* is closely related to *N. viridis*. All members of *Nephroselmis* except *N. olivacea* occur in marine habitats. This suggests that an ancestral population of *N. olivacea* and *N. viridis* could have moved from a marine to a freshwater habitat. This could possibly have occurred if the organism was washed into an estuary or freshwater environment as a result of, for example, a marine overwash event. The organism in the freshwater habitat may have been able to adapt to this environment and is what is termed *N. olivacea* today. The ancestor remaining in the marine environment evolved into what is termed *N. viridis* today. Longer branch lengths are found for *N. olivacea* than for *N. viridis* in all three analyses: 4 for *N. olivacea* and 1 for *N. viridis* in the first of two trees from the unweighted morphological analysis (Figure 3.17A), 5 and 1 in the second of these two trees (Figure 3.17B), 10 and 1 in the partial 18S molecular analysis (Figure 3.21) and 7 and 3 in the combined analysis (Figure 3.22). This shows that there have been many more evolutionary changes in the *N. olivacea* lineage compared to the *N. viridis* lineage. These changes could be attributed to adaptations to a freshwater habitat. Both marine and freshwater species are found in other green algal genera – the type species of *Pyramimonas*, *P. tetrarhynchus*, is the only freshwater species in the genus (SD Sym, pers. comm., 2008).

4.5 Comparisons of Outgroups with Previous 18S Molecular Studies

Several previous 18S molecular studies involving the prasinophytes have been undertaken. The taxa which were included varied between the studies. The results of the present study are compared to these previous results below.

In four studies (Kantz *et al.*, 1990; Steinkötter *et al.*, 1994; Friedl, 1997; Nayakama *et al.*, 1998) *Pseudoscourfieldia marina* appears as sister to *Nephroselmis*, although in all cases the number of taxa which could provide resolution between these two genera is limited. *Tetraselmis* is distantly related to *Nephroselmis* in studies by Kantz *et al.* (1990), Steinkötter *et al.* (1994) and Nayakama *et al.* (1998), but appears as sister in the studies by Friedl (1997), Nayakama *et al.* (1998) and Marin and Melkonian (1999). The position of *Pseudoscourfieldia marina* in the present study is more distant, as it appears in a clade, sister to *Nephroselmis*, with *Tetraselmis Dolichomastix* and *Mamiella* (Figure 3.21). This may be a result of including only the first 900 bases of the 18S region.

The present study places *Pyramimonas* as sister to *Halosphaera*, which supports the findings of Nayakama *et al.* (1998). The findings of Fawley *et al.* (2000) show that *Tetraselmis* is more closely related to *Nephroselmis* than is *Pseudoscourfieldia marina*. In contrast to these findings, these two species appear in a clade together in the present study. The present study supports the findings of Nayakama *et al.* (1998) and Fawley *et al.* (2000) which place *Halosphaera* and *Pyramimonas* as sister genera. *Pseudoscourfieldia marina* and *Pycnococcus* appear as sister in studies by Marin and Melkonian (1999) and Fawley *et al.* (2000). *Pycnococcus* sequences from GenBank which were included in preliminary analyses in the present study (not shown here) grouped with *Pseudoscourfieldia marina* sequences from GenBank (see Section 3.10.5). Results from Nayakama *et al.* (1998) place *Pycnococcus* as sister to a clade containing *Nephroselmis* and *Pseudoscourfieldia marina*. The results of the present study agree with those of Nakayama *et al.* (2007) in the placement of *Pseudoscourfieldia marina* as sister to *Nephroselmis*, *Halosphaera* as sister to *Pyramimonas*, *Dolichomastix* in a clade sister to the one in which *Pyramimonas* and *Halosphaera* appear and *Prasinoderma* as sister to *Prasinococcus*.

4.6 Conclusions

The monophyly of the genus *Nephroselmis* (consisting of *N. anterostigmatica*, *N. astigmatica*, *N. olivacea*, *N. pyriformis*, *N. rotunda*, *N. spinosa* and *N. viridis*) has been confirmed. *Nephroselmis* is characterized by an approximately round to ovate cell in lateral view, flattened in the left-right plane, two heterodynamic, unequal, blunt-ended, scaly flagella, two or three flagellar scale layers, in addition to flagellar hair scales, two to five layers of non-mineralised organic body scales, with the second layer of scales having a Maltese cross, paper windmill or stellate shape, a swimming action in which the short flagellum is directed forwards, with the long flagellum trailing, a flagellar root system which consists of (only) three microtubular roots (one of which is multilayered) and a rhizoplast and a single, intraplastidial eyespot, typically located under the short flagellum (located on the anterior surface in *N. anterostigmatica* and absent in *N. astigmatica*). The morphology and ultrastructure of the seven species in the genus has been examined in detail, resulting in true synapomorphies being found for each clade. Autapomorphies for each species, except *N. pyriformis*, were determined. A lack of published data and fresh material prevented *N. fissa*, *N. gaoae*, *N. marina* and *N. minuta* from being included in this study.

Reweighted morphological cladistic analysis revealed distinct clades within the genus, grouped predominantly by body scale number and scale morphology (together termed "scale complexity" below). Partial 18S molecular cladistic analysis agreed well with the morphological analysis, as did an analysis which combined morphological and molecular data. *N. pyriformis*, which shows the greatest number of plesiomorphic features and possesses the simplest scale morphology, was placed in a basal position in all three analyses. The greatest scale complexity is found in *N. anterostigmatica* and *N. astigmatica*, which occured as sister species in all three analyses. Eyespot modifications are found in these two species only: *N. astigmatica* lacks an eyespot and the eyespot of *N. anterostigmatica* is atypically located on the anterior surface of the cell. *N. olivacea* and *N. viridis* showed intermediate scale complexity and were placed as sister species in all three analyses.

The relationship between *N. rotunda* and *N. spinosa* varied between the three analyses. The reweighted morphological cladistic analysis placed *N. rotunda*, which has three body scale layers, in its own clade, between *N. pyriformis*, which has two body scale layers, and the clade consisting of all other *Nephroselmis* species, which possess four or five body scale layers. The partial 18S molecular cladistic analysis grouped *N. rotunda* and *N. spinosa* in a clade sister to the *N. olivacea* / *N. viridis* clade. The combined analysis grouped *N. rotunda* and *N. spinosa* in a clade sister to the remaining *Nephroselmis* species.

While each of the three cladistic methods produced reliable trees with distinct and similar clades, there was not sufficient similarity between them to propose erecting subgenera at this stage. This may be possible in the future once the relationship between *N. rotunda* and *N. spinosa* has been resolved.

The only freshwater species, *N. olivacea*, occured in a clade with *N. viridis* (in a more derived position), rather than in a basal position or alone in a clade. Branch lengths indicate that many more evolutionary changes have occurred in the *N. olivacea* lineage when compared to *N. viridis*, which is present in the same clade. This is consistent with *N. olivacea* having adapted to a freshwater environment as a result of, for example, a marine overwash event. Of the nine other genera included in the molecular analysis, *Dolichomastix*, *Mamiella*, *Pseudoscourfieldia* and *Tetraselmis* appeared as the sister clade of *Nephroselmis*.

4.7 Future Work

The following aspects of the biology of *Nephroselmis* could provide further clarity on the phylogenetic and taxonomic history of the genus:

1. Investigations into whether evidence of sexual reproduction can be found in species of *Nephroselmis* other than *N. olivacea*; investigations into factors which may induce sexual reproduction.
2. Comparative investigations in cell division cycles and growth studies [as undertaken on *N. viridis* by Young (1991)] may reveal differences between species and may inform or assist with sexual reproduction studies.
3. Motility studies (see Section 1.6), which may be useful in confirming or resolving phylogenetic relationships within the genus.
4. Investigations into the halotolerance of species of *Nephroselmis*. All but one species (*N. olivacea*) are marine, although no halotolerance studies on the genus have been reported. Preliminary halotolerance experiments undertaken briefly during this study (not shown here) suggest that *N. viridis* may be tolerant at a salinity of 20‰.
5. Morphological and molecular cladistic investigations of those species of *Nephroselmis* not included in this study (*N. fissa*, *N. marina* and *N. minuta*), as well as several potential new species (Nakayama *et al.*, 2007) would further elucidate the phylogeny of the genus and possibly add to its robustness.
6. Comparative investigations into other gene regions, such as the *rbc*L region for example, could further enhance the understanding of the phylogeny of the genus. In addition to this, the results from an investigation involving the entire 18S gene region of all confirmed species could be compared to the results of the present study.
7. Resolving the relationships between problematic species (such as *N. rotunda* and *N. spinosa*) would further elucidate the phylogeny of the genus and possibly allow for the erection of subgenera.
8. Further investigations into the differences in pigment types found in *Nephroselmis* species, as it has previously been shown that pigmentation varies across *Nephroselmis* species (Yoshii *et al.*, 2005; Yoshii, 2006).

Literature Cited

Altschul, S. F., Gish, W., Miller, W., Myers, E. W. and Lipman, D. J. (1990). Basic Local Alignment Search Tool. *Journal of Molecular Biology* **215**: 403–410.

Andersen, R. A. and Kawachi, M. (2005). Traditional microalgae isolation techniques. In: **Andersen, R. A.** (Ed.), *Algal Culturing Techniques.* Elsevier Academic Press.

Andersen, R. A., Berges, J. A., Harrison, P. J. and Watanabe, M. M. (2005). Appendix A – Recipes for freshwater and seawater media. In: **Andersen, R. A.** (Ed.), *Algal Culturing Techniques.* Elsevier Academic Press.

Baker, R. H., Yu, X. and DeSalle, R. (1998). Assessing the relative contribution of molecular and morphological characters in simultaneous analysis trees. *Molecular Phylogenetics and Evolution* **9**: 427–436.

Barrett, M., Donoghue, M. J. and Sober, E. (1991). Against consensus. *Systematic Zoology* **40**: 486–493.

Becker, B., Marin, B. and Melkonian, M. (1994). Structure, composition, and biogenesis of prasinophyte cell coverings. *Protoplasma* **181**: 233–244.

Becker, D., Becker, B., Satir, P. and Melkonian, M. (1990). Isolation, purification and characterization of flagellar scales from the green flagellate *Tetraselmis striata* (Prasinophyceae). *Protoplasma* **156**: 103–112.

Beitz, E. (2000). TEXshade: shading and labeling of multiple sequence alignments using LaTeX 2ε. *Bioinformatics* **16**: 135–139.

Benson, D. A., Karsch-Mizrachi, I., Lipman, D. J., Ostell, J. and Wheeler, D. (2005). GenBank. *Nucleic Acids Research* **33**: D34–D38.

Bourrelly, P. (1951). Volvocales rares ou nouvelles. *Hydrobiologia* **3**: 251–281.

Bourrelly, P. (1972). *Les Algues D'Eau Douce: Initiation à la systématique: Tome I: Les Algues Vertes.* Éditions N. Boubée & Cie, Saint-André-Des-Arts, Paris.

Butcher, R. W. (1959). *An introductory account of the smaller algae of British coastal waters. Part I: Introduction and Chlorophyceae.* Ministry of Agriculture, Fisheries and Food, Fisheries Investigations, Series IV, London.

Bütschli, O. (1884). Die Protozoen. In: **Bronn, H. G.** (Ed.), *Klassen und Ordnungen des Tierreichs, Bd. I, Abt. II. Mastigophora.* C. F. Winter, Leipzig and Heidelberg.

Cachon, M. and Caram, B. (1979). A symbiotic green alga, *Pedinomonas symbiotica* sp. nov. (Prasinophyceae), in the radiolarian *Thalassolampe margarodes. Phycologia* **18**: 177–184.

Carter, N. (1937). New or interesting algae from brackish water. *Archiv für Protistenkunde* **90**: 1–68.

Cavalier-Smith, T. (1981). Eukaryote kingdoms: seven or nine? *BioSystems* **14**: 461–481.

Cavalier-Smith, T. (1993). The origin, losses and gains of the chloroplast. In: **Lewin, R. E.** (Ed.), *Origin of the plastid: symbiogenesis, prochlorophytes and the origins of the chloroplast*, pp. 291–348. Chapman and Hall, New York.

Cavalier-Smith, T. (1998). A revised six-kingdom system of life. *Biological Review of the Cambridge Philosophical Society* **73**: 203–266.

Chadefaud, M. (1960). Les végétaux non vasculaires (Cryptogamie). In: **Chadefaud, M. and Emberger, L.** (Eds.), *Traité de Botanique Systématique, Tome I.* Masson, Paris.

Chadefaud, M. (1977). Les Prasinophyceés. Remarques historiques, critiques et phylogénétiques. *Bulletin* *de la Société phycologique de France* **22**: 1–18.

Chrétiennot-Dinet, M. J., Courties, C., Vaquer, A., Neveux, J., Claustre, H., Lautier, J. and Machado, M. C. (1995). A new marine picoeukaryote: *Ostreococcus tauri* gen. et sp. nov. (Chlorophyta, Prasinophyceae). *Phycologia* **34**: 285–292.

Christensen, T. (1962). Alger. In: **Böcher, T. W., Lange, M. and Sørensen, T.** (Eds.), *Botanik 2 (Systematik Botanik) 2*, pp. 1–178. Munksgaard, Copenhagen.

Coleman, A. W. and Mai, J. C. (1997). Ribosomal DNA ITS-1 and ITS-2 sequence comparisons as a tool for predicting genetic relatedness. *Journal of Molecular Evolution* **45**: 168–177.

Coleman, A. W. and Vacquier, V. D. (2002). Exploring the phylogenetic utility of ITS sequences for animals: a test case for abalone (*Haliotis*). *Journal of Molecular Evolution* **54**: 246–257.

Compère, P. (1987). Observations taxonomiques et nomenclaturales sur quelques phytoflagellates de Belgique. *Bulletin du Jardin botanique national de Belgique / Bulletin van de National Plantentuin van België* **57**: 325–350.

Courties, C., Vaquer, A., Troussellier, M., Lautier, J., Chrétiennot-Dinet, M. J., Neveux, J., Machado, C. and Claustre, H. (1994). Smallest eukaryotic organism. *Nature* **370**: 255.

Cracraft, J. (1983). Species concepts and speciation analysis. In: **Johnston, R. F.** (Ed.), *Current Ornithology, Volume 1*, pp. 159–187. Plenum Press, New York.

Cron, G. V. (2005). *Cineraria L. (Senecioneae, Asteraceae) – its taxonomy, phylogeny, phytogeography and conservation.* Ph.D. thesis, University of the Witwatersrand, Johannesburg.

Cunningham, C. W. (1997a). Can three incongruence tests predict when data should be combined? *Molecular Biology and Evolution* **14**: 733–740.

Cunningham, C. W. (1997b). Is congruence between data partitions a reliable predictor of phylogenetic accuracy? Empirically testing an iterative procedure for choosing among phylogenetic methods. *Systematic Biology* **46**: 464–478.

Darwin, C. (1872). *On the origin of species by means of natural selection; or the preservation of favoured races in the struggle for existence, Sixth Edition.* Random House Inc., New York, 1998 Printing.

Daugbjerg, N., Moestrup, Ø. and Arctander, P. (1995). Phylogeny of genera of Prasinophyceae and Pedinophyceae (Chlorophyta) deduced from molecular analysis of the *rbc*L gene. *Phycological Research* **43**: 203–213.

De Queiroz, A. (1993). For consensus (sometimes). *Systematic Biology* **42**: 368–372.

De Queiroz, A. (1995). Separate versus combined analysis of phylogenetic evidence. *Annual Review of Ecology and Systematics* **26**: 657–681.

De Queiroz, K. (2000). Logical problems associated with including and excluding characters during tree reconstruction and their implications for the study of morphological character evolution. In: **Wiens, J. J.** (Ed.), *Phylogenetic analysis of morphological data*, pp. 192–212. Smithsonian Institution Press, Washington, D.C.

Doyle, J. J. (1992). Gene trees and species trees: molecular systematics as one-character taxonomy. *Systematic Botany* **17**: 144–163.

Edgar, R. C. (2004a). MUSCLE: a multiple sequence alignment method with reduced time and space complexity. *BMC Bioinformatics* **5**: 113 (doi:10.1186/1471–2105–5–113).

Edgar, R. C. (2004b). MUSCLE: multiple sequence alignment with high accuracy and high throughput. *Nucleic Acids Research* **32**: 1792–1797.

Ettl, H. (1982). Taxonomische Namensänderungen und Neubeschreibungen unter den Phytomonadina (Chlorophyta). *Nova Hedwigia* **35**: 731–736.

Ettl, H. (1983). *Süßwasserflora von Mitteleuropa. Band 9: Chlorophyta I.* Gustav Fischer Verlag, Stuttgart.

Farris, J. S. (1974). Formal definitions of paraphyly and polyphyly. *Systematic Zoology* **23**: 548–554.

Farris, J. S. (1988). Hennig86, version 1.5. Distributed by the author. Port Jefferson Station, N. Y.

Farris, J. S. (1989). The retention index and the rescaled consistency index. *Cladistics* **5**: 417–419.

Farris, J. S., Källersjö, M., Kluge, A. G. and Bult, C. (1995). Testing significance of incongruence. *Cladistics* **10**: 315–319.

Fawley, M. W., Qin, M. and Yun, Y. (1999). The relationship between *Pseudoscourfieldia marina* and *Pycnococcus provasolii* (Prasinophyceae, Chlorophyta): evidence from 18S rDNA sequence data. *Journal of Phycology* **35**: 838–843.

Fawley, M. W., Yun, Y. and Qin, M. (2000). Phylogenetic analyses of 18S rDNA sequences reveal a new coccoid lineage of the Prasinophyceae (Chlorophyta). *Journal of Phycology* **36**: 387–393.

Felsenstein, J. (2007). PHYLIP (Phylogeny Inference Package), Version 3.67. Distributed by the author. Department of Genome Sciences, University of Washington, Seattle.

Fott, B. (1971). Taxonomische Übertragungen und Namensänderung enunter den Algen IV. Chlorophyceae und Euglenophyceae. *Preslia* **43**: 289–303.

Freudenstein, J. V. (2005). Characters, states, and homology. *Systematic Biology* pp. 965–973.

Friedl, T. (1997). The evolution of the green algae. In: **Bhattacharya, D.** (Ed.), *Origins of Algae and their Plastids*. Springer-Verlag, Wien.

Friedl, T. and O'Kelly, C. J. (2002). Phylogenetic relationships of green algae assigned to the genus *Planophila* (Chlorophyta): evidence from 18S rDNA sequence data and ultrastructure. *European Journal of Phycology* **37**: 373–384.

Funk, V. A. (1995). Cladistic Methods. In: **Wagner, W. L. and Funk, V. A.** (Eds.), *Hawaiian biogeography: evolution on a hot spot archipelago*, pp. 30–38. Smithsonian Institution Press, Washington.

Gilbert, D. (2001). ReadSeq: Java application to read and reformat biological sequence data. *http://iubio.bio.indiana.edu/soft/molbio/readseq/java/* .

Graham, L. and Wilcox, E. (2000). *Algae*. Prentice-Hall International, London.

Guillard, R. R. L., Keller, M. D., O'Kelly, C. J. and Floyd, G. L. (1991). *Pycnococcus provasolii* gen. et sp. nov., a coccoid prasinoxanthin-containing phytoplankter from the western North Atlantic and Gulf of Mexico. *Journal of Phycology* **27**: 39–47.

Guillou, L., Eikrem, W., Chrétiennot-Dinet, M. J., Le Gall, F., Massana, R., Romari, K., Pedrós-Alió, C. and Vaulot, D. (2004). Diversity of picoplanktonic Prasinophytes assessed by direct nuclear SSU rDNA sequencing of environmental samples and novel isolates retrieved from oceanic and coastal marine ecosystems. *Protist* **155**: 193–214.

Guiry, M. D. and Guiry, G. M. (2008). *AlgaeBase version 4.2*. World-wide electronic publication, National University of Ireland, Galway. *http://www.algaebase.org*, accessed on 13 September 2007, 12 February 2008 and 17 May 2008.

Hall, T. A. (1999). BioEdit: a user-friendly biological sequence alignment editor and analysis program for Windows 95/98/NT. *Nucleic Acids Symposium Series* **41**: 95–98.

Hamby, R., Sims, L. E., Issel, L. E. and Zimmer, E. A. (1988). Direct ribosomal RNA sequencing: optimization of extraction and sequencing methods for work with higher plants. *Plant Molecular Biology Reports* **6**: 175–192.

Hayat, M. A. (1986). *Basic techniques for transmission electron microscopy*. Academic Press, Orlando.

Hillis, D. M. (1987). Molecular versus morphological approaches to systematics. *Annual Review of Ecology and Systematics* **18**: 23–42.

Hillis, D. M. and Wiens, J. J. (2000). Molecules versus morphology in systematics: conflicts, artifacts and misconceptions. In: **Wiens, J. J.** (Ed.), *Phylogenetic analysis of morphological data*, pp. 1–19. Smithsonian Institution Press, Washington, D.C.

Hillis, D. M., Huelsenbeck, J. P. and Cunningham, C. W. (1994). Application and accuracy of molecular phylogenies. *Science* **264**: 671–677.

Huss, V. A. R., C., F., Hartmann, E. C., Hirmer, M., Kloboucek, A., Seidel, B. M., Wenzeler, P. and Kessler, E. (1999). Biochemical taxonomy and molecular phylogeny of the genus *Chlorella* sensu lato (Chlorophyta). *Journal of Phycology* **35**: 587–598.

Inouye, I. (1993). Flagella and flagellar apparatuses of algae. In: **Berner, T.** (Ed.), *Ultrastructure of microalgae*. CRC Press, Inc, Boca Raton.

Inouye, I. and Hori, T. (1991). High-speed video analysis of the flagellar beat and swimming patterns of algae: possible evolutionary trends in green algae. *Protoplasma* **164**: 54–69.

Inouye, I. and Pienaar, R. N. (1984). Light and electron microscope observations on *Nephroselmis astigmatica* sp. nov. (Prasinophyceae). *Nordic Journal of Botany* **4**: 409–423.

Inouye, I., Pienaar, R. N., Suda, S. and Chihara, M. (1991). A scaly marine flagellate *Nephroselmis viridis* sp. nov. (Chlorophyta, Prasinophyceae) a possible phyletic link between freshwater and marine representatives. *Japanese Journal of Phycology* **Unpublished**.

John, D. M. and Maggs, C. A. (1997). Species problems in eukaryotic algae: A modern perspective. In: **Claridge, M. F., Dawah, H. A. and Wilson, M. R.** (Eds.), *Species: The Units of Biodiversity.* Chapman and Hall, London.

Kantz, T. S., Theriot, E. C., Zimmer, E. A. and Chapman, R. L. (1990). The Pleurastrophyceae and Micromonadophyceae: a cladistics analysis of nuclear rRNA sequence data. *Journal of Phycology* **26**: 711–721.

Kluge, A. G. and Wolf, A. J. (1993). Cladistics: what's in a word? *Cladistics* **9**: 183–199.

Krienitz, L., Ustinova, I., Friedl, T. and Huss, V. A. R. (2001). Traditional generic concepts versus 18S rDNA gene phylogeny in the green algal families Selenastraceae (Chlorophyceae, Chlorophyta). *Journal of Phycology* **37**: 852–865.

Kufferath, H. (1942). Récoltes algologiques à Onoz, Gezmbloux, Rouge-Cloître, Lierre, Herenthals et en Campine. IV, Cyanophycées, Flagellés et divers. *Bulletin de la Société Royale Botanique de Belgique* **74**: 94–107.

Lackey, J. B. (1940). Some new flagellates from the Woods Hole area. *American Midland Naturalist* **23**: 463–471.

Leadbeater, B. S. C. and McCready, S. M. M. (2000). The flagellates: historial perspectives. In: **Leadbeater, B. S. C. and Green, J. C.** (Eds.), *The flagellates: unity, diversity and evolution*, pp. 1–26. Taylor and Francis, London.

Lee, M. S. Y. (2001). Uninformative characters and apparant conflict between molecular and morphology. *Molecular Biology and Evolution* **18**: 676–680.

Levasseur, C. and Lapointe, F. (2001). War and peace in phylogenetics: a rejoinder on total evidence and consensus. *Systematic Biology* **50**: 881–891.

Lipscomb, D. L., Farris, J. S., Källersjö, M. and Tehler, A. (1998). Support, ribosomal sequences and the phylogeny of the Eukaryotes. *Cladistics* **14**: 303–338.

Mai, J. C. and Coleman, A. W. (1997). The internal transcribed spacer 2 exhibits a common secondary structure in green algae and flowering plants. *Journal of Molecular Evolution* **44**: 258–271.

Manton, I. (1966). Observations on scale production in *Pyramimonas amylifera* Conrad. *Journal of Cell Science* **1**: 429–438.

Manton, I. (1975). Observations on the microanatomy of *Scourfieldia marina* Throndsen and *Scourfieldia caeca* (Korsch.) Belcher *et* Swale. *Archiv für Protistenkunde* **117**: 358–368.

Manton, I. (1977). *Dolichomastix* (Prasinophyceae) from arctic Canada, Alaska and South Africa: a new genus of flagellates with scaly flagella. *Phycologia* **16**: 427–438.

Manton, I. and Parke, M. (1960). Further observations on small green flagellates with special reference to possible relatives of *Chromulina pusilla* Butcher. *Journal of the Marine and Biological Association of the UK* **39**: 275–298.

Manton, I., Rayns, D. G., Ettl, H. and Parke, M. (1965). Further observations on green flagellates with scaly flagella: the genus *Heteromastix* Korshikov. *Journal of the Marine and Biological Association of the UK* **45**: 241–255.

Marin, B. and Melkonian, M. (1994). Flagellar hairs in prasinophytes (Chlorophyta): ultrastructure and distribution on the flagellar surface. *Journal of Phycology* **30**: 659–678.

Marin, B. and Melkonian, M. (1999). Mesostigmatophyceae, a new class of streptophyte green algae revealed by SSU rRNA sequence comparisons. *Protist* **150**: 399–417.

Mattox, K. R. and Stewart, K. D. (1977). Cell division in the scaly green flagellate *Heteromastix angulata* and its bearing on the origin of the Chlorophyceae. *American Journal of Botany* **64(8)**: 931–945.

Mattox, K. R. and Stewart, K. D. (1984). Classification of the green algae: a concept based on comparative cytology. In: **Irvine, D. E. G. and John, D. M.** (Eds.), *Systematics of the Green Algae*, pp. 29–72. Academic Press, London.

Mayr, E. (1969). *Principles of systematic zoology.* McGraw-Hill, New York.

McLachlan, J. (1973). Growth Media – Marine. In: **Stein, J. R.** (Ed.), *Handbook of Phycological Methods: Culture Methods and Growth Measurements*, p. 460. Cambridge University Press, Cambridge.

Medlin, L., Elwood, H. J., Stickel, S. and Sogin, M. L. (1988). The characterization of enzymatically amplified eukaryotic 16S-like rRNA-coding regions. *Gene* **71**: 491–499.

Melkonian, M. (1982). The functional analysis of the flagellar apparatus in green algae. In: *Prokaryotic and eukaryotic flagella*. Cambridge University Press, Cambridge.

Melkonian, M. (1984). Flagellar apparatus ultrastructure in relation to green algal classification. In: **Irvine, D. E. G. and John, D. M.** (Eds.), *Systematics of the green algae*, pp. 73–120. Academic Press, London.

Melkonian, M. (1990). Phylum Chlorophyta, Class Prasinophyceae. In: **Margulis, L., Corliss, J. O., Melkonian, M. and Chapman, D. J.** (Eds.), *Handbook of Protoctista*, pp. 600–607. Jones and Bartlett Publishers, Boston.

Melkonian, M. and Robenek, H. (1984). The eyespot apparatus of flagellated green algae: a critical review. In: **Round, F. E. and Chapman, D. J.** (Eds.), *Progress in phycological research, volume 3*, pp. 193–268. Biopress Ltd, Bristol.

Mishler, B. D. and Theriot, E. C. (2000). The phylogenetic species concept (*sensu* Mishler and Theriot): monophyly, apomorphy, and phylogenetic species concepts. In: **Wheeler, Q. D. and Meier, R.** (Eds.), *Species concepts and phylogenetic theory: a debate*. Columbia University Press, New York.

Moestrup, Ø. (1978). On the phylogenetic validity of the flagellar apparatus in green algae and other chlorophyll *a* and *b* containing plants. *BioSystems* **10**: 117–144.

Moestrup, Ø. (1982). Flagellar structure in algae: a review, with observations particularly on the Chrysophyceae, Phaeophyceae (Fucophyceae), Euglenophyceae, and *Reckertia*. *Phycologia* **21**: 427–528.

Moestrup, Ø. (1983). Further studies on *Nephroselmis* and its allies (Prasinophyceae). I. The question of the genus *Bipedinomonas*. *Nordic Journal of Botany* **3**: 609–627.

Moestrup, Ø. (1984a). Further studies on *Nephroselmis* and its allies (Prasinophyceae). II. *Mamiella* gen. nov., Mamiellaceae fam. nov., Mamiellales ord. nov. *Nordic Journal of Botany* **4**: 109–121.

Moestrup, Ø. (1984b). On *Nephroselmis pyriformis* (N. Carter) Ettl. *Williams, D. M.* **4**: 122.

Moestrup, Ø. (1991). Further studies of presumedly primitive green algae, including the description of Pedinophyceae class. nov. and *Resultor* gen. nov. *Journal of Phycology* **27**: 119–133.

Moestrup, Ø. (2000). The flagellate cytoskeleton: Introduction of a general terminology for microtubular flagellar roots in protists. In: **Leadbeater, B. S. C. and Green, J. C.** (Eds.), *The Flagellates*. Taylor and Francis, London.

Moestrup, Ø. and Ettl, H. (1979). A light and electron microscopical study of *Nephroselmis olivacea* (Pracinophyceae). *Opera Botanica* **49**: 1–39.

Moestrup, Ø. and Throndsen, J. (1988). Light and electron microscopical studies on *Pseudoscourfieldia marina*, a primitive scaly green flagellate (Prasinophyceae) with posterior flagella. *Canadian Journal of Botany* **66**: 1415–1434.

Moon-van der Staay, S. Y., van der Staay, G. W. M., Guillou, L., Vaulot, D., Claustre, H. and Medlin, L. K. (2000). Abundance and diversity of prymnesiophytes in the picoplankton community from the equatorial Pacific Ocean inferred from 18S rDNA sequences. *Limnology and Oceanography* **45**: 98–109.

Moon-van der Staay, S. Y., De Wachter, R. and Vaulot, D. (2001). Oceanic 18S rDNA sequences from picoplankton reveal unsuspected eukaryotic diversity. *Nature* **409**: 607–610.

Moritz, C. and Hillis, D. M. (1996). Molecular systematics: context and controversies. In: **Hillis, D. M., Moritz, C. and Mable, B. K.** (Eds.), *Molecular systematics*. Sinauer Associates, Inc., Canada.

Nakayama, T., Suda, S., Kawachi, M. and Inouye, I. (2003). Taxonomic and phylogenetic study on a new prasinophycean alga, *Nephroselmis intermedia* sp. nov. (Chlorophyta), based on ultrastructural and molecular characters. Unpublished reference from GenBank.

Nakayama, T., Suda, S., Kawachi, M. and Inouye, I. (2007). Phylogeny and ultrastructure of *Nephroselmis* and *Pseudoscourfieldia* (Chlorophyta), including the description of *Nephroselmis anterostigmatica* sp. nov. and a proposal for the Nephroselmidales ord. nov. *Phycologia* **46**: 680–697.

Nayakama, T., Marin, B., Kranz, H. D., Surek, B., Huss, V. A. R., Inouye, I. and Melkonian, M. (1998). The basal position of scaly green flagellates among the green algae (Chlorophyta) is revealed by analyses of nuclear-encoded SSU rRNA sequences. *Protist* **149**: 367–380.

Needleman, S. B. and Wunsch, C. D. (1970). A general method applicable to the search for similarities in the amino acid sequence of two proteins. *Journal of Molecular Biology* **48**: 443–453.

Norris, R. E. (1980). Prasinophytes. In: **Cox, E. R.** (Ed.), *Phytoflagellates: developments in marine biology 2*, pp. 85–145. Elsevier/North, Holland.

Okamoto, N. and Inouye, I. (2005). A secondary symbiosis in progress? *Science* **310**: 287.

Okamoto, N. and Inouye, I. (2006). *Hatena arenicola* gen. et sp. nov., a Katablepharid undergoing probable plastid acquisition. *Protist* **157**: 401–419.

Omland, K. E. (1994). Character congruence between a molecular and morphological phylogeny for dabbling ducks (*Anas*). *Systematic Biology* **43**: 369–386.

Oosterbroek, P. (1987). More appropriate definitions of paraphyly and polyphyly, with a comment on the Farris 1974 model. *Systematc Zoology* **36**: 103–108.

Page, R. D. M. (1996). TREEVIEW: An application to display phylogenetic trees on personal computers. *Computer Applications in the Biosciences* **12**: 357–358.

Parke, M. and Dixon, P. S. (1964). A revised check-list of British marine algae. *Journal of the Marine and Biological Association of the UK* **45**: 537–557.

Parke, M. and Manton, I. (1967). The specific identity of the algal symbiont in *Convoluta roscoffensis. Journal of the Marine and Biological Association of the UK* **47**: 445–464.

Parke, M. and Rayns, D. G. (1964). Studies on marine flagellates VII. *Nephroselmis gilva* sp. nov. and some allied forms. *Journal of the Marine and Biological Association of the UK* **44**: 209–217.

Pienaar, R. N. and Sym, S. D. (2002). The genus *Pyramimonas* (Prasinophyceae) from southern African inshore waters. *South African Journal of Botany* **68**: 283–298.

Poe, S. and Wiens, J. J. (2000). Character selection and the methodology of morphological phylogenetics. In: **Wiens, J. J.** (Ed.), *Phylogenetic analysis of morphological data*, pp. 20–36. Smithsonian Institution Press, Washington, D.C.

Raven, P. H., Evert, R. F. and Eichhorn, S. E. (1992). *Biology of Plants.* Worth, New York, fifth edition edition.

Reynolds, E. S. (1963). The use of lead citrate at high pH as an electron-opaque stain in electron microscopy. *Journal of Cell Biology* **17**: 208–212.

Rice, P., Longden, I. and Bleasby, A. (2000). EMBOSS: The European Molecular Biology Open Software Suite. *Trends in Genetics* **16**: 276–277.

Romari, K. and Vaulot, D. (2004). Composition and temporal variability of picoeukaryote communities at a coastal site of the English Channel from 18S rDNA sequences. *Limnology and Oceanography* **49**: 784–798.

Rowan, R. and Powers, D. A. (1992). Ribosomal RNA sequences and the diversity of symbiotic dinoflagellates (zooxanthellae). *Proceedings of the National Academy of Sciences USA* **89**: 3639–3643.

Schiller, J. (1926). Die planktonischen Vegetationen des adriatischen Meeres. B. Chrysomonadina, Heterokontae, Cryptomonadina, Eugleninae, Volvocales. I. Systematischer Teil. *Archiv für Protistenkunde* **63**: 59–123.

Sieburth, J. M. (1979). *Sea microbes.* Oxford University Press.

Simmons, M. P. and Ochoterena, H. (2000). Gaps as characters in sequence-based phylogenetic analyses. *Systematic Biology* **49**: 369–381.

Skelton, P. and Smith, A. (2002). *Cladistics: a practical primer on CD-ROM.* Cambridge University Press, Cambridge.

Skuja, H. (1948). Taxonomie des Phytoplanktons einiger Seen in Uppland, Schweden. *Symb. Bot. Upsal.* **9**: 1–399.

Smith, T. F. and Waterman, M. S. (1981). Identificaiton of common molecular subsequences. *Journal of Molecular Biology* **147**: 195–197.

Spurr, A. R. (1969). A low-viscosity epoxy resin embedding medium for electron microscopy. *Journal of*

Ultrastructure Research **26**: 31–43.

Stein, F. R. (1878). *Der Organismus der Infusionsthiere. III. Der Organismus der Flagellaten. I.* Willhelm Engelmann, Leipzig.

Steinkötter, J., Bhattacharya, D., Semmelroth, I., Bibeau, C. and Melkonian, M. (1994). Prasinophytes form independent lineages within the Chlorophyta: evidence from ribosomal RNA sequence comparisons. *Journal of Phycology* **30**: 340–345.

Suda, S. (2003). Light microscopy and electron microscopy of *Nephroselmis spinosa* sp. nov. (Prasinophyceae, Chlorophyta). *Journal of Phycology* **39**: 590–599.

Suda, S. and Watanabe, M. M. (1989). Evidence for sexual reproduction in the primitive green alga *Nephroselmis olivacea* (Prasinophyceae). *Journal of Phycology* **25**: 596–600.

Suda, S., Watanabe, M. M. and Inouye, I. (2004). Electron microscopy of sexual reproduction in *Nephroselmis olivacea* (Prasinophycea, Chlorophyta). *Phycological Research* **52**: 273–283.

Sweeney, B. M. (1976). *Pedinomonas noctilucae* (Prasinophyceae), the flagellate symbiont in *Noctiluca* (Dinophyceae) in Southeast Asia. *Journal of Phycology* **12**: 460–464.

Swofford, D. L. (2003). PAUP*. Phylogenetic Analysis Using Parsimony (*and Other Mehthods), Version 4. Sinauer Associates, Sunderland, Massachusetts.

Swofford, D. L. and Begle, D. P. (1993). *PAUP* User's Manual, Version 3.1.* Laboratory of Molecular Systematics, Smithsonian Institution, Washington DC.

Swofford, D. L., Olsen, G. J., Waddell, P. J. and Hillis, D. M. (1996). Phylogenetic inference. In: **Hillis, D. M., Moritz, C. and Mable, B. K.** (Eds.), *Molecular Systematics.* Sinauer Associates, Inc., Canada.

Sym, S. D. and Pienaar, R. N. (1993). The class Prasinophyceae. In: **Round, F. E. and Chapman, D. J.** (Eds.), *Progress in phycological research, volume 9*, pp. 281–376. Biopress Ltd, Bristol.

Sym, S. D. and Pienaar, R. N. (1997). Further observations on the type subgenus of *Pyramimonas* (Prasinophyceae), with particular reference to a new species, *P. chlorina*, and the flagellar apparatus of *P. propulsa*. *Canadian Journal of Botany* **75**: 2196–2215.

Sym, S. D. and Pienaar, R. N. (1999). An additional punctate species of *Pyramimonas*, *P. formosa* sp. nov., and its impact on the subgenera *Punctatae* and *Pyramimonas* (Prasinophyceae, Chlorophyta). *Journal of Phycology* **35**: 1313–1321.

Sym, S. D., Kawachi, M. and Inouye, I. (2000). Diversity of swimming behaviour in *Pyramimonas* (Prasinophyceae). *Phycological Research* **48**: 149–154.

Tamura, K., Dudley, J., Nei, M. and Kumar, S. (2007). MEGA4: Molecular Evolutionary Genetics Analysis (MEGA) Software, Version 4.0. Molecular Biology and Evolution 10.1093/molbev/msm092.

Thompson, J. D., Higgins, D. G. and Gibson, T. J. (1994). CLUSTAL W: improving the sensitivity of progressive multiple sequence alignment through sequence weighting, position specific gap penalties and weight matrix choice. *Nucleic Acids Research* **22**: 4673–4680.

Throndsen, J. (1997). The planktonic marine flagellates. In: **Tomas, C. R.** (Ed.), *Identifying marine phytoplankton.* Academic Press, San Diego, California.

Throndsen, J. and Zingone, A. (1997). *Dolichomastix tenuilepis* sp. nov., a first insight into the microanatomy of the genus *Dolichomastix* (Mamiellales, Prasinophyceae, Chlorophyta). *Phycologia* **36**: 244–254.

Tomas, C. (1997). *Identifying marine phytoplankton.* Academic Press, San Diego, California.

Tseng, C. K., Chen, J., Zhang, Z. and Zhang, H. (1994). Light and electron microscope observations on *Nephroselmis gaoae* sp. nov. (Prasinophyceae). *Chinese Journal of Oceanology and Limnology* **12**: 201–207.

Watanabe, S., Himizu, A., Lewis, L. A., Floyd, G. L. and Fuerst, P. A. (2000). *Pseudoneochloris marina* (Chlorophyta), a new coccoid ulvophycean alga, and its phylogenetic position inferred from morphological and molecular data. *Journal of Phycology* **36**: 596–604.

Whatley, J. M. (1993). Chloroplast ultrastructure. In: **Berner, T.** (Ed.), *Ultrastructure of microalgae.* CRC Press, Inc, Boca Raton.

Wheeler, Q. D. and Platnick, N. I. (2000a). A critique from the Wheeler and Platnick phylogenetic species concept perspective: problems with alternative concepts of species. In: **Wheeler, Q. D. and**

Meier, R. (Eds.), *Species concepts and phylogenetic theory: a debate*. Columbia University Press, New York.

Wheeler, Q. D. and Platnick, N. I. (2000b). The phylogenetic species concept (*sensu* Wheeler and Platnick). In: **Wheeler, Q. D. and Meier, R.** (Eds.), *Species concepts and phylogenetic theory: a debate*. Columbia University Press, New York.

White, T. J., Bruns, T., Lee, S. and Taylor, T. (1990). Amplification and direct sequencing of fungal ribosomal RNA genes for phylogenetics. In: **Innis, M. A., Gelfand, D. H., Sninsky, J. J. and White, T. J.** (Eds.), *PCR protocols: a guide to methods and applications*. Academic Press, Inc., San Diego.

Wiens, J. J. (2000). Preface. In: **Wiens, J. J.** (Ed.), *Phylogenetic analysis of morphological data*. Smithsonian Institution Press, Washington, D.C.

Wiley, E. O., Siegel-Causey, D., Brooks, D. R. and Funk, V. A. (1993). *The compleat cladist*. The University of Kansas Museum of Natural History Special Publication No. 19.

Yoshii, Y. (2006). Diversity and evolution of photosynthetic antenna systems in green plants. *Phycological Research* **54**: 220–229.

Yoshii, Y., Takaichi, S., Maoka, T., Suda, S., Sekiguchi, H., Nakayama, T. and Inouye, I. (2005). Variation in siphonaxanthin series among the genus *Nephroselmis* (Prasinophyceae, Chlorophyta), including a novel primary methoxy carotenoid. *Journal of Phycology* **41**: 827–834.

Young, A. V. (1991). *A developmental study of* Nephroselmis viridis *Inouye, Suda* et *Pienaar.* Master's thesis, University of the Witwatersrand, Johannesburg.

Young, N. D. and Healy, J. (2003). GapCoder automates the use of indel characters in phylogenetic analysis. *BMC Bioinformatics* **4**: 6.

Zingone, A., Borra, M., Brunet, C., Forlani, G., Kooistra, W. H. C. F. and Procaccini, G. (2002). Phylogenetic position of *Crustomastix stigmatica* sp. nov. and *Dolichomastix tenuilepis* in relation to the Mamiellales (Prasinophyceae, Chlorophyta). *Journal of Phycology* **38**: 1024–1039.

Appendix A

Electron Microscopy Preparation Techniques

A.1 Formvar Film

Formvar film for coating of electron microscope grids was prepared as follows. A 0.5% solution of Formvar in Dichloroethane was used, which was prepared by mixing 0.5 g of Formvar in 100 mℓ of Dichloroethane. Microscope slides were cleaned with alcohol and impurities were burned off over an open alcohol flame. Lens tissue was used to remove any surface reside from the ultrapure Millipore water in a glass basin. Glass slides were heated over an open alcohol flame and lowered for half their length into Formvar in a small beaker. The Formvar film on the slide was scored on the top, bottom, left and right edges, as well as down the middle, with a sharp blade. The slide was lowered carefully into the basin of ultrapure Millipore water, causing the Formvar film to detach from the slide and float onto the surface of the water. Grids (#300 Mesh or Slot) were placed into the floating Formvar film, with the shiny surface facing up. Small sections of Parafilm were submerged against each Formvar film in order to be able to remove the Formvar from the basin.

A.2 Whole Mounts

A JEM 100S transmission electron microscope was used for all whole mount viewing. Micrograph negatives were scanned electronically (see section 2.4 on page 37). Details of the fixative used for freshwater samples are provided in section A.6 on page 98. The following procedure was used (Marin and Melkonian, 1994). A fixative consisting of a final concentration of 5% gluteraldehyde in growth medium was prepared. 4 $\mu\ell$ of fixative was placed onto a #300 mesh electron microscope grid which had been coated with Formvar and 4 $\mu\ell$ of cell suspension was added. This was left to stand for 5 minutes and the liquid was then removed with wedges of filter paper and 4 $\mu\ell$ of ultrapure Millipore water and 4 $\mu\ell$ of 2% aqueous Uranyl Acetate was addd. This was left to stand for 90 seconds. The liquid was removed with wedges of filter paper and the grid was washed once with 4 $\mu\ell$ of distilled water.

A.3 Sodium Cacodylate Fixation and Embedding for Ultrathin Sectioning

18 mℓ of 0.5 M sucrose in 0.1 M sodium cacodylate[20] was placed into a clean glass polytop vial in a fume hood and 2mℓ of 25% gluteraldehyde (GTA) was addd. Centrifuge tubes were filled with 5 mℓ of culture each and 5 mℓ of the GTA as prepared above was added to each. Tubes were sealed with Parafilm and gently inverted once to mix. The samples were allowed to fix for 1 hour at room temperature in the fume hood. The tubes were then centrifuged for 5 minutes at 1000 g and then for 10 minutes at 3000 g and the supernatant was discarded. The tubes were washed in each of the following in sequence, care being taken to not resuspend the pellet: (a) 0.5 M sucrose 0.1 M sodium cacodylate, (b) 0.4 M sucrose 0.1 M sodium cacodylate, (c) 0.2 M sucrose 0.1 M sodium cacodylate and (d) 0.1 M sucrose 0.1 M sodium cacodylate. All tubes were bulked into one after the final wash. The pellet was post-fixed for 1 hour at room temperature in 2% Osmium Tetroxide (OsO_4) in 0.1 M sodium cacodylate buffer (no sucrose). The pellet was resuspended in the Osmium Tetroxide to ensure uniform post-fixation. After post-fixation the tube(s) were centrifuged again to form a pellet. The pellet was washed three times in 0.1 M buffer (no sucrose), care being taken to not resuspend the pellet. The pellet was dehydrated for 15 minutes in each of the following: 10%, 20%, 50%, 80% and 90% alcohol. This was followed by two washes in 100% alcohol for 20 minutes each. Spurr's Resin[21] was prepared. The pellet was infiltrated in the following resin to alcohol mixtures for 20 minutes each: (a) 3 alcohol (100%) to 1 resin, (b) 1 alcohol (100%) to 1 resin and (c) 1 alcohol (100%) to 3 resin. Finally the pellet was infiltrated in 100% resin for 30 minutes. Tin foil dishes with a catalogue number were prepared and filled with 100% resin. The pellet was gently broken into small pieces in the centrifuge tube and transferred them to the tin foil dish. The pellet fragments were allowed to settle completely before the dish was placed into a Memmert oven at 70°C for 16 hours. A small amount of the pellet was fully suspended in resin and a small drop was placed onto a clean slide, covered with a cover slip, labelled and placed into the oven for 16 hours. The resin mould was removed from the tin foil dish after 16 hours and small blocks small blocks containing cells were cut out of the resin using a jeweler's hacksaw. Each block was glued onto a resin bullet from a beem capsule. Blocks were trimmed with glass knives and 50 nm sections were cut with a Reichert Ultracut E microtome. Sections were stained and viewed as detailed in section A.5 on page 98. Micrograph negatives were scanned electronically (see section 2.4 on page 37).

A.4 Freshwater/Seawater Fixation and Embedding for Ultrathin Sectioning

Centrifuge tubes were filled with 9.5 mℓ of culture each and 0.5 mℓ of either 25% gluterelde-hyde (GTA) (seawater) or 25% Gluteraldehyde-Phosphate Buffer[22] (freshwater) was added. Tubes were sealed with Parafilm and gently inverted once to mix. The samples were allowed to fix for 1 hour at room temperature in the fume hood. The tubes were then centrifuged for 5 minutes at 1000 g and then for 10 minutes at 3000 g and the supernatant was discarded. The tubes were washed three times with freshwater/seawater, care being taken to not resuspend the pellet. The pellet was post-fixed for 1 hour at room temperature in 2% Osmium Tetroxide (OsO_4) in freshwater/seawater. The pellet was resuspended

[20] Recipe provided in section C.7 on page 102
[21] Recipe provided in section C.1 on page 101
[22] Recipe provided in section A.6 on page 98

in the Osmium Tetroxide to ensure uniform post-fixation. After post-fixation the samples were bulked and centrifuged again to form a pellet. The pellet was washed three times with freshwater/seawater, care being tkane to not resuspend the pellet. The pellet was dehydrated for 15 minutes in each of the following: 10%, 20%, 50%, 80% and 90% alcohol. This was followed by two washes in 100% alcohol for 20 minutes each. Spurr's Resin[23] was prepared. The pellet was infiltrated in the following resin to alcohol mixtures for 20 minutes each: (a) 3 alcohol (100%) to 1 resin, (b) 1 alcohol (100%) to 1 resin and (c) 1 alcohol (100%) to 3 resin. Finally, the pellet was infiltrated in 100% resin for 30 minutes. Tin foil dishes with a catalogue number were prepared and filled with 100% resin. The pellet was gently broken into small pieces in the centrifuge tube and transferred them to the tin foil dish. The pellet fragments were allowed to settle completely before the dish was placed into a Memmert oven at 70°C for 16 hours. A small amount of the pellet was fully suspended in resin and a small drop was placed onto a clean slide, covered with a cover slip, labelled and placed into the oven for 16 hours. The resin mould was removed from the tin foil dish after 16 hours and small blocks small blocks containing cells were cut out of the resin using a jeweler's hacksaw. Each block was glued onto a resin bullet from a beem capsule. Blocks were trimmed with glass knives and 50 nm sections were cut with a Reichert Ultracut E microtome. Sections were stained and viewed as detailed in section A.5 on page 98. Micrograph negatives were scanned electronically (see section 2.4 on page 37).

A.5 Staining and Viewing of Ultrathin Sections

Sections were collection onto slot or mesh microscope grids and double-stained with Uranyl Acetate and Lead Citrate as follows. Drops of freshly-made Lead Citrate[24] were dispensed onto Parafilm in an air-tight container such as a Petri dish. Wet pellets of sodium hydroxide (NaOH) were placed into the container and left to stand until required. Each microscope grid was stained by placing it onto a drop of Uranyl Acetate on Parafilm for 15 minutes. Each microscope grid was then rinsed by placing it onto a drop of distilled water on Parafilm or by dipping it carefully into a beaker of fresh ultrapure Millipore water. Each microscope grid was then stained by placing it onto a drop of Lead Citrate as prepared above for 10 minutes. Each microscope grid was then placed onto a drop of weak sodium hydroxide (NaOH) on Parafilm and finally rinsed again with water as above. A JEM 100S transmission electron microscope was used for viewing. Micrograph negatives were scanned electronically (see section 2.4 on page 37).

A.6 Freshwater Fixative

A Glutaraldehyde-Phosphate Buffer, as follows (Hayat, 1986: 15), was used as a fixative for freshwater samples (see section A.4 on page 97). The fixative contains 2.5% glutaraldehyde and has a pH of 7.4.

$NaH_2PO_4.H_2O$	3.31 g
$Na_2HPO_4.7H_2O$	33.71 g
25% Glutaraldehyde in water	40 mℓ

Distilled water was added to make the final volume up to 1ℓ.

[23] Recipe provided in section C.1 on page 101

[24] Recipe provided in section C.3 on page 101

Appendix B

Media Recipes

B.1 3N-BBM+V Medium (Freshwater)

This recipe is a modification, provided by CCAP[25], of the standard *Bold Basal Medium* (BBM) as described in Andersen *et al.* (2005). The modification includes threefold nitrogen (3N) and added vitamins (V). Add all of the following components, make up to 1ℓ with distilled water, autoclave at 15 psi for 15 minutes and ensure that the final pH is 6.6 by adding either 1 N NaOH or 1 N HCl.

Component	**Stock Solution ($g.\ell^{-1}$ distilled water)**	**Quantity Used for 1ℓ Medium**
Macronutrients		
$NaNO_3$	25.00	30 $m\ell$
$CaCl_2.2H_2O$	2.50	10 $m\ell$
$MgSO_4.7H_2O$	7.50	10 $m\ell$
K_2HPO_4	7.50	10 $m\ell$
KH_2PO_4	17.50	10 $m\ell$
NaCl	2.50	10 $m\ell$
Trace Element Solution		6 $m\ell$
Add 0.75g Na_2EDTA and the minerals in the following order to 1 ℓ of distilled water		
$FeCl_2.6H_2O$		97.0 mg
$MnCl_2.4H_2O$		41.0 mg
$ZnCl_2.6H_2O$		5.0 mg
$CoCl_2.6H_2O$		2.0 mg
$Na_2MoO_4.2H_2O$		4.0 mg
Vitamin B_1		1 $m\ell$
0.12 g Thiaminhydrochloride in 100 $m\ell$ distilled water; filter sterile		
Vitamin B_{12}		1 $m\ell$
Make up 0.1 g Cyanocobalamin in 100 $m\ell$ distilled water		
Take 1 $m\ell$ of this solution and add 99 $m\ell$ distilled water; filter sterile		

B.2 Soil Extract (Freshwater)

Unfertilized soil was mixed with distilled water, agitated and left to stand for three days. The water was then fine-filtered and autoclaved to produce soil extract medium. This was added to distilled water at 10 $m\ell$ per ℓ.

[25] Website: *http://www.ccap.ac.uk*

B.3 Provasoli's Enriched Seawater (PES) Medium

McLachlan (1973)

Stock 1 – Major Salts – Made up to 1 ℓ with distilled water

- 5.61 g $NaNO_3$
- 0.78 g $NL2.C_3H_5(OH_2)PO_4.5H_2O$
- 0.26 g Fe.EDTA
- 7.99 g Tris. Buffer

Stock 2 – PII Trace Metals – Made up to 1 ℓ with distilled water

- 230 mg $ZnSO_4.7H_2O$
- 163 mg $MnSO_4.4H_2O$
- 5 mg $CoSO_4.7H_2O$
- 114 0mg H_3BO_3
- 1000 mg NL2.EDTA
- 60 mg Fe.Citrate

Stock 3 – Vitamins – Made up to 500 mℓ with distilled water

- 0.8 mg Cyanocobalamin
- 0.4 mg Biotin
- 10 mg Thiamine (Aneurine).HCl

Method
1 ℓ of enriched seawater is made by combining the following, and making the volume up to 1 ℓ with distilled water:

- 10 mℓ of Stock 1
- 10 mℓ of Stock 2
- 1 mℓ of Stock 3

PES stock solutions were filter-sterilized through a 0.45 Millipore filter membrane. The pH of all stock solutions was adjusted to pH 7.5 using either 1 N HCl or 1 N NaOH.

Appendix C

Chemicals

C.1 Spurr's Low Viscosity Resin (Spurr, 1969)

The following components were added in the order in which they are listed. The mixture was stirred continuously at a moderate speed with a magnetic stirrer.

- 10 g Vinylcyclohexene Dioxide (VDC or ERL 4206)
- 6 g Diflycide Ether of Polypropylene Glycol (DER 736)
- 26 g Nonenyl Succinic Anhydride (NSA)
- 0.4 g Dumethylaminoethanol (S-1 DMAE)

C.2 Uranyl Acetate

A 2% aqueous solution of uranyl acetate was prepared by mixing 1 g of powdered uranyl acetate into 50 ml of distilled water. The mixture was agitated to ensure that all of the uranyl acetate dissolved and then allowed to settle. The solution was wrapped in tin foil to protect it from the light and stored in the refridgerater.

C.3 Reynold's Lead Citrate (Reynolds, 1963)

Lead Citrate was prepared as follows. 3.2 mℓ of water was added to 0.6 mℓ of Trisodium Citrate (37.7 g/100 mℓ water) and stirred. 0.4 mℓ of Lead Nitrate (33.1 g/100 mℓ water) was then added and the mixture was stirred to make it homogenous. 0.8 mℓ of 1 N Sodium Hydroxide (4 g/100 mℓ water) was added an stirred until the precipitate dissolved.

C.4 Germanium Dioxide

Germanium Dioxide (GeO_2) was prepared as follows. 100 mg of GeO_2 was placed into test tube. Four to six pellets of potassium hydroxide (KOH) were added, followed by 3 mℓ of distilled water. The mixture was boiled slowly until the GeO_2 is in solution. It may be necessary to add an additional ten to twelve more potassium hydroxide (KOH) pellets during this time (approximately 15 minutes). When the GeO_2 is in solution, the volume was brought to 10 mℓ with distilled water. The pH was adjusted to approximately 8 with 2 N HCl (or KOH) as required. Distilled water was added to bring the volume to 25 mℓ, which is 4 mg GeO_2 per mℓ. 0.25 mℓ GeO_2 per ℓ growth medium was used as required (1 mg GeO_2 per ℓ growth medium).

C.5 Chromic Acid

In a fume hood, 5 g of Potassium Dichromate ($K_2Cr_2O_7$) was added to 10 mℓ of distilled water. Concentrated Sulphuric Acid (H_2SO_4) was then added until the potassium dichromate is fully dissolved. Chromic acid will dissolve organic matter and was used on occassion to clean flasks.

C.6 Tris (TAE) Electrophoresis Buffer

A 50 times strength 500 mℓ stock solution of Tris (TAE) Electrophoresis Buffer was prepared as follows. 121 g of Tris base, 18.6 g of $Na_2EDTA.2H_2O$ and 400 mℓ of distilled water were mixed on a hot plate set on a low heat. The solution was allowed to cool before 28.6 mℓ Glacial Acetic Acid was added. The pH of the mixture was adjusted to 8.1 using Glacial Acetic Acid and then brought to 500 mℓ with distilled water.

C.7 Sucrose and Sodium Cacodylate Series

Osmolarity Media

Sucrose, with a molecular weight of 342.3, was used. 100 mℓ of each of the following were prepared, except where otherwise indicated:

- 0.5 M sucrose: 17.120 g sucrose per 100 mℓ distilled water. Make up to 500 mℓ.
- 0.4 M sucrose: 13.692 g sucrose per 100 mℓ distilled water.
- 0.2 M sucrose: 6.846 g sucrose per 100 mℓ distilled water.
- 0.1 M sucrose: 3.423 g sucrose per 100 mℓ distilled water.

Preparation of Buffer

In volumetric flasks, 100 mℓ of the following solutions were prepared, except where otherwise indicated:

- A: 250 mℓ of 0.2 M sodium cacodylate in 0.5 M sucrose. Make up to 500 mℓ.
- B: 50 mℓ of 0.2 M sodium cacodylate in 0.4 M sucrose.
- C: 50 mℓ of 0.2 M sodium cacodylate in 0.2 M sucrose.
- D: 50 mℓ of 0.2 M sodium cacodylate in 0.1 M sucrose.
- E: 50 mℓ of 0.2 M sodium cacodylate (no sucrose).

The molecular weight of sodium cacodylate is 214.03. Therefore, 0.2 M sodium cacodylate is 2.1403 g in 50 mℓ.

Optimization of Buffer

50 mℓ of 0.2 M HCl was prepared. Concentrated HCl is 10 N = 10 M. Therefore, 0.2 M HCl is 1 mℓ of 10 N HCl in 49 mℓ of distilled water. The pH of each solution A to E above was adjusted to approximately 7.5 by adding 12.5 mℓ of 0.2 M HCl to solution A above and 2.5 mℓ of 0.2 M HCl to solutions B to E above. Each solution A to E above was made up to the mark with the relevant concentration of sucrose solution. Distilled water was used in solution E (no sucrose).

C.8 Alcohol Dilution Series

A stock solution of 100% ethanol was diluted with ultrapure Millipore water to produce a series of alcohol dilutions, as follows: 10%, 20%, 50%, 70%, 80%, 90% and 95%.

Appendix D

Custom *Python* Programs

 Source code is available from the author via email (*bell@gecko.biol.wits.ac.za*). See section 2.5.6 for more information on the use of these programs in this study.

morph.py This program formats character state data from the clipboard (typically copied from a spreadsheet) into Phylip and PAUP* (Nexus) formats and writes the formatted data to disk (see section 2.2.

penaltytester.py This program runs a *ClustalW* multiple sequence alignment with a range of gap-opening and gap-extension parameters for slow pairwise and multiple sequence alignment, called *ReadSeq* to convert the output file to Nexus format and runs PAUP* to perform a heuristic search and bootstrap analysis on the data, which can be redirected to a log file. The input file must be named "infile.fasta". See section 2.5.3.

penaltyparser.py This program parses the output log file from *penaltytester* to display the parameters used and the consistency index (CI) of the trees produced from the PAUP* analysis. See section 2.5.3.

seqcomp.py This program runs the *water* program from EMBOSS to complete pairwise comparisons between all the FASTA files in the current folder and outputs the similarity score data as a table. See section 3.10.

seqindelcode.py This program codes indels in molecular data based on the species groupings specified by the user. See section 2.5.5.

seqscanner.py This program is a front-end for the *fuzznuc* program from EMBOSS. Multiple searches of all possible substrings between the specified minimum and maximum length across an entire target sequence are conducted. See section 3.10.

Appendix E

Partial 18S Sequence Data

The edited and aligned partial 18S sequence data which was used in the molecular analysis is provided on the following pages. The LaTeX TeXshade package (Beitz, 2000) was used to format the sequence data for printing. The insertion of 437 bases found starting at position 329 in *Nephroselmis viridis* sp. ined. is provided after the sequence data.

```
GCATGTCTA.GTATAA.CTATTTATACTGGGAAACTGCGAATGGCTCATTAAATCAGTTA   58  Nephroselmis_anterostigmatica_MBIC11158
GCATGTCTAAGTATAA.CTATTTATACTGGGAAACTGCGAATGGCTCATTAAATCAGTTA   59  Nephroselmis_anterostigmatica_AB158372
GCATGTCTAAGTATAA.CTATTTATACTGGGAAACTGCGAATGGCTCATTAAATCAGTTA   59  Nephroselmis_anterostigmatica_AB158373
..............AA.CTATTTATACTGGGAAACTGCGAATGGCTCATTAAATCAGTTA   45  Nephroselmis_astigmatica_NIES252
GCATGTCTAAGTATAA.CTATTTATACTGGGAAACTGCGAATGGCTCATTAAATCAGTTA   59  Nephroselmis_astigmatica_AB158374
GCATGTCTAAGTATAA.CTATT.ATACTGGGAAACTGCGAATGGCTCATTAAATCAGTTA   58  Nephroselmis_olivacae_X74754
GCATGTCTAAGTATAA.CTGCTTATACTGGGAAACTGCGAATGGCTCATTAAATCAGTTA   59  Nephroselmis_pyriformis_WW02
GCATGTCTAAGTATAA.CTGCTTATACTGGGAAACTGCGAATGGCTCATTAAATCAGTTA   59  Nephroselmis_pyriformis_AB158376
GCATGTCTAAGTATAA.CTGCTTATACTGGGAAACTGCGAATGGCTCATTAAATCAGTTA   59  Nephroselmis_pyriformis_AB058378
GCATGTCTAAGTATAA.CTGCTTATACTGGGAAACTGCGAATGGCTCATTAAATCAGTTA   59  Nephroselmis_pyriformis_AB058391
GCATGTCTAAGTATAA.CTGCTTATACTGGGAAACTGCGAATGGCTCATTAAATCAGTTA   59  Pseudoscourfieldia_marina_X75565
GCATGTCTAAGTATAA.CTATTTATACTGGGAAACTGCGAATGGCTCATTAAATCAGTTA   59  Nephroselmis_rotunda_CCAP1960_3
....GTCTA.GT.TA..CTATTTATACTGGGAAACTGCGAATGGCTCATTAAATCAGTTA   52  Nephroselmis_rotunda_BB2
GCATGTCTAAGTATAA.CTGCTTATACTGGGAAACTGCGAATGGCTCATTAAATCAGTTA   59  MBIC11149_AB214975
...........TA..A.CTTTT.ATACTGGGAA.CTGCGAATGGCTCATTAAATCAGTTA   44  Nephroselmis_spinosa_NIES935
GCATGTGTCTGTATAA.CTTTT.ATACTGGGAAACTGCGAATGGCTCATTAAATCAGTTA   58  Nephroselmis_spinosa_AB158375
.............TAA.CTATTTATACTGGGAAACTGCGAATGGCTCATTAAATCAGTTA   46  Nephroselmis_viridis_NIES486
GCATGTCTAAGTATAA.CTNTTTATACTGGGAAACTGCGAATGGCTCATTNAATCAGTTA   59  Nephroselmis_viridis_AB214976
GCATGTCTAAGTATA...CCGTTATACTGGGAAACTGCGAATGGCTCATTAAATCAGTTA   57  Pseudoscourfieldia_marina_AF122888
GCATGTCTAAGTATA...CCGTTATACTGGGAAACTGCGAATGGCTCATTAAATCAGTTA   57  Pseudoscourfieldia_marina_AJ132619
GCATGTCTAAGTATAAGC..ATTATACAGTGAAACTGCGAATGGCTCATTAAATCAGTTA   58  Dolichomastix_tenuilepis
GCATGTCTAAGTATAAAT...TTATACAGTGAAACTGCGAATGGCTCATTAAATCAGTTA   57  Dolichomastix_tenuilepis_AF509625
GCATGTCTAAGTATAAGC..GTTATACTGTGAAACTGCGAATGGCTCATTAAATCAGCAA   58  Mamiella_gilva_AB017129
GCATGTCTAAGTATA.GCTGATTATACTGTGAAACTGCGAATGGCTCATTAAATCAGTTA   59  Pyramimonas_mucifera
GCATGTCTAAGTATAAGCTGATTATACTGTGAAACTGCGAATGGCTCATTAAATCAGTTA   60  Pyramimonas_olivacea_AB017122
GCATGTCTAAGTATAAGCTGATTATACTGTGAAACTGCGAATGGCTCATTAAATCAGTTA   60  Pyramimonas_parkeae_AB017124
GCCTGTCTAAGTATAA.CTGCTTATACTGTGAAACTGCGAATGGCTCATTAAATCAGTTA   59  Tetraselmis
GCATGTCTAAGTATAAACTGCTTATACTGTGAAACTGCGAATGGCTCATTAAATCAGTTA   60  Tetraselmis_convolutae_U05039
..ATGTCTAAGTATAAACTGCTTATACTGTGAACCTGCGAATGGATCATTAAATCAGTTA   58  Tetraselmis_kochiensis_AJ431370
GCATGTCTAAGTATAAGCTTATTATACTGTGAAACTGCGAATGGCTCATTAAATCAGTTA   60  Halosphaera_AB017125
.............TAAA.GCTTTATACGGTGAAACTGCGAATGGCTCATTAAATCAGTTA   46  Pseudoscourfieldia_marina_Wits_(?)
GCATGTCTAAGTATAAG.CTTTTATACGGTGAAACTGCGAATGGCTCATTAAATCAGTTA   59  Prasinoderma_coloniale_AB058379
GCATGTCTAAGTATAAACGCTTTATACTGTGAAACTGCGAATGGCTCATTAAATCAGTTA   60  Prasinococcus_capsulatus_AB058384
```

TAGTTTATTTGATGGTACCTTACTACTCGGATAACCGTAGTAATTCTAGAGCTAATACGT	118	Nephroselmis_anterostigmatica_MBIC11158
TAGTTTATTTGATGGTACCTTACTACTCGGATAACCGTAGTAATTCTAGAGCTAATACGT	119	Nephroselmis_anterostigmatica_AB158372
TAGTTTATTTGATGGTACCTTACTACTCGGATAACCGTAGTAATTCTAGAGCTAATACGT	119	Nephroselmis_anterostigmatica_AB158373
TAGTTTATTTGATGGTACCTTACTACTCGGATAACCGTAGTAATTCTAGAGCTAATACGT	105	Nephroselmis_astigmatica_NIES252
TAGTTTATTTGATGGTACCTTACTACTCGGATAACCGTAGTAATTCTAGAGCTAATACGT	119	Nephroselmis_astigmatica_AB158374
TAGTTTATTTGATGGTACCTTACTACTCGGATAACCGTAGTAATTCTAGAGCTAATACGT	118	Nephroselmis_olivacae_X74754
TAGTTTATTTGATGGTACCTTACTACTCGGATAACCGTAGTAATTCTAGAGCTAATACGT	119	Nephroselmis_pyriformis_WW02
TAGTTTATTTGATGGTACCTTACTACTCGGATAACCGTAGTAATTCTAGAGCTAATACGT	119	Nephroselmis_pyriformis_AB158376
TAGTTTATTTGATGGTACCTTACTACTCGGATAACCGTAGTAATTCTAGAGCTAATACGT	119	Nephroselmis_pyriformis_AB058378
TAGTTTATTTGATGGTACCTTACTACTCGGATAACCGTAGTAATTCTAGAGCTAATACGT	119	Nephroselmis_pyriformis_AB058391
TAGTTTATTTGATGGTACCTTACTACTCGGATAACCGTAGTAATTCTAGAGCTAATACGT	119	Pseudoscourfieldia_marina_X75565
TAGTTTATTTGATGGTACCTTACTACTCGGATAACCGTAGTAATTCTAGAGCTAATACGT	119	Nephroselmis_rotunda_CCAP1960_3
TAGTTTATTTGATGGTACCTTACTACTCGGATAACCGTAGTAATTCTAGAGCTAATACGT	112	Nephroselmis_rotunda_BB2
TAGTTTATTTGATGGTACCTTACTACTCGGATAACCGTAGTAATTCTAGAGCTAATACGT	119	MBIC11149_AB214975
TAGTTTATTTGATGGTACCTTACTACTCGGATAACCGTAGTAATTCTAGAGCTAATACGT	104	Nephroselmis_spinosa_NIES935
TAGTTTATTTGATGGTACCTTACTACTCGGATAACCGTAGTAATTCTAGAGCTAATACGT	118	Nephroselmis_spinosa_AB158375
TAGTTTATTTGATGGTACCTTACTACTCGGATAACCGTAGTAATTCTAGAGCTAATACGT	106	Nephroselmis_viridis_NIES486
TAGTTTATTTGATGGTACCTTACTACTCGGATAACCGTANTAATTCTAGAGCTAATACGT	119	Nephroselmis_viridis_AB214976
TAGTTTATTTGATGGTACCTTACTACTCGGATAACCGTAGTAATTCTAGAGCTAATACGT	117	Pseudoscourfieldia_marina_AF122888
TAGTTTATTTGATGGTACCTTACTACTCGGATAACCGTAGTAATTCTAGAGCTAATACGT	117	Pseudoscourfieldia_marina_AJ132619
TAGTTTATTTGATGGTGT.TT.TTACTCGGATAACCGTAGTAATTCTAGAGCTAATACGT	116	Dolichomastix_tenuilepis
TAGTTTATTTGATGGTAC.TT..TACTCGGATAACTGTAGTAATTCTAGAGCTAATACGT	114	Dolichomastix_tenuilepis_AF509625
TAGTTTCTTTGGTGGTGT.TTACTACTCGGATAACCGTAGTAATTCTAGAGCTAATACGT	117	Mamiella_gilva_AB017129
TAGTTTATTTGATGGTAC.CTACTACTCGGATAACCGTAGTAATTCTAGAGCTAATACGT	118	Pyramimonas_mucifera
TAGTTTATTTGATGGTAC.CTACTACTCGGATAACCGTAGTAATTCTAGAGCTAATACGT	119	Pyramimonas_olivacea_AB017122
TAGTTTATTTGATGGTAC..TACTACTCGGATAACCGTAGTAATTCTAGAGCTAATACGT	118	Pyramimonas_parkeae_AB017124
TAGTTTATTTGATGGTAC.CTACTACTCGGATAACCGTAGTAATTCTAGAGCTAATACGT	118	Tetraselmis
TAGTTTATTTGATGGTAC.CTACTACTCGGATAACCGTAGTAATTCTAGGGCTAATACGT	119	Tetraselmis_convolutae_U05039
TAGTTTATTTGATGGTAC.CTACTACTCGGATAACCGTAGTAATTCTAGAGCTAATACGT	117	Tetraselmis_kochiensis_AJ431370
TAGTTTATTTGATGGTAC.CTACTACTCGGATAACCGTAGTAATTCTAGAGCTAATACGT	119	Halosphaera_AB017125
TAGTTTATTTGATGGT...CTTGTACTCGGATACCTGTTGGAATCCAAGAGCTAATACGT	103	Pseudoscourfieldia_marina_Wits_(?)
TAGTTTATTTGATGGT...CT.GTACTCGGATACCTGTTGGAATCCAAGAGCTAATACGT	115	Prasinoderma_coloniale_AB058379
TAGTTTATTTGATGGTAC.CTACTACTCGGATAACCGTAGTAATTCTAGAGCTAATACGT	119	Prasinococcus_capsulatus_AB058384

```
GCGCAACTCCCGACTCTT.GGAAGGGACGTATATATTAGATAAAAGACCGACCGG.CTTT   176  Nephroselmis_anterostigmatica_MBIC11158
GCGCAACTCCCGACTCTT.GGAAGGGACGTATATATTAGATAAAAGACCGGCCGG.GCTT   177  Nephroselmis_anterostigmatica_AB158372
GCGCAACTCCCGACTCTT.GGAAGGGACGTATATATTAGATAAAAGACCGACCGG.CTTT   177  Nephroselmis_anterostigmatica_AB158373
GCGCAACTCCCGACTTCT.GGAAGGGACGTATATATTAGATAAAAGACCGACCGG.GCTT   163  Nephroselmis_astigmatica_NIES252
GCGCAACTCCCGACTTCT.GGAAGGGACGTATATATTAGATAAAAGACCGACCGG.GCTT   177  Nephroselmis_astigmatica_AB158374
GCGCAACTCCCGACTTC..GGAAGGGACGTATATATTAGATCAAAGACCGACCGG.GCTT   175  Nephroselmis_olivacae_X74754
GCGCAACACCCGACTTC..GGAAGGGTTGTATATATTAGATAAAAGACCGACCG...CTT   174  Nephroselmis_pyriformis_WW02
GCGCAACACCCGACTTC..GGAAGGGTTGTATATATTAGATAAAAGACCGACCG...CTT   174  Nephroselmis_pyriformis_AB158376
GCGCACCACCCGACTTC..GGAAGGGTTGTATATATTAGATAAAAGACCGACCG...CTT   174  Nephroselmis_pyriformis_AB058378
GCGCAACACCCGACTTC..GGAAGGGTTGTATATATTAGATAAAAGACCGACCG...CTT   174  Nephroselmis_pyriformis_AB058391
GCGCAACACCCGACTTC..GGAAGGGTTGTATATATTAGATAAAAGACCGACCG...CTT   174  Pseudoscourfieldia_marina_X75565
GCGCAACTCCCGACTCTT.GGAAGGGACGTATATATTAGATAAAAGGCCGACCGG.GCTT   177  Nephroselmis_rotunda_CCAP1960_3
GCGCAACTCCCGACTCTT.GGAAGGGACGTATATATTAGATAAAAGGCCGACCGG.GCTT   170  Nephroselmis_rotunda_BB2
GCGCAACTCCCGACTCTT.GGAAGGGACGTATATATTAGATAAAAGGCCGACCGG.GCTT   177  MBIC11149_AB214975
GCGCAACTCCCGACTTTTTGGAAGGGACGTATATATTGGATAAAAGGCCGACCGG.GCTT   163  Nephroselmis_spinosa_NIES935
GCGCAACTCCCGACTTTTTGGAAGGGACGTATATATTGGATAAAAGGCCGACCGG.GCTT   177  Nephroselmis_spinosa_AB158375
GCGCAACTCCCGACTTC..GGAAGGGACGTATATATTAGATAAAAGACCGACCGG.GCTT   163  Nephroselmis_viridis_NIES486
GCGCAACTCCCGACTTC..GGAAGGGACGTATATNTTAGATNAAAGACCGACCGG.GCTT   176  Nephroselmis_viridis_AB214976
GCGTAAATCTCGACTTC..GGAAGAGACGTATTTATTAGATTAAAGACCAACCCT.TC..   172  Pseudoscourfieldia_marina_AF122888
GCGTAAATCTCGACTTC..GGAAGAGACGTATTTATTAGATTAAAGACCAACCCT.TC..   172  Pseudoscourfieldia_marina_AJ132619
GCTTAAATCCCGACTCA..CGAAGGGACGTGTTTATTAGATAAAAGACCAGCCGC.CCTC   173  Dolichomastix_tenuilepis
GCTTAAATCCCGACTTA..CGAAGGGACGTGTTTATTAGATAAAAGACCAGCCTC.CGAC   171  Dolichomastix_tenuilepis_AF509625
GCGTAAATCCCGACTTC..GGAAGGGACGTATTTATTAGATAAA.GACCGGCCTC.....   169  Mamiella_gilva_AB017129
GCGCAACTCCCGACCTCT.GGAAGGGACGTATTTATTAGATAAAAGACCAGCCGC.CTTC   176  Pyramimonas_mucifera
GCGCAACTCCCGACTTCT.GGAAGGGACGTATTTATTAGATAAAAGACCAGCCGC.CTTC   177  Pyramimonas_olivacea_AB017122
GCGCAACTCCCGACTTCT.GGAAGGGACGTATTTATTAGATAAAAGACCAGCCGC.CTTC   176  Pyramimonas_parkeae_AB017124
GCGTAAATCCCGACTTCT.GGAAGGGACGTATATATTAGATTTAAGGCCGACCGAGCTTT   177  Tetraselmis
GCGTAAATCCTGACTTCT.GGAAGGGACGTATTTATTAGATTTAAGGCCGACCGAGCTTT   178  Tetraselmis_convolutae_U05039
GCGTAAATCCCGACTTCT.GGAAGGGACGTATTTATTAGATTTAAGGCCAACCGAGCTTT   176  Tetraselmis_kochiensis_AJ431370
GCGCAACTCCCGACTTCT.GGAAGGGATGTATTTATTAGATAAAAGACCAGCCG..CTTC   176  Halosphaera_AB017125
GCGCAACTCCCGACTTCT.GGAAGGGACGTATTTATTAGATAAAAAACCAAA....CTTG   158  Pseudoscourfieldia_marina_Wits_(?)
GCGCAACTCCCGACTTCT.GGAAGGGACGTATTTATTAGATAAAAAACCAAA....CTTG   170  Prasinoderma_coloniale_AB058379
GCATAAATCCCGAC........AGGGACGTATATATTAGATAAAAAACCACTCG..CTTG   169  Prasinococcus_capsulatus_AB058384
```

```
GCC.GTTTTTCGGTGAATCATGATATTTCCACGAATCGCATGGTC.TTGCAC..CGGCGA   232  Nephroselmis_anterostigmatica_MBIC11158
GCCCGATTTTCGGTGAATCATGATATTTCCACGAATCGCATGGTC.TTGCAC..CGGCGA   234  Nephroselmis_anterostigmatica_AB158372
GCC.GTTTTTCGGTGAATCATGATATTTCCACGAATCGCATGGTC.TTGCAC..CGGCGA   233  Nephroselmis_anterostigmatica_AB158373
GCCCGTTTTTCGGTGAATCATGATATTTCCACGAATCGCATGGTC.T.GCAC..CGGCGA   219  Nephroselmis_astigmatica_NIES252
GCCCGTTTTTCGGTGAATCATGATATTTCCACGAATCGCATGGTC.TTGCAC..CGGCGA   234  Nephroselmis_astigmatica_AB158374
GCCCGTTTTTCGGTGAATCATGATATTTCCACGAATCGCATGGCC.TCGTGC..GGGCGA   232  Nephroselmis_olivacae_X74754
CGGCGTTCTTCGGTGAATCATGATATTTCCACGGATCGCATGGGC.TTGCCC..CGGCGA   231  Nephroselmis_pyriformis_WW02
CGGCGTTCTTCGGTGAATCATGATATTTCCACGGATCGCATGGGC.TCGCCC..CGGCGA   231  Nephroselmis_pyriformis_AB158376
CGGCGTTCTTCGGTGAATCATGATATTTCCACGAATCGCATGGGC.TTGCCC..CGGCGA   231  Nephroselmis_pyriformis_AB058378
CGGCGTTCTTCGGTGAATCATGATATTTCCACGGATCGCATGGGC.TTGCCC..CGGCGA   231  Nephroselmis_pyriformis_AB058391
CGGCGTTCTTCGGTGAATCATGATATTTCCACGGATCGCATGGGC.TTGCCC..CGGCGA   231  Pseudoscourfieldia_marina_X75565
GCCCGTTTTTTGGCGACTCATGATATTTCCACGAATCGCATGGCCCTCGCGC..CGGCGA   235  Nephroselmis_rotunda_CCAP1960_3
GCCCGTTTTTTGGCGACTCATGATATTTCCACGAATCGCATGGCCCTCGCGC..CGGCGA   228  Nephroselmis_rotunda_BB2
GCCCGTTTCTTGGCGAATCATGATATTTCCACGAATCGCACGGCCCTCGTGC..CGGCGA   235  MBIC11149_AB214975
GCCCGTTTTCTGGCGAATCATGATATTTCCACGAATCGCATGGCCCTTGCGC..CGGCGA   221  Nephroselmis_spinosa_NIES935
GCCCGTTTTCTGGCGAATCATGATATTTCCACGAATCGCATGGCCCTTGCGC..CGGCGA   235  Nephroselmis_spinosa_AB158375
GCCCGTTTTTCGGTGAATCATGATATTTCCACGAATCGCATGGCT.TTGTGC..CGGCGA   220  Nephroselmis_viridis_NIES486
GCCCGTTTTTCGGTGAATCATGATATTTCCACGAATCGCATGGCT.TTGTGC..CGGCGA   233  Nephroselmis_viridis_AB214976
..GGGACCGTTGGTGATTCATAATAACTGGACGAATCGCATGGGCTT.GCCC..CGGCGA   227  Pseudoscourfieldia_marina_AF122888
..GGGACCGTTGGTGATTCATAATAACTGGACGAATCGCATGGGCTT.GCCC..CGGCGA   227  Pseudoscourfieldia_marina_AJ132619
GGGCGTTTCTTGGCGAATCATGATAACTTTACGGATCGCATGGCCTT.GCGC..CGGCGA   230  Dolichomastix_tenuilepis
GGGTGTCTTGGGGTGAATCATGATAACCTAACGGATCGCATGGCCTT.GTGC..CGGCGA   228  Dolichomastix_tenuilepis_AF509625
....GTTCTACGGTGAATCATGATAACTATACGGATCGCATGGCCTT.GTGC..CGGCGA   222  Mamiella_gilva_AB017129
GGGCGTTTTGTGGTGAATCATGATAACTTGTCGGATCGCATGGCCTTTGTGC..CGGCGA   234  Pyramimonas_mucifera
GGGCGTTTTGTGGTGAATCATGATAACTTGTCGGATCGCATGGCCTTCGTGC..CGGCGA   235  Pyramimonas_olivacea_AB017122
GGGCGTTTTGTGGTGAATCATGATAACTTGTCGGATCGCATGGCCTT.GTGC..CGGCGA   233  Pyramimonas_parkeae_AB017124
GCTCGTCTTGCGGTGAATCATGATATCTTCACGAATCGCATGGCCTTCGTGC..CGGCGA   235  Tetraselmis
GCTCGTCTTGCGGTGAATCATGATAACTTCACGAATCGCATGGCCTCCGCGCGCCGGCGA   238  Tetraselmis_convolutae_U05039
GCTCGTCTTTTGGTGAATCATGATAACTTCACGAATCGCATGGCCTT.GCGC..CGGCGA   233  Tetraselmis_kochiensis_AJ431370
.GGCGTTTTGTGGTGAATCATGATAATTTAACGGATCGCATGGCCTT.GCGC..TGGCGA   232  Halosphaera_AB017125
.....TTTCTCGGTGACTCATGATAACTGATCGGATCGCATGGCCTC.GTGC..CGGCGA   210  Pseudoscourfieldia_marina_Wits_(?)
.....TTTCTCGGTGACTCATGATAACTGATCGGATCGCATGGCCTC.GTGC..CGGCGA   222  Prasinoderma_coloniale_AB058379
CGGCGTCTGGAGGTGAATCATGATATCTTATCGGATCGCACGGGCTT.GCCC..CGGCGA   226  Prasinococcus_capsulatus_AB058384
```

TGTTTCATTCAAATTTCTGCCCTATCAACTTTCGATGGTAGGATAGAGGCCTACCATGGT	292	Nephroselmis_anterostigmatica_MBIC11158
TGTTTCATTCAAATTTCTGCCCTATCAACTTTCGATGGTAGGATAGAGGCCTACCATGGT	294	Nephroselmis_anterostigmatica_AB158372
TGTTTCATTCAAATTTCTGCCCTATCAACTTTCGATGGTAGGATAGAGGCCTACCATGGT	293	Nephroselmis_anterostigmatica_AB158373
TGTTTCATTCAAATTTCTGCCCTATCAACTTTCGATGGTAGGATAGAGGCCTACCATGGT	279	Nephroselmis_astigmatica_NIES252
TGTTTCATTCAAATTTCTGCCCTATCAACTTTCGATGGTAGGATAGAGGCCTACCATGGT	294	Nephroselmis_astigmatica_AB158374
TGTTTCATTCAAATTTCTGCCCTATCAACTTTCGATGGTAGGATAGAGGCCTACCATGGT	292	Nephroselmis_olivacae_X74754
TGTTTCATTCAAATTTCTGCCCTATCAACTTTCGATGGTAGGATAGAGGCCTACCATGGT	291	Nephroselmis_pyriformis_WW02
TGTTTCATTCAAATTTCTGCCCTATCAACTTTCGATGGTAGGATAGAGGCCTACCATGGT	291	Nephroselmis_pyriformis_AB158376
TGTTTCATTCAAATTTCTGCCCTATCAACTTTCGATGGTAGGATAGAGGCCTACCATGGT	291	Nephroselmis_pyriformis_AB058378
TGTTTCATTCAAATTTCTGCCCTATCAACTTTCGATGGTAGGATAGAGGCCTACCATGGT	291	Nephroselmis_pyriformis_AB058391
TGTTTCATTCAAATTTCTGCCCTATCAACTTTCGATGGTAGGATAGAGGCCTACCATGGT	291	Pseudoscourfieldia_marina_X75565
TGTTTCATTCAAATTTCTGCCCTATCAACTTTCGATGGTAGGATATAGGCCTACCATGGT	295	Nephroselmis_rotunda_CCAP1960_3
TGTTTCATTCAAATTTCTGCCCTATCAACTTTCGATGGTAGGATATAGGCCTACCATGGT	288	Nephroselmis_rotunda_BB2
TGTTTCATTCAAATTTCTGCCCTATCAACTTTCGATGGTAGGATATAGGCCTACCATGGT	295	MBIC11149_AB214975
TGTTTCATTCAAATTTCTGCCCTATCAACTTTCGATGGTAGGATATAGGCCTACCATGGT	281	Nephroselmis_spinosa_NIES935
TGTTTCATTCAAATTTCTGCCCTATCAACTTTCGATGGTAGGATATAGGCCTACCATGGT	295	Nephroselmis_spinosa_AB158375
TGTTTCATTCAAATTTCTGCCCTATCAACTTTCGATGGTAGGATAGAGGCCTACCATGGT	280	Nephroselmis_viridis_NIES486
TGTTTCATTCAAATTTCTGCCCTATCAACTTTCGATGGTAGGATAGAGGCCTACCATGGT	293	Nephroselmis_viridis_AB214976
TGTTTCATTCAAATTTCTGCCCTATCACGTTTCGATGGTAGTATAGAGGACTACCATGCG	287	Pseudoscourfieldia_marina_AF122888
TGTTTCATTCAAATTTCTGCCCTATCACGTTTCGATGGTAGTATAGAGGACTACCATGCG	287	Pseudoscourfieldia_marina_AJ132619
TGTTTCATTCAAATTTCTGCCCTATCAACTTTCGATGGTAGGATAGAGGCCTACCATGGT	290	Dolichomastix_tenuilepis
TGTTTCATTCAAATTTCTGCCCTATCAACTTTCGATGGTAGGATAGAGGCCTACCATGGT	288	Dolichomastix_tenuilepis_AF509625
TGTTCCATTCAAATTTCTGCCCTATCAACTTTCGATGGTAGTATAGAGGACTACCATGGT	282	Mamiella_gilva_AB017129
CGTTTCATTCAAATTTCTGCCCTATCAACTTTCGATGGTAGGATAGAGGCCTACCATGGT	294	Pyramimonas_mucifera
CGTTTCATTCAAATTTCTGCCCTATCAACTTTCGATGGTAGGATAGAGGCCTACCATGGT	295	Pyramimonas_olivacea_AB017122
CGTTTCATTCAAATTTCTGCCCTATCAACTTTCGATGGTAGGATAGAGGCCTACCATGGT	293	Pyramimonas_parkeae_AB017124
TATTTCATTCAAATTTCTGCCCTATCAATTTGCGATGGTAGGATAGAGGCCTACCATGGT	295	Tetraselmis
TGTTTCATTCAAATTTCTGCCCTATCAATTTGCGATGGTAGGATAGAGGCCTACCATGGT	298	Tetraselmis_convolutae_U05039
TATTTCATTCAAATTTCTGCCCTATCAATTGGCGATGGTAGGATAGAGGCCTACCATGGT	293	Tetraselmis_kochiensis_AJ431370
CGGTTCATTCAAATTTCTGCCCTATCAACTTTCGATGGTAGGATAGAGGCCTACCATGGT	292	Halosphaera_AB017125
CGTTTCATTCAAATTTCTGCCCTATCAACTGTCGATGGTAGGATAGAGGCCTACCATGGT	270	Pseudoscourfieldia_marina_Wits_(?)
CGTTTCATTCAAATTTCTGCCCTATCAACTGTCGATGGTAGGATAGAGGCCTACCATGGT	282	Prasinoderma_coloniale_AB058379
CGTCTCATTCAAATTTCTGCCCTATCAACTTTCGATGGTAGGATAGAGGCCTACCATGGT	286	Prasinococcus_capsulatus_AB058384

GGTAACGGGTAACGGAGGATTAGGGTTCGATTCCGGAGAGGGAGCCTGAGAGACGGCTAC	352	Nephroselmis_anterostigmatica_MBIC11158
GGTAACGGGTAACGGAGGATTAGGGTTCGATTCCGGAGAGGGAGCCTGAGAGACGGCTAC	354	Nephroselmis_anterostigmatica_AB158372
GGTAACGGGTAACGGAGGATTAGGGTTCGATTCCGGAGAGGGAGCCTGAGAGACGGCTAC	353	Nephroselmis_anterostigmatica_AB158373
GGTAACGGGTGACGGAGGATTAGGGTTCGATTCCGGAGAGGGAGCCTGAGAGACGGCTAC	339	Nephroselmis_astigmatica_NIES252
GGTAACGGGTGACGGAGGATTAGGGTTCGATTCCGGAGAGGGAGCCTGAGAGACGGCTAC	354	Nephroselmis_astigmatica_AB158374
GGTAACGGGTGACGGAGGATTAGGGTTCGATTCCGGAGAGGGAGCCTGAGAGACGGCTAC	352	Nephroselmis_olivacae_X74754
GGTAACGGGTGACGGAGGATTAGGGTTCGATTCCGGAGAGGGAGCCTGAGAGACGGCTAC	351	Nephroselmis_pyriformis_WW02
GGTAACGGGTGACGGAGGATTAGGGTTCGATTCCGGAGAGGGAGCCTGAGAGACGGCTAC	351	Nephroselmis_pyriformis_AB158376
GGTAACGGGTGACGGAGGATTAGGGTTCGATTCCGGAGAGGGAGCCTGAGAGACGGCTAC	351	Nephroselmis_pyriformis_AB058378
GGTAACGGGTGACGGAGGATTAGGGTTCGATTCCGGAGAGGGAGCCTGAGAGACGGCTAC	351	Nephroselmis_pyriformis_AB058391
GGTAACGGGTGACGGAGGATTAGGGTTCGATTCCGGAGAGGGAGCCTGAGAGACGGCTAC	351	Pseudoscourfieldia_marina_X75565
GGTAACGGGTGACGGAGGATTAGGGTTCGATTCCGGAGAGGGAGCCTGAGAGACGGCTAC	355	Nephroselmis_rotunda_CCAP1960_3
GGTAACGGGTGACGGAGGATTAGGGTTCGATTCCGGAGAGGGAGCCTGAGAGACGGCTAC	348	Nephroselmis_rotunda_BB2
GGTAACGGGTGACGGAGGATTAGGGTTCGATTCCGGAGAGGGAGCCTGAGAGACGGCTAC	355	MBIC11149_AB214975
GGTAACGGGTGACGGAGGATTAGGGTTCGATTCCGGAGAGGGAGCCTGAGAGACGGCTAC	341	Nephroselmis_spinosa_NIES935
GGTAACGGGTGACGGAGGATTAGGGTTCGATTCCGGAGAGGGAGCCTGAGAGACGGCTAC	355	Nephroselmis_spinosa_AB158375
GGTAACGGGTGACGGAGGATTAGGGTTCGATTCCGGAGAGGGAGCCTGAGAGACGGCTAC	340	Nephroselmis_viridis_NIES486
GGTAACGGGTGACGGAGGATTAGGGTTCGATTCCGGAGAGGGAGCCTGAGAGACGGCTAC	353	Nephroselmis_viridis_AB214976
AGTAACGGGTGACGGAGAATTAGGGTTCGATTCCGGAGAGGGAGCCTGAGAAACGGCTAC	347	Pseudoscourfieldia_marina_AF122888
AGTAACGGGTGACGGAGAATTAGGGTTCGATTCCGGAGAGGGAGCCTGAGAAACGGCTAC	347	Pseudoscourfieldia_marina_AJ132619
GGTAACGGGTGACGGAGAATTAGGGTTCGATTCCGGAGAGGGAGCCTGAGAAACGGCTAC	350	Dolichomastix_tenuilepis
GGTAACGGGTGACGGAGAATTAGGGTTCGATTCCGGAGAGGGAGCCTGAGAAACGGCTAC	348	Dolichomastix_tenuilepis_AF509625
GTTAACGGGTGACGGAGAATTAGGGTTCGATTCCGGAGAGGGAGCCTGAGAAACGGCTAC	342	Mamiella_gilva_AB017129
GGTAACGGGTGACGGAGAATTAGGGTTCGATTCCGGAGAGGGAGCCTGAGAAACGGCTAC	354	Pyramimonas_mucifera
GGTAACGGGTGACGGAGAATTAGGGTTCGATTCCGGAGAGGGAGACTGAGAAACGGCTAC	355	Pyramimonas_olivacea_AB017122
GGTAACGGGTGACGGAGAATTAGGGTTCGATTCCGGAGAGGGAGCCTGAGAAACGGCTAC	353	Pyramimonas_parkeae_AB017124
GTTAACGGGTGACGGAGAATTAGGGTTCGATTCCGGAGAGGGAGCCTGAGAAACGGCTAC	355	Tetraselmis
GGTAACGGGTGACGGAGAATTAGGGTTCGATTCCGGATAGGGAGCCTGAGAAACGGCTAC	358	Tetraselmis_convolutae_U05039
GTTAACGGGTGACGGGGAATTAGGGTTCGATTCCGGAGAGGGAGCCTGAGAAACGGCTAC	353	Tetraselmis_kochiensis_AJ431370
GGTAACGGGTGACGGAGAATTAGGGTTCGATTCCGGAGAGGGAGCCTGAGAAACGGCTAC	352	Halosphaera_AB017125
GGTAACGGGTGACGGAGAATTAGGGTTCGATTCCGGAGAGGGAGCCTGAGAAATGGCTAC	330	Pseudoscourfieldia_marina_Wits_(?)
GGTAACGGGTGACGGAGAATTAGGGTTCGATTCCGGAGAGGGAGCCTGAGAAATGGCTAC	342	Prasinoderma_coloniale_AB058379
GGTAACGGGTGACGGAGAATTAGGGTTCGATTCCGGAGAGGGAGCCTGAGAGACGGCTAC	346	Prasinococcus_capsulatus_AB058384

↑
Insertion of 437 bases in "N. viridis"

CACATCCAAGGAAGGCAGCAGGCGCGCAAATTACCCAATCCTAATTCAGGGAGGTAGTGA	412	Nephroselmis_anterostigmatica_MBIC11158
CACATCCAAGGAAGGCAGCAGGCGCGCAAATTACCCAATCCTAATTCAGGGAGGTAGTGA	414	Nephroselmis_anterostigmatica_AB158372
CACATCCAAGGAAGGCAGCAGGCGCGCAAATTACCCAATCCTAATTCAGGGAGGTAGTGA	413	Nephroselmis_anterostigmatica_AB158373
CACATCCAAGGAAGGCAGCAGGCGCGCAAATTACCCAATCCTAATTCAGGGAGGTAGTGA	399	Nephroselmis_astigmatica_NIES252
CACATCCAAGGAAGGCAGCAGGCGCGCAAATTACCCAATCCTAATTCAGGGAGGTAGTGA	414	Nephroselmis_astigmatica_AB158374
CACATCCAAGGAAGGCAGCAGGCGCGCAAATTACCCAATCCTGACTCAGGGAGGTAGTGA	412	Nephroselmis_olivacae_X74754
CACATCCAAGGAAGGCAGCAGGCGCGCAAATTACCCAATCCTGACACAGGGAGGTAGTGA	411	Nephroselmis_pyriformis_WW02
CACATCCAAGGAAGGCAGCAGGCGCGCAAATTACCCAATCCTGACACAGGGAGGTAGTGA	411	Nephroselmis_pyriformis_AB158376
CACATCCAAGGAAGGCAGCAGGCGCGCAAATTACCCAATCCTGACACAGGGAGGTAGTGA	411	Nephroselmis_pyriformis_AB058378
CACATCCAAGGAAGGCAGCAGGCGCGCAAATTACCCAATCCTGACACAGGGAGGTAGTGA	411	Nephroselmis_pyriformis_AB058391
CACATCCAAGGAAGGCAGCAGGCGCGCAAATTACCCAATCCTGACACAGGGAGGTAGTGA	411	Pseudoscourfieldia_marina_X75565
CACATCCAAGGAAGGCAGCAGGCGCGCAAATTACCCAATCCTGACACAGGGAGGTAGTGA	415	Nephroselmis_rotunda_CCAP1960_3
CACATCCAAGGAAGGCAGCAGGCGCGCAAATTACCCAATCCTGACACAGGGAGGTAGTGA	408	Nephroselmis_rotunda_BB2
CACATCCAAGGAAGGCAGCAGGCGCGCAAATTACCCAATCCTGACACAGGGAGGTAGTGA	415	MBIC11149_AB214975
CACATCCAAGGAAGGCAGCAGGCGCGCAAATTACCCAATCCTGACACAGGGAGGTAGTGA	401	Nephroselmis_spinosa_NIES935
CACATCCAAGGAAGGCAGCAGGCGCGCAAATTACCCAATCCTGACACAGGGAGGTAGTGA	415	Nephroselmis_spinosa_AB158375
CACATCCAAGGAAGGCAGCAGGCGCGCAAATTACCCAATCCTGACACAGGGAGGTAGTGA	400	Nephroselmis_viridis_NIES486
CANATCCAAGGAAGGCAGCAGGCGCGCAAATNACCCAATCCTGACANAGGGAGGTAGTGA	413	Nephroselmis_viridis_AB214976
CACATCCAAGGAAGGCAGCAGGCGCGCAAATTACCCAATCCTGACACAGGGAGGTAGTGA	407	Pseudoscourfieldia_marina_AF122888
CACATCCAAGGAAGGCAGCAGGCGCGCAAATTACCCAATCCTGACACAGGGAGGTAGTGA	407	Pseudoscourfieldia_marina_AJ132619
CACATCCAAGGAAGGCAGCAGGCGCGCAAATTACCCAATCCTGACACAGGGAGGTAGTGA	410	Dolichomastix_tenuilepis
CACATCCAAGGAAGGCAGCAGGCGCGCAAATTACCCAATCCTGACACAGGGAGGTAGTGA	408	Dolichomastix_tenuilepis_AF509625
CACATCCAAGGAAGGCAGCAGGCGCGCAAATTACCCAATCCTGACACAGGGAGGTAGTGA	402	Mamiella_gilva_AB017129
CACATCCAAGGAAGGCAGCAGGCGCGCAAATTACCCAATCCTGACACAGGGAGGTAGTGA	414	Pyramimonas_mucifera
CACATCCAAGGAAGGCAGAAGGCGCGCAATTTACCCAATCCTGACACAGGGAGGTAGTGA	415	Pyramimonas_olivacea_AB017122
CACATCCAAGGAAGGCAGCAGGCGCGCAAATTACCCAATCCTGACACAGGGAGGTAGTGA	413	Pyramimonas_parkeae_AB017124
CACATCCAAGGAAGGCAGCAGGCGCGCAAATTACCCAATCCTGATACAGGGAGGTAGTGA	415	Tetraselmis
CACATCCAAGGAAGGCAGCAGGCGCGCAAATTACCCAATCCTGACACAGGGAGGTAGTGA	418	Tetraselmis_convolutae_U05039
CACATCCAAGGAAGGCAGCAGGCGCGCAAATTACCCAATCCTGATACAGGGAGGTAGTGA	413	Tetraselmis_kochiensis_AJ431370
CACATCCAAGGAAGGCAGCAGGCGCGCAAATTACCCANTCCTGACACAGGGAGGTAGTGA	412	Halosphaera_AB017125
CACATCCAAGGATGGCAGCAGGCGCGCAAATTACCCAATCCTGACACAGGGAGGTAGTGA	390	Pseudoscourfieldia_marina_Wits_(?)
CACATCCAAGGATGGCAGCAGGCGCGCAAATTACCCAATCCTGACACAGGGAGGTAGTGA	402	Prasinoderma_coloniale_AB058379
CACATCCAAGGAAGGCAGCAGGCGCGCAAATTACCCAATCCTGACACAGGGAGGTAGTGA	406	Prasinococcus_capsulatus_AB058384

CAATAAATAACAATACCGGGCTTTTTCAAGTCTGGTAATTGGAATGAGAACAATCTAAAT	472	Nephroselmis_anterostigmatica_MBIC11158
CAATAAATAACAATACCGGGCTTTTTCAAGTCTGGTAATTGGAATGAGAACAATCTAAAT	474	Nephroselmis_anterostigmatica_AB158372
CAATAAATAACAATACCGGGCTTTTTCAAGTCTGGTAATTGGAATGAGAACAATCTAAAT	473	Nephroselmis_anterostigmatica_AB158373
CAATAAATAACAATACCGGGCTTTTTCAAGTCTGGTAATTGGAATGAGAACAATCTAAAT	459	Nephroselmis_astigmatica_NIES252
CAATAAATAACAATACCGGGCTTTTTCAAGTCTGGTAATTGGAATGAGAACAATCTAAAT	474	Nephroselmis_astigmatica_AB158374
CAATAAATAACAATACCGGGCTTTTTCAAGTCTGGTAATTGGAATGAGAACAATCTAAAT	472	Nephroselmis_olivacae_X74754
CAATAAATAACAATACCGGGCTTTTTCAAGTCTGGTAATTGGAATGAGTACAATCTAAAC	471	Nephroselmis_pyriformis_WW02
CAATAAATAAGAATACCGGGCTTTTTCAAGTCTGGTAATTGGAATGAGTACAATCTAAAC	471	Nephroselmis_pyriformis_AB158376
CAATAAATAACAATACCGGGCTTTTTCAAGTCTGGTAATTGGAATGAGTACAATCTAAAC	471	Nephroselmis_pyriformis_AB058378
CAATAAATAACAATACCGGGCTTTTTCAAGTCTGGTAATTGGAATGAGTACAATCTAAAC	471	Nephroselmis_pyriformis_AB058391
CAATAAATAACAATACCGGGCTTTTTCAAGTCTGGTAATTGGAATGAGTACAATCTAAAC	471	Pseudoscourfieldia_marina_X75565
CAATAAATAACAATACCGGGCTTTTTCAAGTCTGGTAATTGGAATGAGAACAATCTAAAT	475	Nephroselmis_rotunda_CCAP1960_3
CAATAAATAACAATACCGGGCTTTTTCAAGTCTGGTAATTGGAATGAGAACAATCTAAAT	468	Nephroselmis_rotunda_BB2
CAATAAATAACAATACCGGGCTTTTTCAAGTCTGGTAATTGGAATGAGAACAATCTAAAT	475	MBIC11149_AB214975
CAATAAATAACAATACCGGGCTTTTTCAAGTCTGGTAATTGGAATGAGAACAATTTAAAT	461	Nephroselmis_spinosa_NIES935
CAATAAATAACAATACCGGGCTTTTTCAAGTCTGGTAATTGGAATGAGAACAATTTAAAT	475	Nephroselmis_spinosa_AB158375
CAATAAATAACAATACCGGGCTTTTTCAAGTCTGGTAATTGGAATGAGAACAATCTAAAT	460	Nephroselmis_viridis_NIES486
CAATAAATAACAATACCGGGCTTTTTCAAGTCTGGTAATTGGAATGAGAACAATCTAAAT	473	Nephroselmis_viridis_AB214976
CAATAAATAACAATACCGGGCGTTTTTACGTCTGGTAATTGGAATGAGAACAATCTAAAT	467	Pseudoscourfieldia_marina_AF122888
CAATAAATAACAATACCGGGCGTTTTTACGTCTGGTAATTGGAATGAGAACAATCTAAAT	467	Pseudoscourfieldia_marina_AJ132619
CAATAAATAACAATACCGGGCTTTTTCAAGTCTGGTAATTGGAATGAGAACAATCTAAAT	470	Dolichomastix_tenuilepis
CAATAAATAACAATACCGGGCTTTTTTAAGTCTGGTAATTGGAATGAGAACAATCTAAAT	468	Dolichomastix_tenuilepis_AF509625
CAATAAATAACAATACCGAGGCTTTTCACTTCTGGTAATTGGAATGAGAACAATCTAAAT	462	Mamiella_gilva_AB017129
CAATAAATAACAATACCGGGCTTTTTCAAGTCTGGTAATTGGAATGAGAACAATCTAAAT	474	Pyramimonas_mucifera
CAATAAATAACAATACCGGGCTTTTTCAAGTCTGGTAATTGGAATGAGAACAATCTAAAT	475	Pyramimonas_olivacea_AB017122
CAATAAATAACAATACCGGGCTTTTTCAAGTCTGGTAATTGGAATGAGAACAATCTAAAT	473	Pyramimonas_parkeae_AB017124
CAATAAATAACAATACCGGGCTTTT.CAAGTCTGGTAATTGGAATGAGTACAATCTAAAC	474	Tetraselmis
CAATAAATAACAATACCGGGCTTTT.CAAGTCTGGTAATTGGAATGAGTACAATCTAAAC	477	Tetraselmis_convolutae_U05039
CAATAAATAACAATACCGGGCTTCT.AAAGTCTGGTAATTGGAATGAGTACAATCTAAAT	472	Tetraselmis_kochiensis_AJ431370
CAATAAATAACGATACCGGACTTTTTCAAGCCTGGTAATTGGAATGAGAACAATCTAAAT	472	Halosphaera_AB017125
CAATAAATAACAATACCGGGCTTTTTCAAGTCTGGTACTTGGAATGAGAACAATCTAAAC	450	Pseudoscourfieldia_marina_Wits_(?)
CAATAAATAACAATACCGGGCTTTTTCAAGTCTGGTACTTGGAATGAGAACAATCTAAAC	462	Prasinoderma_coloniale_AB058379
CAATAAATAACAATACCGGGCTTTT.CAGGTCTGGTAATTGGAATGAGTACAATCTAAAC	465	Prasinococcus_capsulatus_AB058384

C.CCTTAACGAGGATCCATTGGAGGGCAAGTCTGGT.GCCAGCAGCCGCGGTAATTCCAG	530	Nephroselmis_anterostigmatica_MBIC11158
C.CCTTAACGAGGATCCATTGGAGGGCAAGTCTGGT.GCCAGCAGCCGCGGTAATTCCAG	532	Nephroselmis_anterostigmatica_AB158372
C.CCTTAACGAGGATCCATTGGAGGGCAAGTCTGGT.GCCAGCAGCCGCGGTAATTCCAG	531	Nephroselmis_anterostigmatica_AB158373
C.CCTTAACGAGGATCCATTGGAGGGCAAGTCTGGT.GCCAGCAGCCGCGGTAATTCCAG	517	Nephroselmis_astigmatica_NIES252
C.CCTTAACGAGGATCCATTGGAGGGCAAGTCTGGT.GCCAGCAGCCGCGGTAATTCCAG	532	Nephroselmis_astigmatica_AB158374
C.CCTTAACGAGGATCCATTGGAGGGCAAGTCTGGT.GCCAGCAGCCGCGGTAATTCCAG	530	Nephroselmis_olivacae_X74754
C.CCTTAACGAGGATCCATTGGAGGGCAAGTCTGGT.GCCAGCAGCCGCGGTAATTCCAG	529	Nephroselmis_pyriformis_WW02
C.CCTTAACGAGGATCCATTGGAGGGCAAGTCTGGT.GCCAGCAGCCGCGGTAATTCCAG	529	Nephroselmis_pyriformis_AB158376
C.CCTTAACGAGGATCCATTGGAGGGCAAGTCTGGT.GCCAGCAGCCGCGGTAATTCCAG	529	Nephroselmis_pyriformis_AB058378
C.CCTTAACGAGGATCCATTGGAGGGCAAGTCTGGT.GCCAGCAGCCGCGGTAATTCCAG	529	Nephroselmis_pyriformis_AB058391
C.CCTTAACGAGGATCCATTGGAGGGCAAGTCTGGT.GCCAGCAGCCGCGGTAATTCCAG	529	Pseudoscourfieldia_marina_X75565
C.CCTTATCGAGGATCCATTGGAGGGCAAGTCTGGT.GCCAGCAGCCGCGGTAATTCCAG	533	Nephroselmis_rotunda_CCAP1960_3
C.CCTTATCGAGGATCCATTGGAGGGCAAGTCTGGT.GCCAGCAGCCGCGGTAATTCCAG	526	Nephroselmis_rotunda_BB2
C.CCTTATCGAGGATCCATTGGAGGGCAAGTCTGGT.GCCAGCAGCCGCGGTAATTCCAG	533	MBIC11149_AB214975
C.CCTTATCGAGGATCCATTGGAGGGCAAGTCTGGT.GCCAGCAGCCGCGGTAATTCCAG	519	Nephroselmis_spinosa_NIES935
C.CCTTATCGAGGATCCATTGGAGGGCAAGTCTGGT.GCCAGCAGCCGCGGTAATTCCAG	533	Nephroselmis_spinosa_AB158375
C.CCTTAACGAGGATCCATTGGAGGGCAAGTCTGGT.GCCAGCAGCCGCGGTAATTCCAG	518	Nephroselmis_viridis_NIES486
C.CCTTAACGAGGATCCATTGGAGGGCAAGTCTGGT.GCCAGCAGCCGCGGTAATTCCAG	531	Nephroselmis_viridis_AB214976
C.CCTTATCGAGGATCAATTGGAGGGCAAGTCTGGT.GCCAGCAGCCGCGGTAATTCCAG	525	Pseudoscourfieldia_marina_AF122888
C.CCTTATCGAGGATCAATTGGAGGGCAAGTCTGGT.GCCAGCAGCCGCGGTAATTCCAG	525	Pseudoscourfieldia_marina_AJ132619
C.CCTTAACGAA.ATCCATTGGAGGGCAAGTCTGGT.GCCAGCAGCCGCGGTAATTCCAG	527	Dolichomastix_tenuilepis
C.CCTTAACGAGGATCCATTGGAGGGCAAGTCTGGT.GCCAGCAGCCGCGGTAATTCCAG	526	Dolichomastix_tenuilepis_AF509625
C.CCTTAACGAGGATCCATTGGAGGGCAAGTCTGGT.GCCAGCAGCCGCGGTAATTCCAG	520	Mamiella_gilva_AB017129
C.CCTTAACGAGGATCCATTGGAGGGCAAGTCTGGT.GCCAGCAGCCGCGGTAATTCCAG	532	Pyramimonas_mucifera
C.CCTTAACGAGGATCCATTGGAGGGCAAGTCTGGT.GCCAGCAGCCGCGGTAATTCCAG	533	Pyramimonas_olivacea_AB017122
C.CCTTAACGAGGATCCATTGGAGGGCAAGTCTGGT.GCCAGCAGCCGCGGTAATTCCAG	531	Pyramimonas_parkeae_AB017124
AACCTTAACGAGGATCCATTGGAGGGCAAGTCTGGT.GCCAGCAGCCGCGGTAATTCCAG	533	Tetraselmis
AACCTTAACGAGGATCCATTGGAGGGCAAGTCTGGTTGCCAGCAGCCGCG.TAATTCCAG	536	Tetraselmis_convolutae_U05039
C.CCTTAACGAGGATCCATTGGAGGGCAAGTCTGGT.GCCAGCAGCCGCGGTAATTCCAG	530	Tetraselmis_kochiensis_AJ431370
C.CCTTAACGAGGATCCATTGGAGGGCAAGTCTGGT.GCCAGCAGCCGCGGTAATTCCAG	530	Halosphaera_AB017125
C.CCTTACCGAGGATCCATTGGAGGGCAAGTCTGGT.GCCAGCAGCCGCGGTAATTCCAG	508	Pseudoscourfieldia_marina_Wits_(?)
C.CCTTACCGAGGATCCATTGGAGGGCAAGTCTGGT.GCCAGCAGCCGCGGTAATTCCAG	520	Prasinoderma_coloniale_AB058379
C.CCTTAACGAGGATCCATTAGAGGGCAAGTCTGGT.GCCAGCAGGCGCGGTAATTCCAG	523	Prasinococcus_capsulatus_AB058384

CTCCAATAGCGTATATTTAAGTTGTTGCAGTTAAAAAGCTCGTAGTTGGATTTCGGGTGG	590	Nephroselmis_anterostigmatica_MBIC11158
CTCCAATAGCGTATATTTAAGTTGTTGCAGTTAAAAAGCTCGTAGTTGGATTTCGGGTGG	592	Nephroselmis_anterostigmatica_AB158372
CTCCAATAGCGTATATTTAAGTTGTTGCAGTTAAAAAGCTCGTAGTTGGATTTCGGGTGG	591	Nephroselmis_anterostigmatica_AB158373
CTCCAATAGCGTATATTTAAGTTGTTGCAGTTAAAAAGCTCGTAGTTGGATTTCGGGTGT	577	Nephroselmis_astigmatica_NIES252
CTCCAATAGCGTATATTTAAGTTGTTGCAGTTAAAAAGCTCGTAGTTGGATTTCGGGTGT	592	Nephroselmis_astigmatica_AB158374
CTCCAATAGCGTATATTTAAGTTGTTGCAGTTAAAAAGCTCGTAGTTGGATTTCGGGTGG	590	Nephroselmis_olivacae_X74754
CTCCAATAGCGTATATTTAAGTTGTTGCAGTTAAAAAGCTCGTAGTTGGATTTCGGGTGG	589	Nephroselmis_pyriformis_WW02
CTCCAATAGCGTATATTTAAGTTGTTGCAGTTAAAAAGCTCGTAGTTGGATTTCGGGTGG	589	Nephroselmis_pyriformis_AB158376
CTCCAATAGCGTATATTTAAGTTGTTGCAGTTAAAAAGCTCGTAGTTGGATTTCGGGTGG	589	Nephroselmis_pyriformis_AB058378
CTCCAATAGCGTATATTTAAGTTGTTGCAGTTAAAAAGCTCGTAGTTGGATTTCGGGTGG	589	Nephroselmis_pyriformis_AB058391
CTCCAATAGCGTATATTTAAGTTGTTGCAGTTAAAAAGCTCGTAGTTGGATTTCGGGTGG	589	Pseudoscourfieldia_marina_X75565
CTCCAATAGCGTATATTTAAGTTGTTGCAGTTAAAAAGCTCGTAGTTGGATTTCGGATGG	593	Nephroselmis_rotunda_CCAP1960_3
CTCCAATAGCGTATATTTAAGTTGTTGCAGTTAAAAAGCTCGTAGTTGGATTTCGGATGG	586	Nephroselmis_rotunda_BB2
CTCCAATAGCGTATATTTAAGTTGTTGCAGTTAAAAAGCTCGTAGTTGGATTTCGGATGG	593	MBIC11149_AB214975
CTCCAATAGCGTATATTTAAGTTGTTGCAGTTAAAAAGCTCGTAGTTGGATTTCGGATGG	579	Nephroselmis_spinosa_NIES935
CTCCAATAGCGTATATTTAAGTTGTTGCAGTTAAAAAGCTCGTAGTTGGATTTCGGATGG	593	Nephroselmis_spinosa_AB158375
CTCCAATAGCGTATATTTAAGTTGTTGCAGTTAAAAAGCTCGTAGTTGGATTTCGGGTGG	578	Nephroselmis_viridis_NIES486
CTCCAATAGCGTATATTTAAGTTGTTGCAGTTAAAAAGCTCGTAGTTGGATTTCGGGTGG	591	Nephroselmis_viridis_AB214976
CTCCAATAGCGTATATTTAAGTTGTTGCGGTTAAAAAGCTCGTAGTTGGATTTCGGGCGT	585	Pseudoscourfieldia_marina_AF122888
CTCCAATAGCGTATATTTAAGTTGTTGCGGTTAAAAAGCTCGTAGTTGGATTTCGGGCGT	585	Pseudoscourfieldia_marina_AJ132619
CTCCAATAGCGTATATTTAAGTTGTTGCAGTTAAAAAGCTCGTAGTTGGATTTTGGGCGA	587	Dolichomastix_tenuilepis
CTCCAATAGCGTATATTTAAGTTGTTGCAGTTAAAAAGCTCGTAGTTGGATTTCGGGCGA	586	Dolichomastix_tenuilepis_AF509625
CTCCAATAGCGTATATTTAAGTTGTTGCAGTTAAAAAGCTCGTAGTTGGATTTCGGTTGG	580	Mamiella_gilva_AB017129
CTCCAATAGCGTATATTTAAGTTGTTGCAGTTAAAAAGCTCGTAGTTGGATTTCGGATGG	592	Pyramimonas_mucifera
CTCCAATAGCGGATATTTAAGTTGTTGCAGTTAAAAAGCTCGTAGTTGGATTTCGGATGG	593	Pyramimonas_olivacea_AB017122
CTCCAATAGCGTATATTTAAGTTGTTGCAGTTAAAAAGCTCGTAGTTGGATTTCGGATGG	591	Pyramimonas_parkeae_AB017124
CTCCAATAGCGTATATTTAAGTTGCTGCAGTTAAAAAGCTCGTAGTTGGATTTCGGATGG	593	Tetraselmis
CTCCAATAGCGTATATTTAAGTTGCTGCAGTTAAAAAGCTCGTAGTTGGATTTCGGATGG	596	Tetraselmis_convolutae_U05039
CTCCAATAGCGTATATTTAAGTTGTTGCAGTTAAAAAGCTCGTAGTTGGATTTCGGATGG	590	Tetraselmis_kochiensis_AJ431370
CTCCAATAGCGTATATTTAAGTTGTTGCAGTTAAAAAGCTCGTAGTTGGATTTCAGGTGG	590	Halosphaera_AB017125
CTCCAATAGCGTATATTTAAGTTGTTGCAGTTAAAAAGCTCGTAGTTGGATTTTGGGTCG	568	Pseudoscourfieldia_marina_Wits_(?)
CTCCAATAGCGTATATTTAAGTTGTTGCAGTTAAAAAGCTCGTAGTTGGATTTTGGGTCG	580	Prasinoderma_coloniale_AB058379
CTCTAATAGCGTATATTTAAGTTGTTGCAGTTAAAAAGCTCGTAGTTGGATTTGGGGTCG	583	Prasinococcus_capsulatus_AB058384

GGTTCACCGGTCCGCCGTCT.CGGTGTGCACTGGTGAGG.CCCATCTTTCTGTCGGGGAC	648	Nephroselmis_anterostigmatica_MBIC11158
GGTNCACCGGTCCGCCGTTT.CGGTGTGCACTGGTTGGT.CCCATCTTTCTGTCGGGGAC	650	Nephroselmis_anterostigmatica_AB158372
GGTTCACCGGTCCGCCGTCT.CGGTGTGCACTGGTGAGG.CCCATCTTTCTGTCGGGGAC	649	Nephroselmis_anterostigmatica_AB158373
GGCTGGCCGGTCCGCCGTCT.CGGTGTGCACTGGCATAG.CCCATCTTCTTGTCGAGGGC	635	Nephroselmis_astigmatica_NIES252
GGCTGGCCGGTCCGCCGTCT.CGGTGTGCACTGGCATAG.CCCATCTTCTTGTCGAGGGC	650	Nephroselmis_astigmatica_AB158374
GGATCGCCGGTCCGTCGTCT.CGATGTGCACTGGCGCGC.CCCATCTTCTTGTCGGGGAC	648	Nephroselmis_olivacae_X74754
GCGAGGCCGGTCCGCCGTCT.CGGTGTGCACTGGC.TGCGCCCATCTTCTTGCTGGGGAC	647	Nephroselmis_pyriformis_WW02
GCGAGGCCGGTCCGCCGTCT.CGGTGTGCACTGGCGTTCGCCCAT.TTCTTGCTGGGGAC	647	Nephroselmis_pyriformis_AB158376
GTGAGGCCGGTCCGCCGTCT.CGGTGTGCACTGGCGTT.GCCCATCTTCTTGCTGGGGAC	647	Nephroselmis_pyriformis_AB058378
GCGAGGCCGGTCCGCCGTCT.CGGTGTGCACTGGC.TGCGCCCATCTTCTTGCTGGGGAC	647	Nephroselmis_pyriformis_AB058391
GCGAGGCCGGTCCGCCGTCT.CGGTGTGCACTGGC.TGCGCCCATCTTCTTGCTGGGGAC	647	Pseudoscourfieldia_marina_X75565
GCAGCGTCGGTCCGCCGTCT.CGGTGTGCACTGACGCGC.CTCATCTTCTTGCCGGGGAC	651	Nephroselmis_rotunda_CCAP1960_3
GCAGCGTCGGTCCGCCGTCT.CGGTGTGCACTGACGCGC.CTCATCTTCTTGCCGGGGAC	644	Nephroselmis_rotunda_BB2
GCAGTGTCGGTCCGCCGTCT.CGGTGTGCACTGACACGC.CTCATCTTCTTGCCGGGGAC	651	MBIC11149_AB214975
ACAGCGTCGGTCCGCTGTTTACAGTGTGCACTGACGCGT.CTCATCTTCTTGCCGGGGAC	638	Nephroselmis_spinosa_NIES935
ACAGCGTCGGTCCGCTGTTTACAGTGTGCACTGACGCGT.CTCATCTTCTTGCCGGGGAC	652	Nephroselmis_spinosa_AB158375
GATGCGCCGGTCCGTCGTCT.CGATGTGCACTGGTGCGT.CCCATCTTCTTGTCGGGGAC	636	Nephroselmis_viridis_NIES486
GATGCGCCGGTCCGTCGTCT.CGATGTGCACTGGTGCGT.CCCATCTTCTTGTCGGGGAC	649	Nephroselmis_viridis_AB214976
GGAGGTTCGGTCCGCCGTTT.CGGTGTGCACTGTCTTTC.TGCGTCTTTCTGTCGGGGAC	643	Pseudoscourfieldia_marina_AF122888
GGAGGTTCGGTCCGCCGTTT.CGGTGTGCACTGTCTTTC.TGCGTCTTTCTGTCGGGGAC	643	Pseudoscourfieldia_marina_AJ132619
TGCGGGCCGGTCCGCCGTTG.CGGTGTGCACTGGCTGGC.GCCGTCTTCTTGTCGAGGAC	645	Dolichomastix_tenuilepis
CGCTGGCCGGTCCGCCGTTT.CGGTGTGCACTGGCCGGC.ATTGTCTTCTTGTCGAGGAC	644	Dolichomastix_tenuilepis_AF509625
GGGCGGCCGGTCCGCCGTT..CGGTGTGCACTGGCTGGT.CCCAGCTTCCTGTCGAGGAC	637	Mamiella_gilva_AB017129
GGACAACCGGTCCGCCGTTG.CGGTGTGCACTGGTGGTG.TCCATCTTAATGTCGGGGAC	650	Pyramimonas_mucifera
TGACGACCGGTCCGCCGTTT.CGGTGTGCACTGGGTGTT.GTTATCTTGATGTCGGGGAC	651	Pyramimonas_olivacea_AB017122
GAACGACCGGTCCGCCGTTT.CGGTGTGCACTGGACGAT.TCTATCTTGTTGTCGGGGAC	649	Pyramimonas_parkeae_AB017124
GATTGGCCGGTCCGTCGTTT.CGATGTGCACTGGCTAGT.CCCATCTTGTTGTCGGGGAC	651	Tetraselmis
GATTTGCCGGTCCGCCGTTT.CGGTGTGCACTGGCCAGT.CCCATCTTGTTGTCGGGGAC	654	Tetraselmis_convolutae_U05039
GACCTGCCGGTCCGTCTTTG.AGATGTGTACTGGCAAGT.CCCATCTTGTTGTCGGGGAC	648	Tetraselmis_kochiensis_AJ431370
GAATGATTGGTCCGCCGCTC.TGGTGTGTACTATGACTA.CCTACTTTTCTGTCGGGGAC	648	Halosphaera_AB017125
GGGGCACCGGTCCGCCGTTC.CGGTGTGCACTGGTGGCC.CCTTCCTTTCTGCCGGGGAC	626	Pseudoscourfieldia_marina_Wits_(?)
GGG.CACCGGTCCGCCGTTC.CGGTGTGCACTGGTGGCC.CCTTCCTTTCTGCCGGGGAC	637	Prasinoderma_coloniale_AB058379
GAGCGACCGGTCCGCCGTTC.CGGTGTGCACTGGTGGCT.TCTTCCTTCTTGCCGGGGAC	641	Prasinococcus_capsulatus_AB058384

CTGCTTCTGGCCTTCACTGGCTGGG.ACAGGGA.GTCGGCGATGTTACTTTGAAAAAATT	706	Nephroselmis_anterostigmatica_MBIC11158
TCGCTCCTGGCCTTAATTGACTGGG.ACGAGGA.GTCGGCGATGTTACTTTGAAAAAATT	708	Nephroselmis_anterostigmatica_AB158372
CTGCTTCTGGCCTTCACTGGCTGGG.ACAGGGA.GTCGGCGATGTTACTTTGAAAAAATT	707	Nephroselmis_anterostigmatica_AB158373
GCGCTCTTGGCCTTGATTGGCTGAG.ACGTGATCGTCGGCGATGTTACTTTGAAAAAATT	694	Nephroselmis_astigmatica_NIES252
GCGCTCTTGGCCTTGATTGGCTGAG.ACGTGATCGTCGGCGATGTTACTTTGAAAAAATT	709	Nephroselmis_astigmatica_AB158374
GCACTCCTGGTCTTTACTGCCCGGG.ATGCGGA.GTCGGCGATGTTACTTTGAGTAAATT	706	Nephroselmis_olivacae_X74754
GCGCTCCTGGCCTTTGTTGGCTGGG.ACGTGGA.GTCAGCGATGTTACTTTGAAAAAATT	705	Nephroselmis_pyriformis_WW02
GCGCTCCTGGCCTTAATTGGCTGGG.ACGTGGA.GTCAGCGATGTTACTTTGAAAAAATT	705	Nephroselmis_pyriformis_AB158376
GCGCTCCTGGCCTTGATTGGCTGGG.ACGTGGA.GTCAGCGATGTTACTTTGAAAAAATT	705	Nephroselmis_pyriformis_AB058378
GCGCTCCTGGCCTTTGTTGGCTGGG.ACGTGGA.GTCAGCGATGTTACTTTGAAAAAATT	705	Nephroselmis_pyriformis_AB058391
GCGCTCCTGGCCTTTGTTGGCTGGG.ACGTGGA.GTCAGCGATGTTACTTTGAAAAAATT	705	Pseudoscourfieldia_marina_X75565
GCGCTCGTGGCCTTAATTGACCGCG.ACGCGGA.GTCGGCGATGTTACTTTGAAAAAATT	709	Nephroselmis_rotunda_CCAP1960_3
GCGCTCGTGGCCTTCATTGGCTGCG.ACGCGGA.GTCGGCGATGTTACTTTGAAAAAATT	702	Nephroselmis_rotunda_BB2
GCGCTCGTGGTCTTGATTGATCGCG.ACGCGGA.GTCGGCGCTGTTACTTTGAAGAAATT	709	MBIC11149_AB214975
GCGCTCGTGGCCTTGATTGGCTGCG.ACGCGGA.GTCGGCGATGTTACTTTGAAAAAATT	696	Nephroselmis_spinosa_NIES935
GCGCTCGTGGCCTTGATTGGCTGCG.ACGCGGA.GTCGGCGATGTTACTTTGAAAAAATT	710	Nephroselmis_spinosa_AB158375
ACGCTCCTGGTCTTCATTGCCCGGG.ACGTGGA.GTCGGCGATGTTACTTTGAAAAAATT	694	Nephroselmis_viridis_NIES486
ACGCTCCTGGTCTTCATTGCCCGGG.ACGTGGA.GTCGGCGATGTTACTTTGAAAAAATT	707	Nephroselmis_viridis_AB214976
GCGCTTCTGGCCTTAATTGGCTGGG.ACGTGGA.TTCGACGAGGTTACTTTGAAAAAATT	701	Pseudoscourfieldia_marina_AF122888
GCGCTTCTGGCCTTAATTGGCTGGG.ACGTGGA.TTCGACGAGGTTACTTTGAAAAAATT	701	Pseudoscourfieldia_marina_AJ132619
GCAGTTCTGGCCTTTGTTGGCTAGG.GTGCGGA.GTCGGCGCCGTTACTTTGAAAAAATT	703	Dolichomastix_tenuilepis
GCAGTTCCGGCCTTCGTTGGCCGGG.GTGCGGA.GTCGGCGCTGTTACTTTGAAAAAATT	702	Dolichomastix_tenuilepis_AF509625
GCGCTCCTGGGCTTAACGGCTCGGG.ACGCGGA.GTCGGCGTGGTTACTTTGAAAAAATT	695	Mamiella_gilva_AB017129
GCGCTCCTGGCCTTAATTGGCTGGG.ACGTGGA.GTCGGCGATGTTACTTTGAAAAAATT	708	Pyramimonas_mucifera
GCGCTTCTGGCCTTAACTGGCTGGG.ACGTGGA.GTCGGCGATGTTACTTTGAAAAAATT	709	Pyramimonas_olivacea_AB017122
GCGCTCGTGGGCTTAACTGTCTGCG.ACGCGGA.GTCGGCGGTGTTACTTTGGAAAAATT	707	Pyramimonas_parkeae_AB017124
TAGCTCCTGGGCTTCACTGTCCGGG.ACTAGGA.GCTGACGAGGTTACTTTGAGTAAATT	709	Tetraselmis
TAGCTCCTGGGCTTCACTGTCCGGG.ACTAGGA.GCTGACGAGGTTACTTTGAGTAAATT	712	Tetraselmis_convolutae_U05039
TAGCTCCTGGGCTTCACTGTCCGGGGACTAGGA.GCCGACGAAGTTACTTTGAGTAAATT	707	Tetraselmis_kochiensis_AJ431370
GCGCTACTGGCCTTAACTGGCTCGGTACGCGGA.GTCGGCGATGTTACTTTGAAAAAATT	707	Halosphaera_AB017125
GTGCGTC..GCACTTAATTGGGTGGCGTTCGGA.GTCGGCGTTGTTACTTTGAAAAAATT	683	Pseudoscourfieldia_marina_Wits_(?)
GTGCGTC..GCACTTAATTGGGTGGCGTTCGGA.GTCGGCGTTGTTACTTTGAAAAAATT	694	Prasinoderma_coloniale_AB058379
.TGCGTCTGGCATTCGTTTGCTGGGCGTA.GGA.GTCGGCGTCGTTACTTTGAGTAAATT	698	Prasinococcus_capsulatus_AB058384

AGAGTGTTCAAAGCAGGCAATCGCTCTGAATACATTAGCATGGAATAACACGATAGGACT	766	Nephroselmis_anterostigmatica_MBIC11158
AGAGTGTTCAAAGCAGGCAATCGCTCTGAATACATTAGCATGGAATAACACGATAGGACT	768	Nephroselmis_anterostigmatica_AB158372
AGAGTGTTCAAAGCAGGCAATCGCTCTGAATACATTAGCATGGAATAACACGATAGGACT	767	Nephroselmis_anterostigmatica_AB158373
AGAGTGTTCAAAGCAGGCATTCGCTCTGAATATATTAGCATGGAATAACACGATAGGACT	754	Nephroselmis_astigmatica_NIES252
AGAGTGTTCAAAGCAGGCATTCGCTCTGAATATATTAGCATGGAATAACACGATAGGACT	769	Nephroselmis_astigmatica_AB158374
AGAGTGTTCAAAGCAAGCCTTCGCTCTGAATACGTTAGCATGGAATAACATGATAGGACT	766	Nephroselmis_olivacae_X74754
AGAGTGTTCAAAGCAGGCCTTGGCTCTGAATACATTAGCATGGAATAACACGATAGGACT	765	Nephroselmis_pyriformis_WW02
AGAGTGTTCAAAGCAGGCCTTGGCTCTGAATACATTAGCATGGAATAACACGATAGGACT	765	Nephroselmis_pyriformis_AB158376
AGAGTGTTCAAAGCAGGCCTTGGCTCTGAATACATTAGCATGGAATAACACGATAGGACT	765	Nephroselmis_pyriformis_AB058378
AGAGTGTTCAAAGCAGGCCTTGGCTCTGAATACATTAGCATGGAATAACACGATAGGACT	765	Nephroselmis_pyriformis_AB058391
AGAGTGTTCAAAGCAGGCCTTGGCTCTGAATACATTAGCATGGAATAACACGATAGGACT	765	Pseudoscourfieldia_marina_X75565
AGAGTGTTCAAAGCAGGCCTTCGCTCTGAATACATTAGCATGGAATAACACGATAGGACT	769	Nephroselmis_rotunda_CCAP1960_3
AGAGTGTTCAAAGCAGGCCTTCGCTCTGAATACATTAGCATGGAATAACACGATAGGACT	762	Nephroselmis_rotunda_BB2
AGAGTGTTCAAAGCAGGCCTTCGCTCTGAATACATTAGCATGGAATAACACGATAGGACT	769	MBIC11149_AB214975
AGAGTGTTCAAAGCAGGCCTTCGCTCTGAATACATTAGCATGGAATAACACGATAGGACT	756	Nephroselmis_spinosa_NIES935
AGAGTGTTCAAAGCAGGCCTTCGCTCTGAATACATTAGCATGGAATAACACGATAGGACT	770	Nephroselmis_spinosa_AB158375
AGAGTGTTCAAAGCAAGCCTTCGCTCTGAATACATTAGCATGGAATAACATGATAGGACT	754	Nephroselmis_viridis_NIES486
AGAGTGTTCAAAGCAAGCCTTCGCTCTGAATACATTAGCATGGAATAACATGATAGGACT	767	Nephroselmis_viridis_AB214976
AGAGTGTTCAAAGCAAGCTAAAGCTCTGAATACATTAGCATGGAATAACGCGAGAGGACT	761	Pseudoscourfieldia_marina_AF122888
AGAGTGTTCAAAGCAAGCTAAAGCTCTGAATACATTAGCATGGAATAACGCGAGAGGACT	761	Pseudoscourfieldia_marina_AJ132619
AGAGTGTTCAAAGCGGGCTTACGC.TTGAATATATTAGCATGGAATAACACGATAGGACT	762	Dolichomastix_tenuilepis
AGAGTGTTCAAAGCGGGCTTGCGC.TTGAATATATTAGCATGGAATAACACTATAGGACT	761	Dolichomastix_tenuilepis_AF509625
AGAGTGTTCAAAGCGGGCTTACGC.TTGAATATATTAGCATGGAATAACACTATAGGACT	754	Mamiella_gilva_AB017129
AGAGTGTTCAAAGCAGGCCTAAGCTCTGAATACATTAGCATGGAATAACGCGATAGGACT	768	Pyramimonas_mucifera
AGAGTGTTCAAAGCAGGCCTACGCTCTGAATACATTAGCATGGAATAACGCGATAGGACT	769	Pyramimonas_olivacea_AB017122
AGAGTGTTCAAAGCAGGCAACCGCTCTGAATACATTAGCATGGAATAACGCTATAGGACT	767	Pyramimonas_parkeae_AB017124
AGAGTGTTCAAAGCAAGCCTACGCTCTGAATACATTAGCATGGAATAACATGATAGGACT	769	Tetraselmis
AGAGTGTTCAAAGCAAGCCTACGCTCTGAATACATTAGCATGGAATAACATGATAGGACT	772	Tetraselmis_convolutae_U05039
AGAGTGTTCAAAGCAAGCCTACGCTCTGAATATATTAGCATGGAATAACACGATAGGACT	767	Tetraselmis_kochiensis_AJ431370
AGAGTGTTCAAAGCAGGCCTACGCATTGAATACATTAGCATGGAATAACGCGATAGGACT	767	Halosphaera_AB017125
AGAGTGTTCAAAGCAAGCCATCGCTCTGAATACATTAGCATGGAATAACATGATAGGACT	743	Pseudoscourfieldia_marina_Wits_(?)
AGAGTGTTCAAAGCAAGCCATCGCTCTGAATACATTAGCATGGAATAACATGATAGGACT	754	Prasinoderma_coloniale_AB058379
AGAGTGTTCAAAGCAAGCTTGTGCTCTGCATACTTTAGCATGGAATAACATTATAGGACT	758	Prasinococcus_capsulatus_AB058384

CTGGTCCTATTTTGTTGGTCTTCGGGACCGGAGTAATGACTAATAGGGACAGTTGGGGGC	826	Nephroselmis_anterostigmatica_MBIC11158
CTGGTTCTATTTTGTTGGTCTTCGGGACCGGAGTAATGACTAATAGGGACAGTTGGGGGC	828	Nephroselmis_anterostigmatica_AB158372
CTGGTCCTATTTTGTTGGTCTTCGGGACCGGAGTAATGACTAATAGGGACAGTTGGGGGC	827	Nephroselmis_anterostigmatica_AB158373
CTGGTCCTATTTTGTTGGTCTTCGGGACCGGAGTAATGACTAATAGGGACAGTTGGGGGC	814	Nephroselmis_astigmatica_NIES252
CTGGTCCTATTTTGTTGGTCTTCGGGACCGGAGTAATGACTAATAGGGACAGTTGGGGGC	829	Nephroselmis_astigmatica_AB158374
CTGGTTCTATTTTGTTGGTCTTCGGGACCGGAGTAATGACTAATAGGGACAGTTGGGGGC	826	Nephroselmis_olivacae_X74754
CTGGTCCTATTTTGTTGGTCTTCGGGACCGGAGTAATGATTAATAGGGACAGTTGGGGGC	825	Nephroselmis_pyriformis_WW02
CTGGTCCTATTTTGTTGGTCTTCGGGACCGGAGTAATGATTAATAGGGACAGTTGGGGGC	825	Nephroselmis_pyriformis_AB158376
CTGGTCCTATTTTGTTGGTCTTCGGGACCGGAGTAATGATTAATAGGGACAGTTGGGGGC	825	Nephroselmis_pyriformis_AB058378
CTGGTCCTATTTTGTTGGTCTTCGGGACCGGAGTAATGATTAATAGGGACAGTTGGGGGC	825	Nephroselmis_pyriformis_AB058391
CTGGTCCTATTTTGTTGGTCTTCGGGACCGGAGTAATGATTAATAGGGACAGTTGGGGGC	825	Pseudoscourfieldia_marina_X75565
CTGGTTCTATTTTGTTGGTCTTCGGGACCGGAGTAATGACTAATAGGGACAGTTGGGGGC	829	Nephroselmis_rotunda_CCAP1960_3
CTGGTTCTATTTTGTTGGTCTTCGGGACCGGAGTAATGACTAATAGGGACAGTTGGGGGC	822	Nephroselmis_rotunda_BB2
CTGGTCCTATTCTGTTGGTCTTCGGGACCGGAGTAATGACTAATAGGGACAGTTGGGGGC	829	MBIC11149_AB214975
CTGGTTCTATTTTGTTGGTCTTCGGGACCGGAGTAATGACTAATAGGGACAGTTGGGGGC	816	Nephroselmis_spinosa_NIES935
CTGGTTCTATTTTGTTGGTCTTCGGGACCGGAGTAATGACTAATAGGGACAGTTGGGGGC	830	Nephroselmis_spinosa_AB158375
CTGGTCCTATTTTGTTGGTCTTCAGGACCGGAGTAATGACTAATAGGGACAGTTGGGGGC	814	Nephroselmis_viridis_NIES486
CTGGTCCTATTTTGTTGGTCTTCAGGACCGGAGTAATGACTAATAGGGACAGTTGGGGGC	827	Nephroselmis_viridis_AB214976
CGGTCCTTATTTTGTTGGTCTTCAAGGATGGAGTAATGATTAAGAGGGACAGTTGGGGGC	821	Pseudoscourfieldia_marina_AF122888
CGGTCCTTATTTTGTTGGTCTTCAAGGATGGAGTAATGATTAAGAGGGACAGTTGGGGGC	821	Pseudoscourfieldia_marina_AJ132619
CCGATCCTATTCTGTTGGTCTTCGGGACTGGAGTAATGATTAAGAGGAACAGTTGGGGGC	822	Dolichomastix_tenuilepis
CCGATCCTATTTTGTTGGTCTTCGGGACTGGAGTAATGATTAAGAGGAACAGTTGGGGGC	821	Dolichomastix_tenuilepis_AF509625
CCTATCCTATTTCGTTGGTCT.CGGGACGGGAGTAATGATTAAGAGGAACAGTTGGGGGC	813	Mamiella_gilva_AB017129
CTGGTCTTATTGTGTTGGTCTTCGAGACCGGAGTAATGATTAAGAGGGACAGTTGGGGGC	828	Pyramimonas_mucifera
CTGGTCTTATTGTGTTGGTCTTCGAGACCGGAGTAATGATTAAGAGGGACAGTTGGGGGC	829	Pyramimonas_olivacea_AB017122
CTGGTCTTATTGTGTTGGTCTTCGAGACCGGAGTAATGATTAAGAGGGACAGTTGGGGGC	827	Pyramimonas_parkeae_AB017124
CTGG.CTTATCTTGTTGGTCTGTGAGACCAGAGTAATGATTAAGAGGGACAGTCGGGGAC	828	Tetraselmis
CTGG.CTTATCTTGTTGGTCTGTGAGACCAGAGTAATGATTAAGAGGGACAGTCGGGGGC	831	Tetraselmis_convolutae_U05039
CTGG.CTTATCTTGTTGGTCTGTGAGACCAGAGTAATGATTAAGAGGGACAGTCGGGGAC	826	Tetraselmis_kochiensis_AJ431370
CCTATCCTATTGTGTTGGTCTTCGGGACGGGAGTAATGATTAAGAGGGACAGTTGGGGGC	827	Halosphaera_AB017125
CTGGTCTTATTTTGTTGGTTTCCGAGACTGGAGTAATGATTAAGAGGGACAGTCGGGGGC	803	Pseudoscourfieldia_marina_Wits_(?)
CTGGTCTTATTTTGTTGGTTTCCGAGACTGGAGTAATGATTAAGAGGGACAGTCGGGGGC	814	Prasinoderma_coloniale_AB058379
CTGGTTCTATTTTGTTGGTCTTCGGAACCGGAGTAATGATTAATAGGGACAGTCGGGGGC	818	Prasinococcus_capsulatus_AB058384

ATTCGTATTTCATTGTCAGAAGGTGAAA	854	Nephroselmis_anterostigmatica_MBIC11158
ATTCGTATTTCATTGTCAGA.GGTGAAA	855	Nephroselmis_anterostigmatica_AB158372
ATTCGTATTTCATTGTCAGA.GGTGAAA	854	Nephroselmis_anterostigmatica_AB158373
ATTCGTATTTCAT.GTCAGA.GGTGAAA	840	Nephroselmis_astigmatica_NIES252
ATTCGTATTTCATTGTCAGA.GGTGAAA	856	Nephroselmis_astigmatica_AB158374
ATTCGTATTTCATTGTCAGA.GGTGAAA	853	Nephroselmis_olivacae_X74754
ATTCGTATTTCATTGTCAGA.GGTGAAA	852	Nephroselmis_pyriformis_WW02
ATTCGTATTTCATTGTCAGA.GGTGAAA	852	Nephroselmis_pyriformis_AB158376
ATTCGTATTTCATTGTCAGA.GGTGAAA	852	Nephroselmis_pyriformis_AB058378
ATTCGTATTTCATTGTCAGA.GGTGAAA	852	Nephroselmis_pyriformis_AB058391
ATTCGTATTTCATTGTCAGA.GGTGAAA	852	Pseudoscourfieldia_marina_X75565
ATTCGTATTTCATTGTCAGA.GGTGAAA	856	Nephroselmis_rotunda_CCAP1960_3
ATTCGTATTTCATTGTCAGA.GGTGAAA	849	Nephroselmis_rotunda_BB2
ATTCGTATTTCATTGTCAGA.GGTGAAA	856	MBIC11149_AB214975
ATTCGTATTTCATTGTCAGA.GGTGAAA	843	Nephroselmis_spinosa_NIES935
ATTCGTATTTCATTGTCAGA.GGTGAAA	857	Nephroselmis_spinosa_AB158375
ATTCGTATTTCAT.GTCAGA.GGG....	836	Nephroselmis_viridis_NIES486
ATTCGTATTTCATTGTCAGA.GGTGAAA	854	Nephroselmis_viridis_AB214976
ATTCGTATTTCATTGCTAGA.GGTGAAA	848	Pseudoscourfieldia_marina_AF122888
ATTCGTATTTCATTGCTAGA.GGTGAAA	848	Pseudoscourfieldia_marina_AJ132619
ATTCGTATTTCAT.GTCAGA.GGTGAAA	848	Dolichomastix_tenuilepis
ATTCGTATTTCATTGTCAGA.GGTGAAA	848	Dolichomastix_tenuilepis_AF509625
ATTCGTATTTCATTGTCAGA.GGTGAAA	840	Mamiella_gilva_AB017129
ATTCGTATTTCATTGTCAGA.GGTGAAA	855	Pyramimonas_mucifera
ATTCGTATTTCATTGTCAGA.GGTGAAA	856	Pyramimonas_olivacea_AB017122
ATTCGTATTTCATTGTCAGA.GGTGAAA	854	Pyramimonas_parkeae_AB017124
ATTCGTATTTCATTGTCAGA.GGTGAAA	855	Tetraselmis
ATTCGTATTTCATTGTCAGA.GGTGAAA	858	Tetraselmis_convolutae_U05039
ATTCGTATTTCATTGTCAGA.GGTGAAA	853	Tetraselmis_kochiensis_AJ431370
ATTCGTATTTCATTGTCAGA.GGTGAAA	854	Halosphaera_AB017125
ATCCGTATTTCATTGTCAGA.GGT....	826	Pseudoscourfieldia_marina_Wits_(?)
ATCCGTATTTCATTGTCAGA.GGTGAAA	841	Prasinoderma_coloniale_AB058379
ATCCGTATTTCATTGTCAGA.GGTGAAA	845	Prasinococcus_capsulatus_AB058384

The insertion of 437 bases found starting at position 329 in *Nephroselmis viridis* sp. ined. is as follows:

```
TATTGTACTCATTCGGGCTAGTCGGCTGGCAACAGCTGGCTAGTGACTCG    50
TGGAACTGTTGCAACACCGTCAAATTGCGGGAACACCCTTAGAGCCTTCC   100
CCTACCGCGGCCCGCCGAAAGGTTGGGTGCAGCAGGTGGTATCGTGGCCA   150
CCGGATGGTAAAAACGGGGAAGGATTGGGCGACCACGCAGCCAAGCCCTA   200
AGGGGGCCCGGTCTATCTGGGTTCCTATGGGTGCAGTTCACAGACTAAAT   250
GTCGGTGGGCCGGGAAACGCCCGAGCTGATAGTTCGGGTCTCGGCTTAAG   300
ATATAGTCGGCTCCTTGGGGAAACCCTTGCCGGCAGGAGGATCTGTCCCT   350
TCGAGTTCCACAACTCAGTACGGAGGGCGGGGAGAGCCTGTCGGGGCAGC   400
ACGCTGGACCACCTTCCAGACCCTGTCGAATCAGCGG                437
```

Colophon

This document was prepared using the LaTeX 2_{ε} version of the LaTeX document preparation system and the TeX text-setting program on a notebook computer running Windows XP (SP2) and Kubuntu 8.04 LTS "Hardy Heron". The distributions used were MiKTeX 2.6 (Windows) and TeX live (Kubuntu). The document was set in the standard Computer Modern font (T1) and *cm-super* fonts. Sectional headings set in Sans Serif. Output was compiled directly to PDF via *pdflatex*. Donald Knuth is acknowledged for producing TeX and Leslie Lamport for producing LaTeX. Editing, compiling and project management functions were provided by *TeXnicCenter 1 Beta 7.01* from `ToolsCenter.org` or `www.latex-community.org` (Windows) and by *Kile 2.0* (Kubuntu). The natbib package was used to manage citations within the document and the reference list was maintained using *BibEdt 0.7.2.35* from `bibedt.sourceforge.net` (Windows) and *JabRef* (Kubuntu). Andy Buckley is acknowledged for the hepthesis document class, parts of which were modified and incorporated into this document. The following packages, listed alphabetically, were used: caption, colortbl, enumitem, fancyhdr, fixfoot, fontenc, footmisc, geometry, listings, lscape, multicol, multirow, pdflscape, rotating, sectsty, TeXshade, textcomp, ulem, verbatim and xcolor. Various members of the Internet Usenet Newsgroup comp.text.tex also provided helpful suggestions and assistance.

Atlas of Plates

Plate 1 – Body scale summary

Plate 2 – Flagellar scale summary

Plates 3 – 4 *Nephroselmis anterostigmatica* Nakayama, Suda, Kawachi and Inouye

Plates 5 – 7 *Nephroselmis astigmatica* Inouye and Pienaar

Plate 8 *Nephroselmis olivacea* Stein em. Moestrup *et* Ettl

Plates 9 – 10 *Nephroselmis pyriformis* (Carter) Ettl

Plates 11 – 14 *Nephroselmis rotunda* (Carter) Fott

Plates 15 – 16 *Nephroselmis rotunda* (Carter) Fott (BB2)

Plates 17 – 18 *Nephroselmis rotunda* (Carter) Fott

Plates 19 – 21 *Nephroselmis spinosa* Suda

Plates 22 – 23 *Nephroselmis viridis* Inouye, Suda *et* Pienaar sp. ined.

Plates 1 and 2 were produced in Microsoft Word XP (2002) and the OpenOffice.org Wordprocessor (Version 2.4). Plates 3 to 23 were produced with the open-source desktop publishing program *Scribus*, version 1.3.3.9 (*http://www.scribus.net*) under Windows XP (SP2) and version 1.3.3.11 under Kubuntu Linux.

Plate 1

Body scales found on the seven confirmed members of *Nephroselmis* examined in this study are illustrated in Plate 1. Drawings are not to scale. In order to complete the scale data presented here, scales which were not seen in the examined material are shown redrawn from other sources as cited below. In these instances, the table cells are marked with a heavy border. Scale formulae for third, fourth and fifth layer body scales are provided in Table 3.2.

Body scale layer 1 This scale layer is identical for all species of *Nephroselmis* examined. It is small and square in shape. The left image shows the scale as seen from "above". The small image to the right shows the scale as seen from the side. This scale is approximately 35 nm in size.

Body scale layer 2 Three different types of scale are seen in this position: the "Paper windmill" type, the "Maltese cross" type and small stellate scales. These scales range from 30 to 35 nm in size.

Body scale layer 3 *N. anterostigmatica*: The scale shown on the left is as seen from the side; the right image is the scale as seen from "above". Small unipolar stellate scales are found in the third scale layer position. These scales have 11 spines and are approximately 50 nm in size. *N. astigmatica*: The scale shown on the left is as seen from the side; the right image is the scale as seen from "above". These unipolar scales resemble small a "Eastern temple" or a "Christmas fir tree", have 33 spines and are approximately 180 nm in size. *N. olivacea*: unipolar scales with 11 spines are found in the third scale layer position and are approximately 160 nm in size; image redrawn from Moestrup and Ettl (1979). *N. pyriformis*: Third layer body scales are absent. *N. rotunda*: Large unipolar stellate scales are found in the third scale layer position. The scale on the left is as seen from the side; the right image is the scale as seen from "above". This scale has 11 spines and is approximately 460 nm in height and 330 nm in width. *N. spinosa*: Small unipolar stellate scales with 11 spines are found in the third scale layer position. These scales are approximately 160 nm high and 60 nm in width. The scale on the left is as seen from the side; the right image is the scale as seen from "above". *N. viridis*: Small unipolar stellate scales with 13 spines are found in the third scale layer position. These scales are approximately 180 nm high and 100 nm in width. The scale on the left is as seen from the side; the right image is the scale as seen from "above".

Body scale layer 4 *N. anterostigmatica*: The scale on the left is as seen from the side; the right image is the scale as seen from "above". These are unipolar scales with 16 spines and are approximately 120 nm in height and 150 nm in width. *N. astigmatica*: Complex bipolar scales with 26 spines are present in the fourth scale layer position. Scales are approximately 200 nm in height. Redrawn from Inouye and Pienaar (1984). *N. olivacea*: Multipolar scales with 20 spines are present in the fourth scale layer position. Scales are approximately 250 nm in size. Redrawn from Moestrup and Ettl (1979). *N. pyriformis*: Fourth layer body scales are absent. *N. rotunda*: Fourth layer body scales are absent. *N. spinosa*: Large (1 μm) unipolar spines with four feet and a terminal hook are present in the fourth scale layer. The base of the scale is approximately 180 nm in width. *N. viridis*: The scale on the left is as seen from the side; the right image is the scale as seen from "above".

Large multipolar stellate scales are present in the fourth scale layer position. Scales are approximately 250 nm in size. Image redrawn from Young (1991).

Body scale layer 5 Fifth layer body scales are found in *N. anterostigmatica* only. These bipolar scales are similar to the fourth layer body scales found in *N. astigmatica*, but are not as complex, having only 17 spines. Scales are approximately 250 nm in height and 150 nm in width. Image redrawn from Nakayama *et al.* (2007).

Plate 2

Flagellar scales found on the seven confirmed members of *Nephroselmis* examined in this study. Drawings are not to scale. In order to complete the scale data presented here, scales which were not seen in the examined material are shown redrawn from other sources as cited below. In these instances, the table cells are marked with a heavy border.

Flagellar scale layer 1 This scale layer is identical for all species of *Nephroselmis* examined. It is small and pentagonal in shape, but more rounded than the first layer of body scales. The left image shows the scale as seen from "above". The small image to the right shows the scale as seen from the side. This scale is approximately 35 nm in size.

Flagellar scale layer 2 Small "rod" or "man" scales are found in most species of *Nephroselmis*. These scales are approximately 30 nm in size. The only exception is *N. rotunda*, in which small stellate scales of the same size are found in the second flagellar scale layer position.

Flagellar scale layer 3 Only two species possess flagellar scales in this position. Small scales which resemble curved spines with hooks are found in *N. olivacea*. Image redrawn from Moestrup and Ettl (1979). Small stellate scales of approximately 100 nm in size are found in *N. viridis*. Image redrawn from Young (1991).

Pit scales Pit scales are found in *N. astigmatica* only. These are complex scales approximately 100 nm in size. Image redrawn from Inouye and Pienaar (1984).

Plate 3

Nephroselmis anterostigmatica Nakayama, Suda, Kawachi and Inouye [MBIC 11158]

Figures 1, 2 and 3 Lateral view Nomarski images of fresh material. Note the asymmetrical cell shape and the anterior position of the eyespot.

Figures 4, 5 and 6 Left-right vertical section Nomarski through-focus of fixed material, showing the chloroplast lobes, starch grain and flanges.

Figures 7, 8 and 9 Lateral view Nomarski through-focus of fixed material, showing the chloroplast lobes, pyrenoid and flanges.

Figure 10 Whole mount showing many square underlayer body scales, small stellate third layer body scales (arrow) and large stellate fourth layer scales lying in the field.

Figure 11 Whole mount of flagellum showing the square underlayer scales, the paper windmill second layer scales (arrow), the third layer of small stellate scales and the fourth layer of large stellate scales. Only T-hair scales are visible, suggesting that this is the long flagellum.

Inset The region around the arrow at a higher magnification.

Scale bars = 1 μm

Plate 4

Nephroselmis anterostigmatica Nakayama, Suda, Kawachi and Inouye [MBIC 11158]

Figure 1 Left-right vertical section, with the left of the cell on the left of the image. Note the starch grain surrounding the pyrenoid and ventral penetration of the chloroplast. Stellate scales can be seen in the flagellar pit.

Figure 2 Section through the flagellar pit region, showing the stellate scales. Note the structure of the stellate scales, as can be seen towards the bottom of the image. Paper windmill second layer body scales are visible (arrow). A section of the mitochondrion with cisternae can be seen at the top of the image.

Figure 3 Section showing the square underlayer body scales and the large fourth layer stellate scales. A large lobe of the mitochondrion is visible in the cell.

Figure 4 Section showing the rounded underlayer flagellar scales and a small stellate body scale (arrow).

Figure 5 Glancing section showing the square underlayer body scales, paper windmill scales (horizontal arrow) and large stellate scales. Note the three distinct projections on the stellate scale (vertical arrow).

Figure 6 Cross section through the large stellate scales.

Figure 7 Section showing detail of the large stellate scale at the bottom of the image. Note the three distinct projections on the stellate scale.

Figure 8 Section showing ventral thylakoid penetration.

Scale bars = 1 μm

Plate 5

Nephroselmis astigmatica Inouye and Pienaar [NIES 252]

Figure 1 Left-right view Nomarski image of fresh material. Note the starch grain and the nucleus towards the lower edge of the cell.

Figure 2 Left-right phase contrast image of fresh material showing the flange, the starch grain (appearing green) and the pyrenoid.

Figure 3 Lateral view Nomarski image of fresh material. The cup-shaped chloroplast can be seen in both cells.

Figure 4 Phase contrast image of Figure 3. The chloroplast and pyrenoid (appearing red/orange) are visible.

Figures 5 and 6 Left-right vertical section Nomarski through-focus of fixed material showing the flange and starch grain. The nucleus can be seen on the left of the cell Figure 5.

Figure 7 Lateral view Nomarski image of fixed material, with the starch grain and flagella clearly visible.

Figures 8, 9 and 10 Left-right vertical section Nomarski through-focus of fixed material showing the flange and starch grain.

Black scale bars = 1 μm
White scale bars = 5 μm

Plate 6

Nephroselmis astigmatica Inouye and Pienaar [NIES 252]

Figure 1 Whole mount showing the third layer of body scales.

Figure 2 Whole mount showing detail of the third layer of “temple” body scales, in longitudinal (top arrow) and cross (bottom arrow) sections.

Figure 3 Whole mount of flagellum showing detail of flagellar hair scales (T-hair scales). Pt-hair scales were not seen in this sample.

Figure 4 Glancing section showing the square underlayer body scales, the paper windmill second layer (arrow) and the elaborate "temple" third scale layer. Rounder underlayer scales are seen on the flagellum.

Figure 5 Section showing the square underlayer body scales, the paper windmill scales (arrow) and the "temple" third layer body scales. Scales can be seen in Golgi cisternae within the cell.

Black scale bars = 1 μm
White scale bars = 0.5 μm

Plate 7

Nephroselmis astigmatica Inouye and Pienaar [NIES 252]

Figure 1 Left-right section in the vertical plane, the right of the cell located on the right of the image. The nucleus is visible in the right flange and the Golgi body in the left flange. The pyrenoid, penetrated ventrally by thylakoids of the chloroplast, can be seen. Pit scales are visible in the flagellar pit region and "temple" third layer of body scales can been seen around the periphery of the cell. A pit scale is visible in the region of the Golgi body. The rhizoplast can be seen running towards the dorsal side of the cell, past the nucleus and terminating in the region of the chloroplast. A basal body can be seen at the ventral end of the rhizoplast.

Inset Detail of the pit scales; a pit hair is also visible.

Scale bars = 1 μm

Plate 8

Nephroselmis olivacea Stein em. Moestrup *et* Ettl [NIES 483]

Figures 1, 2 and 3 Lateral view phase contrast and Nomarski images of fresh material. Note the rounded cell shape, the cup-shaped chloroplast and the characteristic position of the flagella.

Figures 4 and 5 Lateral view Nomarski through-focus images of fresh material, showing the cup-shaped chloroplast.

Figure 6 Whole mount showing detail of the large stellate body scales.

Figure 7 Whole mount of flagellum showing detail of the flagella hair scales, lying parallel to the flagellum. A large stellate scale is lying next to the flagellum.

Figure 8 Whole mount of flagellum showing detail of the T-hair scales and Pt-hair scales (arrows).

Figure 9 Whole mount of flagellum showing detail of the T-hair scales.

Black scale bars = 1 μm
White scale bars = 5 μm

Plate 9

Nephroselmis pyriformis (Carter) Ettl [Wits FH01, Wits WW02]

Figure 1 Lateral view Nomarski image of fresh material showing the cup-shaped chloroplast. A refractile granule can be seen within the cell. Note the asymmetrical cell shape.

Figure 2 Left-right Nomarksi image of fresh material showing the cup-shaped chloroplast.

Figures 3 and 4 Left-right vertical section Nomarski through-focus of fixed material showing the chloroplast lobes and the starch grain. The presence of a small flange can be seen in the cells in Figure 4.

Figures 5 and 6 Lateral view Nomarski through-focus of fixed material. Note the cell shape, starch grain and nucleus.

Figure 7 Lateral view Nomarski image of fixed material.

Figures 8 and 9 Left-right vertical section Nomarski through-focus of fixed material showing the chloroplast lobes and the starch grain. A small flange can also be seen.

Scale bars = 1 μm

Plate 10

Nephroselmis pyriformis (Carter) Ettl [Wits FH01, Wits WW02]

Figure 1 Whole mount of flagella, showing the T-hair scales on both flagella and the Pt-hair scales (arrows) on the short flagellum only. Note the blunt-ended flagellum.

Figure 2 Section of flagellum showing the rounded pentagonal underlayer scales.

Figures 3 and 4 Glancing section showing the square underlayer body scales and the small stellate second layer scales.

Figure 5 Left-right section in the vertical plane. The nucleus and Golgi body can be seen, as can the left lobe of the chloroplast. Radial thylakoid penetration is visible. Two distinct layers of body scales can be seen in cross section.

Figure 6 Section through the nucleus. Pit hairs can be seen. A basal body and part of the flagella apparatus is visible.

Figure 7 Section showing pit hairs. Two distinct layers of body scales can been seen in cross section.

Figure 8 Section showing pit hairs.

Scale bars = 1 μm

Plate 11

Nephroselmis rotunda (Carter) Fott [CCAP 1960/1]

Figure 1 Lateral view Nomarski image of fixed material. Note the round shape of the cell, the prominent starch grain and the circular lipid globules.

Figures 2, 3 and 4 Lateral view Nomarski images of fresh material. Note the cup-shaped chloroplast, the starch grain and pyrenoid, and the eyespot located under the short flagellum.

Figure 5 Lateral view and left-right vertical section Nomarski image of fixed material, showing the starch grain in each. The pyrenoid is clearly visible in the lateral view cell.

Figure 6 Dorsal view Nomarski image of fixed material showing the starch grain.

Figure 7 Left-right vertical section Nomarski image of fixed material, showing the starch grain and chloroplast lobes.

Figure 8 Lateral view Nomarski image of fixed material showing the circular shape of the cell and the prominent starch grain.

Black scale bars = 1 μm
White scale bars = 5 μm

Plate 12

Nephroselmis rotunda (Carter) Fott [CCAP 1960/1]

Figure 1 Whole mount showing the cell shape and relative flagellar lengths.

Figure 2 Whole mounts showing flagellar hair scales and a large stellate body scale (arrow).

Figures 3 and 4 Whole mount showing detail of flagellar hair scales. Pt-hair scales can be seen on the short flagellum in Figure 3 (arrows).

Figure 5 Sections through several cells, showing the eyespot (arrow), large circular lipid globules and starch grains.

Figure 6 Detail of eyespot and lipid globule. A basal body and flagellar root (arrow) can be seen on the right of the image.

Figure 7 Lateral section showing the Golgi apparatus, eyespot, lipid globules and large starch grain.

Figure 8 Detail of the eyespot, showing chloroplast membranes, lipid globule and Golgi apparatus. Small square underlayer body scales can also be seen lying in the field.

Scale bars = 1 μm

Plate 13

Nephroselmis rotunda (Carter) Fott [CCAP 1960/1]

Figure 1 Left-right vertical section showing the nucleus, chloroplast lobes, starch grain and pyrenoid. The 9+2 axoneme arrangement of the flagellum can clearly be seen. Note the absence of large stellate scales in this sample.

Figure 2 Section showing stellate scales in the flagellar pit region. Part of the mitochondrion lobe can be seen between the circular lipid globule and the chloroplast.

Figure 3 Left-right vertical section. Note the absence of large stellate body scales and the presence of stellate scales in the flagellar pit region. The nucleus with nucleolus can be seen, as well as the Golgi apparatus in the right cell.

Figure 4 Left-right vertical section. The nucleus and nucleolus can be seen, as well as the Golgi body. Mitochondrion lobes are visible in the sections of the cell flanking the flagellar pit. Note the basal body and the evidence of stellate scales in the flagellar pit. A fibrillar vesicle can also be seen (arrow).

Figure 5 Left-right vertical section. Note the absence of large stellate scales and the presence of stellate pit scales. The characteristic arrangement of cell organelles can be seen – the nucleus on the right of the cell and the Golgi apparatus on the left of the cell. Part of the mitochondrion lobe is visible between the Golgi apparatus and the chloroplast.

Figure 6 Section showing the square underlayer body scales and the small stellate scales of the second body layer (horizontal arrow). Stellate scales in the flagellar pit can be seen in both cells. Stellate second underlayer scales on the flagellum are also visible (vertical arrow).

Figure 7 Detail of the flagellar pit showing the stellate scales. The small stellate body scales of the second layer can be seen (arrow).

Scale bars = 1 μm

Plate 14

Nephroselmis rotunda (Carter) Fott [CCAP 1960/1]

Figure 1 Left-right vertical section (left cell) showing a basal body (black arrow). Glancing section showing square underlayer body scales and small stellate second layer scales (white arrow) (right cell).

Figure 2 Detail of the eyespot, showing the chloroplast membranes and a lipid globule.

Figures 3 and 4 Detail of the radial thylakoid penetration of the pyrenoid.

Scale bars = 1 μm

Plate 15

Nephroselmis rotunda (Carter) Fott [Wits BB2]

Figures 1 and 2 Lateral view Nomarski image of fresh material. Note the circular cell shape, the starch grain and pyrenoid, and the location of the eyespot under the short flagellum.

Figure 3 Left-right view Nomarski image of fresh material, showing starch grain and eyespot.

Figure 4 Lateral view Nomarski image of fixed material. Note the cell shape and starch grain.

Figure 5 Whole mount. Note the large stellate body scales.

Figure 6 Whole mount showing large stellate body scales.

Figure 7 Whole mount showing flagellar T-hair scales and large stellate body scales.

Figure 8 Whole mount showing T-hair scales.

Scale bars = 1 μm

Plate 16

Nephroselmis rotunda (Carter) Fott [Wits BB2]

Figure 1 Dorsal section through the starch grain showing the square underlayer body scales, the small stellate second layer scales and the large stellate third layer scales.

Figure 2 Detail of the three scale layers shown in Figure 1.

Figure 3 Glancing section showing square underlayer body scales and large stellate scales.

Figure 4 Section showing the nucleus, eyespot and three layers of body scales.

Figure 5 Glancing section showing square underlayer body scales and small stellate second layer scales.

Figure 6 The nucleus, eyespot, starch grain, pyrenoid and large stellate scales can be seen in the left cell. The right cell shows detail of the various scale layers found on the body and the flagellum.

Inset The flagella tip at higher magnification. Stellate underlayer scales are visible.

Figure 7 Section showing body scale layers. A flagellum can be seen entering the cell.

Figure 8 Section showing radial thylakoid penetration.

Scale bars = 1 μm

Plate 17

Nephroselmis rotunda (Carter) Fott [CCAP 1960/3]

Figures 1, 2, 3 and 4 Lateral view slide film Nomarski images of fresh material. Note the circular cell shape, the cup-shaped chloroplast, the eyespot located under the short flagellum and the characteristic closed flagellar parking position.

Figure 5 Nomarski image of fixed material in various views. Note the circular cell shape and the lipid globules in the cell on the right.

Figure 6 Left-right vertical section Nomarski image of fixed material showing the starch grain.

Figure 7 Lateral view Nomarski image of fixed material. Note the cell shape, the starch grain and the lipid globules.

Figure 8 Lateral view Nomarski image of dividing cell, from fixed material.

Black scale bars = 1 μm
White scale bars = 5 μm

Plate 18

Nephroselmis rotunda (Carter) Fott [CCAP 1960/3]

Figure 1 Whole mount showing flagellar hair scales.

Figure 2 Detail of flagellar hairs from Figure 1. Pt-hair scales cannot be seen.

Figure 3 Left-right vertical section showing detail of the square underlayer scales and the small stellate second layer body scales. Rounded underlayer scales can be seen on the flagellum. Note the absence of large stellate scales.

Figure 4 Section showing the Golgi apparatus, lipid globule and starch grain. One stellate scale can be seen at the lower right of the image (arrow).

Figure 5 Glancing section showing the square underlayer body scales and the small stellate second layer scales.

Figure 6 Detail of scales from Figure 5 showing the rounded pentagonal underlayer flagellar scales.

Figure 7 Section of the flagellar pit region showing the large stellate scales which appear in this region only in some samples.

Figure 8 Section showing detail of the flagellar basal bodies, positioned at a 90° angle.

Scale bars = 1 μm

Plate 19

Nephroselmis spinosa Suda [NIES 935]

Figures 1 and 2 Lateral view phase contrast and Nomarski images of fresh material. Note the "flattened-circle" cell shape and the starch grain.

Figures 3 and 4 Lateral view Nomarski images of fresh material. Note the cup-shaped chloroplast, the pyrenoid and the eyespot located under the short flagellum.

Figures 5 and 6 Lateral view Phase contrast images of fresh material. Note the cup-shaped chloroplast, the pyrenoid and the eyespot located under the short flagellum.

Figures 7 and 8 Left-right vertical section Nomarski through-focus of fixed material showing the distinctive triangular starch grains. Note the pointed keel of the chloroplast at the dorsal end of the cell (arrow).

Figures 9, 10 and 11 Left-right vertical section Nomarski image through-focus of fixed material showing the distinctive triangular starch grains. Note the pointed keel of the chloroplast at the dorsal end of the cell.

Black scale bars = 1 μm
White scale bars = 5 μm

Plate 20

Nephroselmis spinosa Suda [NIES 935]

Figure 1 Whole mount showing distinctive spine body scales and flagellar hairs.

Figure 2 Whole mount detail of spine scales and flagellar hairs. A single spine scale can be seen in the bottom right of the image, lying next to a bacterium (arrow).

Figure 3 and 4 Whole mount detail of spine scales showing the detail of the four "feet" at the base of the spine (right arrow, Figure 4) and the short terminal hook at the end of the spine (left arrow, Figure 4).

Figure 5 Whole mount of flagellum showing T- and Pt-hair scales (arrow).

Figure 6 Vertical section showing the triangular starch grains, the pointed chloroplast keel at the dorsal end of the cell and the eyespot. Stellate scales as well as spine scales can be seen.

Figure 7 Section showing triangular starch grains, eyespot and scale detail.

Figure 8 Detail of starch grains and dorsal chloroplast keel. Square underlayer body scales can be seen at the bottom of the image.

Scale bars = 1 μm

Plate 21

Nephroselmis spinosa Suda [NIES 935]

Figure 1 Glancing section showing body and flagellar scales.

Figure 2 Section showing nucleus, Golgi apparatus, eyespot and various scales types.

Scale bars = 1 μm

Plate 22

Nephroselmis viridis Inouye, Suda *et* Pienaar sp. ined. [NIES 486]

Figures 1 and 2 Lateral view Nomarski image through-focus showing cup-shaped chloroplast and both flagella in closed parking position.

Figures 3, 4 and 5 Lateral view Nomarski image through-focus showing cup-shaped chloroplast. Note the eyespot located under the short flagellum.

Figures 6, 7 and 8 Lateral view Nomarski image focus-through showing cup-shaped chloroplast, pyrenoid and flagella.

Figure 9 Whole mount showing relative flagellar lengths.

Figure 10 Whole mount showing flagellar T-hair scales and Pt-hair scales (arrow). Many square underlayer body scales can be seen lying in the field.

Scale bars = 1 μm

Plate 23

Nephroselmis viridis Inouye, Suda *et* Pienaar sp. ined. [NIES 486]

Figure 1 Whole mount showing detail of Pt-hair scales.

Figure 2 Whole mount showing Pt-hair scales, square underlayer body scales and a stellate scale in longitudinal (top arrow) and cross (bottom arrow) section.

Figure 3 Vertical section showing nucleus, extensive chloroplast, square underlayer body scales and paper windmill second layer body scales. The structure indicated by the arrow is possibly a polysome.

Figure 4 Vertical section showing the extensive chloroplast and mitochondrion, two underlayer body scales and stellate third layer body scales (arrow).

Figure 5 Vertical section showing the Golgi apparatus with a square underlayer body scale visible in a cisterna and stellate scales in the flagellar pit region. Paper windmill second layer body scales are also visible (arrow).

Figure 6 Vertical section showing ventral thylakoid penetration.

Scale bars = 1 μm